# INFORMATION TO USERS

This manuscript has been reproduced from the microfilm master. UMI films the text directly from the original or copy submitted. Thus, some thesis and dissertation copies are in typewriter face, while others may be from any type of computer printer.

**The quality of this reproduction is dependent upon the quality of the copy submitted.** Broken or indistinct print, colored or poor quality illustrations and photographs, print bleedthrough, substandard margins, and improper alignment can adversely affect reproduction.

In the unlikely event that the author did not send UMI a complete manuscript and there are missing pages, these will be noted. Also, if unauthorized copyright material had to be removed, a note will indicate the deletion.

Oversize materials (e.g., maps, drawings, charts) are reproduced by sectioning the original, beginning at the upper left-hand corner and continuing from left to right in equal sections with small overlaps. Each original is also photographed in one exposure and is included in reduced form at the back of the book.

Photographs included in the original manuscript have been reproduced xerographically in this copy. Higher quality 6" x 9" black and white photographic prints are available for any photographs or illustrations appearing in this copy for an additional charge. Contact UMI directly to order.

**UMI**

A Bell & Howell Information Company
300 North Zeeb Road, Ann Arbor MI 48106-1346 USA
313/761-4700 800/521-0600

# INTERACTION BETWEEN A TRANSIENT PLANE WAVE AND A CONDUCTIVE HALF-SPACE

by

Hsueh-Yuan Pao

---

A Dissertation Submitted to the Faculty of the

DEPARTMENT OF ELECTRICAL AND COMPUTER ENGINEERING

In Partial Fulfillment of the Requirements
For the Degree of

DOCTOR OF PHILOSOPHY

In the Graduate College

THE UNIVERSITY OF ARIZONA

1995

THE UNIVERSITY OF ARIZONA ®
GRADUATE COLLEGE

As members of the Final Examination Committee, we certify that we have read the dissertation prepared by Hsueh-Yuan Pao

entitled Interaction between a Transient Plane Wave and a Conductive Half-Space

and recommend that it be accepted as fulfilling the dissertation requirement for the Degree of Doctor of Philosophy

| | |
|---|---|
| Steven Dvorak | 11/16/95 Date |
| Donald Dudley | 11/16/95 Date |
| Andreas Cangellaris | 11/16/95 Date |
| | Date |
| | Date |

Final approval and acceptance of this dissertation is contingent upon the candidate's submission of the final copy of the dissertation to the Graduate College.

I hereby certify that I have read this dissertation prepared under my direction and recommend that it be accepted as fulfilling the dissertation requirement.

| | |
|---|---|
| Dissertation Director<br>Steven Dvorak | 11/16/95 Date |

## STATEMENT BY AUTHOR

This dissertation has been submitted in partial fulfillment of requirements for an advanced degree at The University of Arizona and is deposited in the University Library to be made available to borrowers under rules of the Library.

Brief quotations from this dissertation are allowable without special permission, provided that accurate acknowledgment of source is made. Requests for permission for extended quotation from or reproduction of this manuscript in whole or in part may be granted by the head of the major department or the Dean of the Graduate College when in his or her judgment the proposed use of the material is in the interests of scholarship. In all other instances, however, permission must be obtained from the author.

SIGNED: 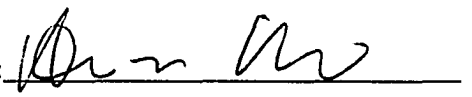

# ACKNOWLEDGEMENTS

I wish to express my deepest gratitude to my advisors, Professor Steven Dvorak and Professor Donald Dudley. For all the caring guidance and encouragement they have given me during the pursuit of my graduate degree, I am deeply indebted to them. I would also like to thank Professor Andreas Cangellaris for providing helpful comments in reviewing my dissertation and for his willingness to serve on my examination committee.

This work was completed with the sponsor by Howard Hughes Doctoral Fellowship. I would like to thank Hughes Aircraft Company in general. In particular, I would like to acknowledge the following individuals for their support and assistance in Hughes Missile Systems Company: Dr. Frank Zak, Mr. Hal Marlin, Mr. Jack Anderson, Mr. Joe Anderson, and many more.

Finally, I would like to thank my wife Ming Chu and my son Hsing-Chia, and my parent Chia-Shan Pao and Feng-Mi Yao, for their love, understanding, patience, and support.

# TABLE OF CONTENTS

# LIST OF FIGURES

# ABSTRACT

A method which allows for the analytical evaluation of the interaction between a transient plane wave and a conductive half-space is presented. We assume that an electromagnetic plane wave is obliquely incident on a conducting half-space, which is modeled by a frequency independent permittivity and conductivity. The general case of the electromagnetic plane wave is divided into two polarizations: transverse electric (TE) and transverse magnetic (TM).

The time-domain expressions for the reflected and transmitted waves are first represented as inverse Laplace transforms. The transient fields are then shown to consist of two canonical integrals, $f(\beta)$ and $e(\beta)$. The canonical integrals, in turn, are solved analytically, thereby yielding closed-form solutions involving incomplete Lipschitz-Hankel integrals (ILHIs). The ILHIs are computed numerically using efficient convergent and asymptotic series expansions, thus enabling the efficient computation of the transient fields. The exact, closed-form expressions are verified by comparing with previously published results and with results obtained using standard numerical integration and fast Fourier transform algorithms.

An asymptotic series representation for the ILHIs is then employed to obtain a relatively simple late-time approximation for the transient fields. This approximate late-time expression is shown to accurately model the fields over a large portion of their time history.

The closed-form transient field expressions are used to investigate the effects of neglecting displacement currents when studying transient wave propagation in the conductive half-space. The diffusion fields are found to yield accurate results at late times.

# CHAPTER 1

## Introduction

It is our intent to study the interaction between a transient plane wave and a conductive half-space. We assume that a transient plane wave is obliquely incident on a conductive half-space which is modeled by the frequency independent electrical parameters $\sigma$, $\epsilon$, and $\mu$. We obtain exact, closed-form solutions for the fields which involve two canonical integrals, namely, $f(\beta)$ and $e(\beta)$, which in turn are expressed as linear combinations of incomplete Lipschitz-Hankel integrals (ILHIs). To the best of our knowledge, this is the first time that the transient fields for this important canonical problem have been represented in closed-form in terms of readily computable special functions.

Our interest in this problem is motivated by the requirement to compute the transient reflected and transmitted fields for various applications, such as stealth technologies, remote sensing, measurement of the electrical properties of conductive substrates, geophysical probing, and subsurface communication. Particularly, the rapidly growing demands on Distributed Interactive Simulation (DIS) stimulate the study of this problem. For example, missile simulation devices require real time simulation of the missile flying environment. As a missile cruises over the earth, the DIS indicates the interaction between the pulse generated by the missile and

the ground. Therefore, an exact, closed-form field solution is valuable for fast and accurate calculation of this interaction.

## 1.1 General Literature Survey

The problem of the interaction between a transient plane wave and a conductive half-space has challenged scientists in electromagnetics for over of a half century because of the difficulties posed by dispersive propagation channels. In this section, we provide an overview of related work.

People started by studying transient wave propagation through a whole space filled with a dispersive medium, under the assumption that the electrical properties of the dispersive space (i.e., $\sigma$, $\epsilon$, and $\mu$) are frequency independent. In 1941, in his famous textbook *Electromagnetic Theory* [37], Stratton employed a Laplace transform pair to solve for the fields associated with an electromagnetic plane wave propagating in a dispersive medium. Later, Wait (1951) calculated the transient electric fields generated by several types of unit-step function current sources, such as electric and magnetic dipoles, and linear grounded current elements of finite and infinite length embedded in a conductive whole space [39]. He used the Laplace transform and neglected the contribution of displacement currents in order to obtain an approximate closed-form solution for the electric field. This method limited the validity of the solution only to low frequencies so that the transient response was only valid at late times. Furthermore, this solution violated causality, which we will discuss in detail

in Chapter 7. Wait (1953) [41] and Richards (1958) [36] extended this work to compute the magnetic field for a pulsed dipole in an infinite conducting medium. They emphasized the attenuation behavior that was observed as a function of the distance. Zisk (1960) [56], and Anderson and Moore (1960) [2] continued Wait and Richard's work and investigated the causes of this behavior. Since they were interested in the transient response for long distances, the displacement current was omitted. Bhattacharyya (1957) later considered the more realistic case of electric dipoles with ramp and sawtooth function current sources immersed in a conducting medium. He noted that the finite rise time strongly affected the fields [5]. He also neglected displacement currents in this study. Later, Bhattacharyya (1957) discussed the propagation of a step-function excited electric dipole in a homogeneous and isotropic conducting medium [6]. This time he took into account the effect of displacement currents. However, the transient response was not expressed in closed-form because he could not analytically evaluate the inverse Laplace transform integrals. In 1969, Wait obtained an exact, closed-form solution for a transient electric field energized by an infinitely thin, unidirectional uniform current sheet. This source gave rise to a normally incident, transient plane wave propagating in a whole space [48].

Wait first studied transient wave propagation in a dispersive half-space in 1951 [40]. In this introductory work, he presented the transient field of a magnetic dipole for a unit-step function excitation placed over a horizontally stratified earth. Once again, the displacement current was neglected. In 1956, Wait derived the transient

fields for a vertical electric dipole over a homogeneous curved ground [43]. The frequency domain solution was facilitated by employing a series expansion. The transient response was then obtained by transformation techniques. Wait (1957) [44, 45], Levy and Keller (1958) [23], and Keilson and Row (1959) [18] investigated the propagation of transient ground or surface waves over curved and planar earth. The transient electric and magnetic fields for a magnetic dipole excited by a step-function current placed close to the surface of the earth were determined by Bhattacharyya in 1959 [7]. In this investigation, the displacement current and the effect of the air were taken into account. Unfortunately, no closed-form result was obtained since the integrals still remained in terms of inverse Laplace transforms. A general analysis for the electromagnetic response of conducting media (either infinite or half-space geometries) due to pulse excitation was presented by Wait (1961) [46]. Mijharends (1962) [27], and Wait and Hill (1971) [52] presented the transient electromagnetic field behavior, generated by a horizontal electrical dipole and magnetic dipole, respectively, embedded in a homogeneous conducting half-space and excited by step-function current. These studies neglected displacement current. Monroe (1969) obtained a three-term approximate expression, consisting of a constant plus two exponentials, for the reflected field of a vertically polarized plane wave in free space with a step-function time variation which was incident obliquely on a planar imperfectly conducting surface [28]. Wait and Spies (1970) investigated the electric and magnetic fields of a step-function excited electric dipole immersed in an infinite homogeneous medium.

The solutions were of series expansion form [49, 50]. Wait (1971) [51], and Hill and Wait (1974) [16] considered the transient electromagnetic field in a conducting half-space which was coupled by a line source (delta function excitation) placed above it. All displacement currents were neglected. Wait and Ott (1972) calculated the transient electromagnetic fields for a small current-carrying loop placed over a homogeneous earth. This study produced the basic theory for time-domain airborne EM surveying [53]. Wait (1972) also studied the electromagnetic transient coupling between two small underground loops [54].

Numerical methods have been used to study transient phenomenon since late 1960. A typical example is the work by Fuller and Wait in 1972 [13]. They studied the effect of the frequency dependence of the conductivity and permittivity of rock for pulse transmission. They used a Debye model in order to model the frequency dependence for the desired properties. A fast Fourier transform technique was then introduced to carry out the numerical solutions. King (1993) analyzed the propagation of a single Gaussian pulse in sea water and a Gaussian pulse envelope for a low-frequency burst. The results were numerically evaluated [20].

In 1954, Vallese investigated a transient plane wave normally incident upon a plane of good conductor [38]. The results were carried out by neglecting displacement currents and reducing the wave equation to a simple diffusion equation. Wait and Froese presented an inverse Laplace transform representation for the reflected field

of a transient transverse magnetic (TM) plane wave which was excited by a unit-step function source and was obliquely incident on a planar interface of a dissipative medium (1955) [42]. The convolution theorem was then used to rewrite the transient field in terms of an exponential function convolved with modified Bessel functions. Approximate early- and late-time expressions were derived as well. They carried out the inverse Laplace transform and obtained closed-form expressions for the transient fields in some special cases. Grumet (1959) reported results on transient transverse electric (TE) plane wave penetration into a semi-infinite conductor. The source he considered was a unit-step function [14]. He obtained an inverse Laplace transform representation for the transient field first. By dropping the displacement current, he then reduced the wave equation to a diffusion equation, and thereby obtained an analytic closed-form solution. He realized that the diffusion fields travel faster than the speed of light (i.e., they violate causality). Baum used numerical inverse Fourier transform techniques to calculate the reflection of a step-function plane wave from a flat ground or water surface (1967) [4]. Nicolis (1967, 1969) [29, 30], and Wait (1969) [47] examined the distortion of plane electromagnetic pulses reflected by total internal reflection. King and Harrison (1968) studied a Gaussian plane wave pulse normally incident on a planar earth [19].

Dudley et al. [8] (1974) carried out a thorough investigation of TE and TM reflected waves associated with a double-exponential, obliquely-incident plane wave. They employed contour integration techniques in order to rewrite the inverse Fourier

transform representation for the reflected fields in terms of a residue term and an integral around the branch cut. The branch cut contribution was computed using numerical integration. Papazoglou [34] (1975) extended the analysis to handle TE and TM transmitted waves. He also investigated a Debye model which accounted for the frequency dependence in the electrical properties of the conductive media. Barnes and Tesche (1984) [3] developed a Neumann series representation for the impulsive reflected field; however, their result is only approximate. Klaasen (1990) [21] showed that the TE transmitted and reflected fields associated with a unit-step, obliquely incident plane wave can be represented in terms of convolution integrals involving exponential functions and modified Bessel functions. Klaasen used a time-matching procedure to evaluate the required convolution integrals numerically.

In summary, up until now, we are unaware of anyone who has been able to represent the transient reflected and transmitted fields for an obliquely incident plane wave in closed-form in terms of readily computable special functions. Reviewing the history leads us to believe that in the early studies, people tried to simplify the problem using approximations so that the integrations could be carried out analytically. The development of high-speed computers has revolutionized the capability for solving transient electromagnetic field problems. This has led more people to directly apply numerical methods to the study of transient fields. However, valuable physical phenomenon can be more readily extracted from analytical solutions. Therefore, we have returned to study the analytic solution for this important canonical problem.

However, instead of finding another approximate result, we have advanced the field by obtaining exact, closed-form analytic solutions.

## 1.2 Outline

The most difficult part of this problem lies in the evaluation of the inverse Laplace transforms. The novel contribution of this work involves new techniques for the analytical evaluation of the integrals in the inverse Laplace transform representations. Recently, Dvorak has found a number of exact, closed-form solutions for some relatively complex canonical electromagnetic problems [10, 12]. All of the new solutions involve incomplete Lipschitz-Hankel integrals (ILHIs). We now demonstrate that this important canonical problem can also be solved using ILHIs.

ILHIs are special functions which involve an integration over Bessel and exponential functions. Thus, one would expect them to be more complicated than Bessel functions. It turns out that ILHIs can be written in terms of an infinite series of Bessel functions. Just like the Bessel functions, ILHIs have various known integral, series, and asymptotic representations [9, 25, 26]. ILHIs also provide solutions to the wave equation [11]. Two factorial-Neumann series expansions together with a Neumann series expansion allow for the efficient computation of the ILHIs [9].

The problem to be studied is introduced in Chapter 2. The coordinate system is first introduced followed by the constitutive parameters. A Laplace transform pair is used to connect the fields in the time-domain and Laplace domain (s-domain).

An arbitrary transient wave can be decomposed into two independent sets of modes: transverse electric (TE) and transverse magnetic (TM). Two sets of fields (transmitted and reflected) are determined using Maxwell's equations and boundary conditions in the s-domain. Some important frequency domain properties are discussed as well.

Chapter 3 is devoted to an overview of the mathematic tools. Two canonical integrals, $f(\beta)$ and $e(\beta)$, are defined by inverse Laplace transform integrals. It is then shown that these two canonical integrals satisfy second-order, non-homogeneous, ordinary differential equations. The differential equations can be solved analytically, yielding closed-form expressions involving incomplete Lipschitz-Hankel integrals (ILHIs).

In Chapters 4 and 5, the transient transmitted fields for the TE and TM modes are represented by inverse Laplace transform integrals, respectively. Using various mathematical techniques, these inverse Laplace transforms are expressed in terms of the two canonical integrals, $f(\beta)$ and $e(\beta)$, plus some other elementary functions. The transient reflected fields are obtained by using the convolution theorem and the transient transmitted field results. Various numerical results are demonstrated for validation purposes. Comparisons between the closed-form solution and the results obtained by both a fast Fourier transform (FFT) algorithm and a numerical integration routine are made to show the advantages of the closed-form solutions.

In Chapter 6, relatively simple late-time expressions for the canonical integrals $f(\beta)$ and $e(\beta)$ are derived by using the asymptotic factorial-Neumann series expansion

for the ILHIs. The numerical result for the late-time transient fields shows good agreement with the closed-form solutions over large potion of the time history.

In Chapter 7, the effects of neglecting displacement currents when studying transient wave propagation in the conductive half-space are discussed. Approximate diffusion fields are compared with the closed-form results.

General conclusions and recommendations for further work are included in Chapter 8.

# CHAPTER 2

## Problem Formulation in the Laplace Domain

This chapter provides a foundation for studying the interaction between a transient plane wave and a conductive half-space. The materials developed in this chapter will be used in following chapters. Since Laplace transforms have received in depth treatment in many textbooks, we refer the reader to the following references [32, 55] for further information. First, the geometry of the problem and the coordinate system are described. Next, we review the procedure for determining the transmitted and reflected fields in the Laplace domain from Maxwell's equations. The Laplace transform pair is employed for this procedure. Invoking the boundary conditions at the interface then leads to the solutions of the transmission and reflection coefficients for both the TE and TM cases. Finally, some frequency domain properties of the reflected and transmitted fields are discussed.

### 2.1 Geometry for the Problem

As depicted in Figure 2.1, a uniform transient plane wave is obliquely incident at an arbitrary angle $\theta_i$ on a conductive half-space (medium II). We assume that the source for the plane wave resides in the air (medium I). To specify the position in this

unbounded space, we employ the coordinates $(x, y, z)$ with respect to a given orthogonal right-hand Cartesian reference frame. The position vector in this coordinate system is given by

$$\mathbf{r} = x\hat{\mathbf{x}} + y\hat{\mathbf{y}} + z\hat{\mathbf{z}}. \tag{2.1}$$

Furthermore, we assume that medium I (air) is homogeneous. The constitutive constants of the air are those of a vacuum, i.e., $\epsilon_0$ and $\mu_0$. The conductive half-space (medium II) is assumed to consist of a homogeneous, isotopic, time-invariant, linear material. The electromagnetic behavior of medium II is characterized by a conductivity $\sigma$, permittivity $\epsilon$, and permeability $\mu$, which are all assumed to be frequency independent. Actually, the permittivities of many media, for instance soil, are quite dependent on frequency and to a smaller extent so are the conductivities. However, as frequency is increased, the permittivity appears to level out. For angular frequencies larger than $\sigma/\epsilon$, the permittivity is somewhat constant [4]. Our problem is clearly two dimensional, since there is no variation in the $y$-direction.

If the time variable is denoted by $t$, then the Laplace transform pair can be written as [32, 55],

$$\mathcal{L}[F(t)] = \tilde{F}(s) = \int_0^\infty e^{-st} F(t) dt, \tag{2.2}$$

and

$$F(t) = \frac{1}{2\pi j} \int_{\xi - j\infty}^{\xi + j\infty} e^{st} \tilde{F}(s) ds, \tag{2.3}$$

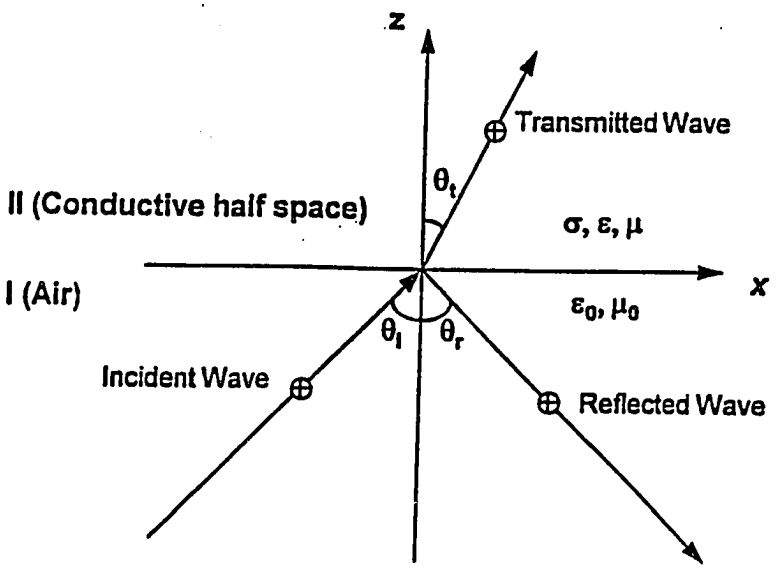


Figure 2.1: Geometry and coordinate system for transient plane wave incident into a conductive half-space

where $\xi$ is a constant which is chosen large enough so that all the singularities lie to the left side of $\xi$ in the complex $s$ plane. The s-domain (Laplace domain) fields are obtained later by applying the Laplace transform (2.2) with respect to time to the wave equation.

An arbitrary transient plane wave in a homogeneous source-free region can be broken up into two sets, i.e., a transverse electric mode (TE) and a transverse magnetic mode (TM). If the incident electric field is polarized perpendicular to the propagation vector, it is defined as a TE mode; otherwise, it is a TM mode. It can be shown that these two sets of fields are independent and that there is no mode coupling in the problem we are studying. For the chosen coordinate system, the TE and TM modes involve the following non-zero field components,

$$TE \begin{cases} E_y \\ H_x \\ H_z \end{cases}, \qquad TM \begin{cases} H_y \\ E_x \\ E_z \end{cases}. \tag{2.4}$$

These six components constitute the field [15]. We wish to determine the transmitted and reflected fields and are going to solve for these two kinds of waves.

## 2.2 Solution for the TE Case

In this section, we find solutions for the TE case. As indicated in (2.4), the principal field component for this case is $E_y$.

We start from Maxwell's equations

$$\left.\begin{aligned} \nabla \times \mathbf{E} + \tfrac{\partial \mathbf{B}}{\partial t} &= 0 \\ \nabla \cdot \mathbf{B} &= 0 \\ \nabla \times \mathbf{H} - \tfrac{\partial \mathbf{D}}{\partial t} &= \mathbf{J} \\ \nabla \cdot \mathbf{D} &= \rho_e \end{aligned}\right\}, \tag{2.5}$$

where $\rho_e$ and $\mathbf{J}$ are the charge density and current density, respectively. The constitutive relations are

$$\left.\begin{aligned} \mathbf{D} = \epsilon \mathbf{E} &= \epsilon_r \epsilon_0 \mathbf{E} \\ \mathbf{B} = \mu \mathbf{H} &= \mu_r \mu_0 \mathbf{H} \\ \mathbf{J} &= \sigma \mathbf{E} \end{aligned}\right\}, \tag{2.6}$$

where $\epsilon_r$ and $\mu_r$ are the relative permittivity and the relative permeability, respectively.

After taking the curl of the first equation in (2.5) and applying the constitutive relations (2.6), we have

$$\nabla \times (\nabla \times \mathbf{E}) = -\nabla \times \frac{\partial \mathbf{B}}{\partial t} = -\mu \frac{\partial}{\partial t}\left(\frac{\partial \mathbf{D}}{\partial t} + \mathbf{J}\right) = -\mu\epsilon \frac{\partial^2 \mathbf{E}}{\partial t^2} - \mu\sigma \frac{\partial \mathbf{E}}{\partial t}. \tag{2.7}$$

Using the vector identity [15]

$$\nabla \times (\nabla \times \mathbf{A}) = \nabla(\nabla \cdot \mathbf{A}) - \nabla^2 \mathbf{A}, \tag{2.8}$$

(2.7) becomes

$$\nabla^2 \mathbf{E} - \mu\epsilon \frac{\partial^2 \mathbf{E}}{\partial t^2} = \mu\sigma \frac{\partial \mathbf{E}}{\partial t} + \frac{1}{\epsilon} \nabla \rho_e. \tag{2.9}$$

Equation (2.9) is a D'Alembertian equation. In source free regions of space, $\rho_e = 0$, so that

$$\nabla^2 \mathbf{E} - \mu\epsilon \frac{\partial^2 \mathbf{E}}{\partial t^2} = \mu\sigma \frac{\partial \mathbf{E}}{\partial t}, \tag{2.10}$$

which is the time-domain wave equation.

If we apply the Laplace transform to both sides of (2.10), we find that the time-domain wave equation reduces to the Helmhotz equation in the s-domain:

$$(\nabla^2 - \gamma_e^2)\tilde{\mathbf{E}}(x, z, s) = 0 \tag{2.11}$$

where

$$\gamma_e = \sqrt{s(s\mu\epsilon + \mu\sigma)} = \frac{1}{\hat{v}}\sqrt{s\left(s + \frac{\sigma}{\epsilon}\right)}; \qquad \Re(\gamma_e) > 0 \tag{2.12}$$

is the complex propagation constant and

$$\hat{v} = \frac{1}{\sqrt{\mu\epsilon}} \tag{2.13}$$

is the speed of light in a lossless medium modeled by $\epsilon$ and $\mu$. The subscript $e$ in the above equations denotes the TE case.

The general solution for Helmholtz's equation (2.11) is

$$\tilde{\mathbf{E}}(x, z, s) = \tilde{E}_y \hat{\mathbf{y}} = \tilde{E}_0(s) e^{\mp \boldsymbol{\gamma}_e \cdot \boldsymbol{r}} \hat{\mathbf{y}}, \tag{2.14}$$

where

$$\boldsymbol{\gamma}_e = \gamma_{ex}\hat{\mathbf{x}} + \gamma_{ez}\hat{\mathbf{z}}. \tag{2.15}$$

The incident electric field, which must satisfy the Helmholtz equation (2.11) with $\epsilon = \epsilon_0$, $\mu = \mu_0$, and $\sigma = 0$, can be written as

$$\tilde{E}_y^{(i)}(x, z, s) = \tilde{E}_0 e^{-\frac{s}{c}(x \sin\theta_i + z \cos\theta_i)}, \tag{2.16}$$

where $\tilde{E}_0$ is the amplitude of the incident waveform and $c$ is the speed of light in free space. Likewise, the reflected and transmitted fields are given by

$$\tilde{E}_y^{(r)}(x, z, s) = \tilde{E}_0 R_e e^{-\frac{s}{c}(x \sin\theta_r - z \cos\theta_r)} \tag{2.17}$$

and

$$\tilde{E}_y^{(t)}(x, z, s) = \tilde{E}_0 T_e e^{-(\gamma_{ex} x + \gamma_{ez} z)}, \tag{2.18}$$

where $R_e$ and $T_e$ are the reflection and transmission coefficients, respectively.

By invoking the phase matching condition along $x$ at $z = 0$, we find that

$$\theta_i = \theta_r \tag{2.19}$$

and

$$\gamma_{ex} = \frac{s}{c} \sin\theta_i. \tag{2.20}$$

In order to satisfy (2.12) and (2.15), we find that

$$\gamma_{ez} = \sqrt{\gamma^2 - \gamma_x^2} = \frac{1}{\hat{v}} \sqrt{\left(1 - \frac{\hat{v}^2}{c^2} \sin^2\theta_i\right) s^2 + \frac{\sigma}{\epsilon} s}. \tag{2.21}$$

If we define $\hat{\theta}_t$ to be the angle of refraction for the lossless case (i.e., $\sigma = 0$), then we can rewrite (2.20) and (2.21) as

$$\gamma_{ex} = \frac{s}{\hat{v}} \sin\hat{\theta}_t \tag{2.22}$$

and

$$\gamma_{ez} = \frac{\cos\hat{\theta}_t}{\hat{v}}\sqrt{s^2+2as}, \tag{2.23}$$

where

$$a = \frac{\sigma}{2\epsilon\cos^2\hat{\theta}_t} \tag{2.24}$$

and

$$\cos\hat{\theta}_t = \sqrt{1-\frac{\hat{v}^2}{c^2}\sin^2\theta_i}. \tag{2.25}$$

The significance of the refraction angle associated with the lossless case will be discussed in following chapters.

Employing Faraday law, $\nabla\times\tilde{\mathbf{E}} = -s\mu\tilde{\mathbf{H}}$, we find that the corresponding magnetic fields are given by

$$\tilde{H}_x^{(i)}(x,z,s) = -\frac{1}{c\mu_0}\cos\theta_i\tilde{E}_0 e^{-\frac{s}{c}(x\sin\theta_i+z\cos\theta_i)}, \tag{2.26}$$

$$\tilde{H}_z^{(i)}(x,z,s) = \frac{1}{c\mu_0}\sin\theta_i\tilde{E}_0 e^{-\frac{s}{c}(x\sin\theta_i+z\cos\theta_i)}, \tag{2.27}$$

$$\tilde{H}_x^{(r)}(x,z,s) = \frac{R_e}{c\mu_0}\cos\theta_i\tilde{E}_0 e^{-\frac{s}{c}(x\sin\theta_i-z\cos\theta_i)}, \tag{2.28}$$

$$\tilde{H}_z^{(r)}(x,z,s) = \frac{R_e}{c\mu_0}\sin\theta_i\tilde{E}_0 e^{-\frac{s}{c}(x\sin\theta_i-z\cos\theta_i)}, \tag{2.29}$$

$$\tilde{H}_x^{(t)}(x,z,s) = -\frac{T_e}{s\mu}\tilde{E}_0\frac{\cos\hat{\theta}_t}{\hat{v}}\sqrt{s^2+2as}\,e^{-(\frac{x}{\hat{v}}s\sin\hat{\theta}_t+\frac{z}{\hat{v}}\cos\hat{\theta}_t\sqrt{s^2+2as})}, \tag{2.30}$$

$$\tilde{H}_z^{(t)}(x,z,s) = \frac{T_e}{c\mu}\sin\theta_i\tilde{E}_0 e^{-(\frac{x}{\hat{v}}s\sin\hat{\theta}_t+\frac{z}{\hat{v}}\cos\hat{\theta}_t\sqrt{s^2+2as})}. \tag{2.31}$$

After enforcing the boundary conditions (i.e., $\tilde{E}_y$ and $\tilde{H}_x$ are continuous at $z=0$), we find that [17]

$$R_e = \frac{s-b_e\sqrt{s^2+2as}}{s+b_e\sqrt{s^2+2as}} \tag{2.32}$$

and

$$T_e = \frac{2s}{s + b_e\sqrt{s^2 + 2as}}, \tag{2.33}$$

where

$$b_e = \sqrt{\frac{\epsilon\mu_0}{\mu\epsilon_0}}\frac{\cos\hat{\theta}_t}{\cos\theta_i}. \tag{2.34}$$

## 2.3 Solution for the TM Case

In this section, we find the solutions for the counterpart of the TE case, the TM case. From (2.4), the principal field component for this case is $H_y$.

To start, we take the curl of Ampere's law (2.5) and use the constitutive relations (2.6), so that

$$\nabla\times(\nabla\times\mathbf{H}) = \nabla\times\mathbf{J}+\nabla\times\frac{\partial\mathbf{D}}{\partial t} = \sigma(\nabla\times\mathbf{E})+\epsilon\frac{\partial}{\partial t}(\nabla\times\mathbf{E}) = -\mu\epsilon\frac{\partial^2\mathbf{H}}{\partial t^2}-\epsilon\sigma\frac{\partial\mathbf{H}}{\partial t}. \tag{2.35}$$

After again using the vector identity in (2.8), we have

$$\nabla^2\mathbf{H} - \mu\epsilon\frac{\partial^2\mathbf{H}}{\partial t^2} = \mu\sigma\frac{\partial\mathbf{H}}{\partial t}, \tag{2.36}$$

which is the TM time-domain wave equation.

If we take the Laplace transform of both sides of (2.36), the wave equation reduces to Helmhotz's equation

$$(\nabla^2 - s^2\mu\epsilon)\tilde{\mathbf{H}}(x,z,s) = \sigma\mu s\tilde{\mathbf{H}}(x,z,s). \tag{2.37}$$

If we define

$$\gamma_h = \sqrt{s(s\mu\epsilon+\mu\sigma)} = \frac{1}{\hat{v}}\sqrt{s\left(s+\frac{\sigma}{\epsilon}\right)}; \qquad \Re(\gamma_h) > 0 \tag{2.38}$$

as the complex propagation constant, then (2.37) becomes

$$(\nabla^2 - \gamma_h^2)\tilde{\mathbf{H}}(x, z, s) = 0 \tag{2.39}$$

in the s-domain. The subscript $h$ denotes the TM case.

The general solution for the Helmholtz equation in (2.39) is

$$\tilde{\mathbf{H}}(x, z, s) = \tilde{H}_y\hat{\mathbf{y}} = \tilde{H}_0(s)e^{\mp\boldsymbol{\gamma}_h \cdot \boldsymbol{r}}\hat{\mathbf{y}}, \tag{2.40}$$

where

$$\boldsymbol{\gamma}_h = \gamma_{hx}\hat{\mathbf{x}} + \gamma_{hz}\hat{\mathbf{z}}. \tag{2.41}$$

The incident magnetic field, which must satisfy Helmholtz's equation (2.39) with $\epsilon = \epsilon_0$, $\mu = \mu_0$, and $\sigma = 0$, can be written as

$$\tilde{H}_y^{(i)}(x, z, s) = \tilde{H}_0 e^{-\frac{s}{c}(x\sin\theta_i + z\cos\theta_i)}, \tag{2.42}$$

where $\tilde{H}_0$ is the amplitude of the incident waveform. Likewise, the reflected and transmitted fields are given by

$$\tilde{H}_y^{(r)}(x, z, s) = \tilde{H}_0 R_h e^{-\frac{s}{c}(x\sin\theta_r - z\cos\theta_r)} \tag{2.43}$$

and

$$\tilde{H}_y^{(t)}(x, z, s) = \tilde{H}_0 T_h e^{-(\gamma_{hx}x + \gamma_{hz}z)}, \tag{2.44}$$

where $R_h$ and $T_h$ are the reflection and transmission coefficients, respectively.

By the phase matching condition (i.e. (2.19)) along $x$ at $z = 0$, we obtain

$$\gamma_{hx} = \frac{s}{c}\sin\theta_i = \frac{s}{\hat{v}}\sin\hat{\theta}_t \tag{2.45}$$

and

$$\gamma_{hz} = \frac{\cos\hat{\theta}_t}{\hat{v}}\sqrt{s^2+2as}, \tag{2.46}$$

where $a$ and $\cos\hat{\theta}_t$ are given by (2.24) and (2.25), respectively.

Employing Ampere's Law $\nabla \times \tilde{\mathbf{H}} = \mathbf{J} + s\epsilon\tilde{\mathbf{E}} = (\sigma + s\epsilon)\tilde{\mathbf{E}}$, we find that the corresponding electric fields are

$$\tilde{E}_x^{(i)}(x,z,s) = \frac{1}{c\epsilon_0}\cos\theta_i\tilde{H}_0 e^{-\frac{s}{c}(x\sin\theta_i + z\cos\theta_i)}, \tag{2.47}$$

$$\tilde{E}_z^{(i)}(x,z,s) = -\frac{1}{c\epsilon_0}\sin\theta_i\tilde{H}_0 e^{-\frac{s}{c}(x\sin\theta_i + z\cos\theta_i)}, \tag{2.48}$$

$$\tilde{E}_x^{(r)}(x,z,s) = -\frac{R_h}{c\epsilon_0}\cos\theta_i\tilde{H}_0 e^{-\frac{s}{c}(x\sin\theta_i - z\cos\theta_i)}, \tag{2.49}$$

$$\tilde{E}_z^{(r)}(x,z,s) = -\frac{R_h}{c\epsilon_0}\sin\theta_i\tilde{H}_0 e^{-\frac{s}{c}(x\sin\theta_i - z\cos\theta_i)}, \tag{2.50}$$

$$\tilde{E}_x^{(t)}(x,z,s) = \frac{T_h}{\sigma+s\epsilon}\tilde{H}_0\frac{\cos\hat{\theta}_t}{\hat{v}}\sqrt{s^2+2as}\, e^{-(\frac{x}{\hat{v}}s\sin\hat{\theta}_t + \frac{z}{\hat{v}}\cos\hat{\theta}_t\sqrt{s^2+2as})}, \tag{2.51}$$

$$\tilde{E}_z^{(t)}(x,z,s) = -\frac{T_h}{\sigma+s\epsilon}\tilde{H}_0 s\frac{\sin\theta_i}{c}e^{-(\frac{x}{\hat{v}}s\sin\hat{\theta}_t + \frac{z}{\hat{v}}\cos\hat{\theta}_t\sqrt{s^2+2as})}. \tag{2.52}$$

Imposing the boundary conditions (i.e., $\tilde{H}_y$ and $\tilde{E}_x$ are continuous at $z = 0$), we find that [17]

$$R_h = \frac{(\sigma+s\epsilon)\hat{v}\cos\theta_i - \epsilon_0 c\cos\hat{\theta}_t\sqrt{s^2+2as}}{(\sigma+s\epsilon)\hat{v}\cos\theta_i + \epsilon_0 c\cos\hat{\theta}_t\sqrt{s^2+2as}} = \frac{(s+\rho) - b_h\sqrt{s^2+2as}}{(s+\rho) + b_h\sqrt{s^2+2as}} \tag{2.53}$$

and

$$T_h = \frac{2(\sigma+s\epsilon)\hat{v}\cos\theta_i}{(\sigma+s\epsilon)\hat{v}\cos\theta_i + \epsilon_0 c\cos\hat{\theta}_t\sqrt{s^2+2as}} = \frac{2(s+\rho)}{(s+\rho) + b_h\sqrt{s^2+2as}}, \tag{2.54}$$

where

$$b_h = \sqrt{\frac{\epsilon_0\mu}{\mu_0\epsilon}}\frac{\cos\hat{\theta}_t}{\cos\theta_i}, \tag{2.55}$$

and

$$\rho = \frac{\sigma}{\epsilon}. \tag{2.56}$$

## 2.4 Properties of the Fields

Some aspects of the reflected and transmitted fields, which will clarify some of the properties of wave propagation in the frequency-domain, are discussed in this section. The expressions in the s-domain are rewritten in the frequency-domain because of the physical importance of the frequency-domain. This is done by simply replacing $s$ by $j\omega$.

### 2.4.1 Propagation of the Transmitted Fields

We demonstrated in the previous sections that the phase terms of the transmitted fields for the TE and TM cases are the same. Now let

$$\boldsymbol{\gamma} = \gamma_x \hat{\mathbf{x}} + \gamma_z \hat{\mathbf{z}} = j(k_x \hat{\mathbf{x}} + k_z \hat{\mathbf{z}}) = j\mathbf{k_1} \tag{2.57}$$

denote the phase term for both the TE and TM transmitted fields. From the previous sections,

$$\gamma_x = \frac{s}{c} \sin\theta_i = j\frac{\omega}{c} \sin\theta_i = jk_0 \sin\theta_i. \tag{2.58}$$

Therefore,

$$k_x = k_0 \sin\theta_i \tag{2.59}$$

in frequency-domain. Similarly,

$$\gamma_z = jk\cos\hat{\theta}_t\sqrt{1-j\frac{\sigma}{\epsilon\omega\cos^2\hat{\theta}_t}} = jk_z. \tag{2.60}$$

Here we have used the radiation condition, $\Re(\gamma_z) > 0$.

In the frequency-domain, the wavenumber in the z-direction can written as

$$k_z = k\cos\hat{\theta}_t\sqrt{1-j\frac{\sigma}{\epsilon\omega\cos^2\hat{\theta}_t}} = k_z' + jk_z''. \tag{2.61}$$

To satisfy the radiation condition, the square root in (2.61) must be chosen such that $\Im(k_z) = k_z'' < 0$. The variables $k_0$ and $k$ denote the lossless wavenumbers in the vacuum and the medium, respectively.

After solving (2.61), we find that

$$k_z' = k\cos\hat{\theta}_t\sqrt{\frac{1}{2}\sqrt{1+\left(\frac{\sigma}{\epsilon\omega\cos\hat{\theta}_t}\right)^2}+\frac{1}{2}} \tag{2.62}$$

and

$$k_z'' = -k\cos\hat{\theta}_t\sqrt{\frac{1}{2}\sqrt{1+\left(\frac{\sigma}{\epsilon\omega\cos\hat{\theta}_t}\right)^2}-\frac{1}{2}}. \tag{2.63}$$

The propagation factor can then be written as

$$e^{-j(xk_x+zk_z)} = e^{zk_z''}e^{-j(xk_x+zk_z')}. \tag{2.64}$$

From (2.64), we conclude that the planes of equal amplitude are given by $z =$ constant, while planes of equal phase are given by $xk_x + zk_z' =$ constant. It is obvious that the transmitted waves are non-uniform waves due to the loss of the medium. Furthermore, the attenuation factor $k_z''$ increases with increasing frequency.

By definition, the phase velocity in the conductive half-space is [24]

$$v = \frac{1}{\sqrt{\frac{\mu\epsilon}{2}\left(\sqrt{1+\frac{\sigma^2}{\omega^2\epsilon^2}}+1\right)}}, \tag{2.65}$$

which is frequency dependent and increases with frequency so long as the constant $\mu$, $\epsilon$ and $\sigma$ are frequency independent. The physical implications of the phase velocity will be discussed in depth after we obtain the analytic solutions for the transient transmitted fields in later chapters.

As shown in Figure 2.1, the general refraction angle $\theta_t$ is the angle between the normal of the interface and the direction of wave propagation. As defined in (2.41) the phase factor of the wave propagation constant is expressed as

$$e^{-j\mathbf{k_1}\cdot\mathbf{r}} = e^{-j(xk_x+zk_z)} = e^{-j(xk_0\sin\theta_i+zk_1\cos\theta_t)} \tag{2.66}$$

where

$$k_1 = \sqrt{k_x^2+k_z^2} = \sqrt{k_0^2\sin^2\theta_i + k_1^2\cos^2\theta_t} \tag{2.67}$$

is the amplitude of the wave propagation vector. From (2.67), we can solve for the general refraction angle $\theta_t$ as

$$\cos\theta_t = \sqrt{1-\frac{k_0^2}{k_1^2\sin^2\theta_i}}, \tag{2.68}$$

which is frequency dependent. With this notation, we can formulate Snell's law for lossy media as

$$k_1\sin\theta_t = k_0\sin\theta_i. \tag{2.69}$$

Notice that if the conductive $\sigma$ vanishes, $\theta_t = \hat{\theta}_t$ resulting in Snell's law for the lossless case.

### 2.4.2 Brewster's Angle Effect

When we study the wave propagation and reflection problem, we shall not forget one important feature: Brewster's angle effect. Brewster's angle is the angle of incidence for which there is no reflected field. For the TM case, we observe from (2.53) that Brewster's angle occurs only if the condition

$$\frac{\epsilon_r(1 - j\frac{\sigma}{\epsilon\omega})\cos\theta_i}{\sqrt{\mu_r\epsilon_r - \sin^2\theta_i - j\frac{\sigma}{\epsilon_0\omega}\mu_r}} = 1 \tag{2.70}$$

is satisfied. If only real angles of incidence are allowed, i.e., the incident wave is uniform, this condition can only be satisfied when $\sigma = 0$, which relies on medium II being lossless. We find that the Brewster angle for the lossless case is defined by

$$\sin\theta_B^{TM} = \sqrt{\frac{\epsilon_r(\epsilon_r - \mu_r)}{\epsilon_r^2 - 1}}. \tag{2.71}$$

Notice that Brewster's angle exists only when $\epsilon_r > \mu_r$. For the special case $\mu = \mu_0$, (2.71) simplifies to

$$\sin\theta_B^{TM} = \sqrt{\frac{\epsilon_r}{\epsilon_r + 1}}. \tag{2.72}$$

Since $\epsilon_r > 1$, Brewster's angle for special case $\mu = \mu_0$ is greater than 45°.

For the lossless case, the reflection coefficient in the frequency domain is

$$R_h = \frac{\epsilon_r\cos\theta_i - \sqrt{\mu_r\epsilon_r - \sin^2\theta_i}}{\epsilon_r\cos\theta_i + \sqrt{\mu_r\epsilon_r - \sin^2\theta_i}}. \tag{2.73}$$

We shall restrict our attention to the situation $\mu = \mu_0$, so (2.73) reduces to

$$R_h = \frac{\epsilon_r \cos\theta_i - \sqrt{\epsilon_r - \sin^2\theta_i}}{\epsilon_r \cos\theta_i + \sqrt{\epsilon_r - \sin^2\theta_i}}. \tag{2.74}$$

If the angle of incidence $\theta_i$ is greater then Brewster's angle $\theta_B^{TM}$, then $\sin\theta_i$ is greater than $\sin\theta_B^{TM}$. We now prove that the reflection coefficient (2.74) is negative when $\theta_i > \theta_B^{TM}$. If $R_h < 0$, then we have

$$\epsilon_r \cos\theta_i - \sqrt{\epsilon - \sin^2\theta_i} < 0, \tag{2.75}$$

which leads to

$$\epsilon_r^2 \cos^2\theta_i = \epsilon_r^2(1 - \sin^2\theta_i) < \epsilon_r - \sin^2\theta_i. \tag{2.76}$$

Solving for $\sin\theta_i$, we find that

$$\sin\theta_i > \sqrt{\frac{\epsilon_r}{\epsilon_r + 1}} = \sin\theta_B^{TM} \tag{2.77}$$

which is what we wanted to show.

As we have demonstrated, a Brewster angle is only defined in the lossless case. However, we can extend this concept to the lossy case by defining the angle which corresponds to a minimum in the reflection coefficient as the pseudo-Brewster's angle.

The reflection coefficient $R_h$ of (2.53) can be written in the frequency-domain as

$$R_h(\omega) = \frac{\epsilon_r - j\frac{\sigma}{\epsilon_0\omega} - \frac{1}{\cos\theta_i}\sqrt{\mu_r\epsilon_r - \sin^2\theta_i - j\frac{\sigma}{\epsilon_0\omega}\mu_r}}{\epsilon_r - j\frac{\sigma}{\epsilon_0\omega} + \frac{1}{\cos\theta_i}\sqrt{\mu_r\epsilon_r - \sin^2\theta_i - j\frac{\sigma}{\epsilon_0\omega}\mu_r}}. \tag{2.78}$$

Let $R_h(\omega) = 0$, which leads to the result

$$\cos\theta_B^{TM} = \sqrt{\frac{\mu_r\epsilon_r - j\frac{\sigma}{\epsilon_0\omega}\mu_r - 1}{\left(\epsilon_r - j\frac{\sigma}{\epsilon_0\omega}\right)^2 - 1}}. \tag{2.79}$$

For the special case $\mu_r = 1$, (2.79) simplifies to

$$\cos\theta_B^{TM} = \frac{1}{\sqrt{\epsilon_r - j\frac{\sigma}{\epsilon_0\omega} + 1}}. \tag{2.80}$$

Although (2.79) and (2.80) only have real solutions in the limiting cases $\omega \rightarrow \infty$ or $\sigma \rightarrow 0$, the reflected field is small when $\theta_i > \theta_B$ provided that the conduction current is small in comparison to the displacement current. Put another way, for the limiting cases $\omega \rightarrow \infty$ or $\sigma \rightarrow 0$, equations (2.79) and (2.80) are approximately satisfied for a given $\sigma$ if $\omega$ is large enough, i.e.,

$$\frac{\sigma}{\epsilon\omega} \ll 1. \tag{2.81}$$

Equation (2.81) shows that the pseudo-Brewster angle effect is stronger in high frequencies. Physically, the higher frequency components are absorbed more than the lower frequency components by the conductive half-space. This effect will be observed in the time-domain as well.

# CHAPTER 3

## Canonical Integrals

In the previous chapter, we obtained expressions for the transmitted and reflected fields in the s-domain. The desired transient field expressions can be now represented by an inverse Laplace transform of the previously derived s-domain results. The task of evaluating the inverse Laplace transform constitutes a difficult mathematical problem. Before deriving the transient field expressions, we want to provide an overview of the mathematical tools employed to solve this difficult problem. In this chapter, we are going to demonstrate a method which allows for the analytical evaluation of the inverse Laplace transforms which are encountered when studying the interaction between a transient plane wave and a conductive half-space. We have found that the transient fields for both the TE and TM cases can be represented as a linear combination of two canonical integrals, $f(\beta)$ and $e(\beta)$. These canonical integrals satisfy second-order, non-homogeneous, ordinary differential equations. The differential equations can be solved analytically, yielding closed-form expressions involving incomplete Lipschitz-Hankel integral (ILHI's).

As mentioned before, we shall show in the following two chapters that computation of the transient fields for both the TE and TM cases relies on the evaluation of the

following inverse Laplace transforms:

$$f(\beta) = -\frac{1}{2\pi j}\int_{\xi-j\infty}^{\xi+j\infty} \frac{e^{ut'-\frac{z}{v}\cos\hat{\theta}_t\sqrt{u^2+\omega_p^2}}}{\sqrt{u^2+\omega_p^2}(u+\beta)}\,du \tag{3.1}$$

and

$$e(\beta) = \frac{1}{2\pi j}\int_{\xi-j\infty}^{\xi+j\infty} \frac{e^{ut'-\frac{z}{v}\cos\hat{\theta}_t\sqrt{u^2+\omega_p^2}}}{u+\beta}\,du. \tag{3.2}$$

Therefore, we must find an efficient method for computing these canonical integrals. But obtaining the exact solutions are very difficult. Many authors have spent considerable effort to solve these integrals approximately [14, 21]. We say it is difficult because these integrals can not be found in a standard table of Laplace transform pairs [1].

Fast Fourier transform (FFT) techniques can be used to evaluate $f(\beta)$ and $e(\beta)$ numerically; however, a large number of points are required in the FFT in order to minimize aliasing and truncation error. Standard numerical integration is another option, but the computation efficiency is relative low and the slow convergence, for some cases, will affect the accuracy. Contour integration techniques can be applied to this problem [8, 34, 10]; however, the procedure of adopting this technique is tedious, complicated, and difficult to follow.

The integrals in (3.1) and (3.2) are difficult to evaluate analytically because they contain both pole and branch singularities. It was demonstrated in [10] that contour integration techniques can be used to obtain the desired closed-form solutions.

However, that technique was relatively complicated. Fortunately, Dvorak and Dudley recently developed a relatively simple method whereby closed-form solution are obtained for $f(\beta)$ and $e(\beta)$ by using a differential-equation-based method [12]. They derived the solutions in the frequency-domain (Fourier domain). We will now demonstrate that the same solutions are obtainable by using the Laplace transform.

We first map $f(\beta)$ and $e(\beta)$ from the $z-t$ plane to a $\psi-\zeta$ plane. Next we prove that $f(\beta)$ satisfies a second-order, non-homogeneous, ordinary differential equation. The variation of parameters method is then employed to solve the differential equation, thereby yielding an exact closed-form solution.

We start by establishing a relationship between $f(\beta)$ and $e(\beta)$ so that we only need to solve one differential equation. To achieve this goal, we employ the following change the variables:

$$t' = \frac{\zeta \cosh \psi}{\omega_p}, \tag{3.3}$$

$$\frac{z}{\hat{v}} \cos \hat{\theta}_t = \frac{\zeta \sinh \psi}{\omega_p}, \tag{3.4}$$

and

$$\zeta = \omega_p \sqrt{t'^2 - \frac{z^2}{v^2} \cos^2 \theta_t}. \tag{3.5}$$

Substituting (3.3) and (3.4) into (3.1) and (3.2), we have

$$f(\beta) = -\frac{1}{2\pi} \int_{\xi-j\infty}^{\xi+j\infty} \frac{e^{\zeta\left((u/\omega_p)\cosh\psi - \sinh\psi\sqrt{(u/\omega_p)^2+1}\right)}}{(u+\beta)\sqrt{u^2+\omega_p^2}} du \tag{3.6}$$

and

$$e(\beta) = \frac{1}{2\pi} \int_{\xi-j\infty}^{\xi+j\infty} \frac{e^{\zeta\left((u/\omega_p)\cosh\psi - \sinh\psi\sqrt{(u/\omega_p)^2+1}\right)}}{(u+\beta)} du \tag{3.7}$$

The Laplace transform pair [1, 29.3.92],

$$J_0\left(\omega_p\sqrt{t'^2-\frac{z^2}{\hat{v}^2}\cos^2\theta_t}\right)u\left(t'-\frac{z}{\hat{v}}\cos\hat{\theta}_t\right)=\frac{1}{2\pi j}\int_{c-j\infty}^{c+j\infty}\frac{e^{ut'-\frac{z}{\hat{v}}\cos\hat{\theta}_t\sqrt{u^2+\omega_p^2}}}{\sqrt{u^2+\omega_p^2}}du;\quad z\geq 0, \tag{3.8}$$

will be employed. Using (3.8), it is straight forward to show that

$$e(\beta)=\frac{1}{\sinh\psi}\left\{\omega_p\frac{\partial f(\beta)}{\partial\zeta}+\cosh\psi[\beta f(\beta)+u(\zeta e^{-\psi}/\omega_p)J_0(\zeta)]\right\}. \tag{3.9}$$

Thus, if we find $f(\beta)$, then $e(\beta)$ can be obtained from (3.9).

With the help of (3.8), it is easy to show that $f(\beta)$ satisfies the following second-order, non-homogeneous, ordinary differential equation:

$$\left(\frac{d^2}{d\zeta^2}+2\cosh\psi\left(\frac{\beta}{\omega_p}\right)\frac{d}{d\zeta}+\left(\frac{\beta}{\omega_p}\right)^2-\sinh^2\psi\right)f(\beta)$$

$$=-\frac{1}{\omega_p^2}\frac{1}{2\pi j}\int_{c-\infty}^{c+\infty}(u\cosh 2\psi-\sinh 2\psi\sqrt{u^2+\omega_p^2}+\beta)\frac{e^{ut'-\frac{z}{\hat{v}}\cos\hat{\theta}_t\sqrt{u^2+\omega_p^2}}}{\sqrt{u^2+\omega_p^2}}du$$

$$=-\frac{1}{\omega_p^2}\left(\cosh 2\psi\frac{\partial}{\partial t'}+\sinh 2\psi\frac{\partial}{\partial(\frac{z}{\hat{v}}\cos\hat{\theta}_t)}+\beta\right)J_0\left(\omega_p\sqrt{t'^2-\frac{z^2}{v^2}\cos^2\theta_t}\right)$$

$$\times u\left(t'-\frac{z}{\hat{v}}\cos\hat{\theta}_t\right)$$

$$=-\frac{1}{\omega_p^2}\left(e^{-2\psi}\delta(\zeta e^{-\psi}/\omega_p)+u(\zeta e^{-\psi}/\omega_p)[\beta J_0(\zeta)-\omega_p\cosh\psi J_1(\zeta)]\right). \tag{3.10}$$

The characteristic equation for (3.10) is

$$D^2+2\cosh\psi\left(\frac{\beta}{\omega_p}\right)D+\left(\frac{\beta}{\omega_p}\right)^2-\sinh^2\psi=0. \tag{3.11}$$

The roots of the above characteristic equation are given by

$$a_{\pm} = \frac{-\beta \cosh\psi \pm \sinh\psi\sqrt{\beta^2+\omega_p^2}}{\omega_p} = \frac{-\beta t \pm \frac{z}{\hat{v}}\cos\hat{\theta}_t\sqrt{\beta^2+\omega_p^2}}{\omega_p\sqrt{t^2-\frac{z^2}{\hat{v}^2}\cos^2\hat{\theta}_t}}. \tag{3.12}$$

The homogeneous solution for the differential equation in (3.10) has the general form

$$f^{(h)}(\beta) = C_+ e^{a_+\zeta} + C_- e^{a_-\zeta}, \tag{3.13}$$

where $C_{\pm}$ are the constants to be determined by the initial conditions.

Using the method of variation of parameters [22], the particular solution is

$$f^{(p)}(\zeta) = -f_1(\zeta)\int \frac{f_2(\tau)r(\tau)}{W(\tau)}d\tau + f_2(\zeta)\int \frac{f_1(\tau)r(\tau)}{W(\tau)}d\tau, \tag{3.14}$$

where $r(\tau)$ is the non-homogeneous term in the differential equation (3.10), and $W(\tau)$ is the Wronskian:

$$W(\zeta) = f_1(\zeta)f_2'(\zeta) - f_1'(\zeta)f_2(\zeta) = -\frac{2\sinh\sqrt{\beta^2+\omega_p^2}}{\omega}e^{-2\beta\frac{\cosh\psi}{\omega}\zeta}. \tag{3.15}$$

The other functions are defined by

$$\left.\begin{aligned} f_1(\zeta) &= e^{a_+\zeta} \\ f_2(\zeta) &= e^{a_-\zeta} \\ f_1'(\zeta) &= a_+ e^{a_+\zeta} \\ f_2'(\zeta) &= a_- e^{a_-\zeta} \end{aligned}\right\}. \tag{3.16}$$

After substituting (3.15) and (3.16) into (3.14), we obtain the following particular solution:

$$f^{(p)}(\beta) = \frac{e^{a_+\zeta}}{2\sinh\psi\sqrt{\beta^2+\omega_p^2}}\left\{-\beta\frac{e^{-2\psi}}{\omega_p} - u\left(\frac{\zeta e^{\psi}}{\omega_p}\right)\int_0^{\zeta}\left[\frac{\beta}{\omega_p}J_0(\tau) - \cosh\psi\, J_1(\tau)\right]\right.$$

$$\times \quad e^{-a_+\tau}\, d\tau\Big\} - \frac{e^{a-\zeta}}{2\sinh\psi\sqrt{\beta^2+\omega_p^2}}\left\{-\beta\frac{e^{-2\psi}}{\omega_p} - u\left(\frac{\zeta e^{\psi}}{\omega_p}\right)\right.$$

$$\times \quad \left.\int_0^{\zeta}\left[\frac{\beta}{\omega_p}J_0(\tau) - \cosh\psi\, J_1(\tau)\right] e^{-a-\tau}\, d\tau\right\}. \tag{3.17}$$

The first term in each curly bracket is constant with respect to $\xi$, so they can be included in the constant terms ($C_{\pm}$) in the homogeneous solution. Thus, the general solution is given by:

$$f(\beta) = -\frac{u(\zeta e^{-\psi}/\omega_p)}{2\sinh\psi\sqrt{\beta^2+\omega_p^2}}\left\{e^{a+\zeta}\left[C_+ + \int_0^{\zeta}[(\beta/\omega_p)J_0(\tau) - \cosh\psi\, J_1(\tau)]e^{-a+\tau}d\tau\right]\right.$$

$$\left. - \; e^{a-\zeta}\left[C_- + \int_0^{\zeta}[(\beta/\omega_p)J_0(\tau) - \cosh\psi\, J_1(\tau)]e^{-a-\tau}d\tau\right]\right\}. \tag{3.18}$$

Employing integration by parts for the second terms in each square bracket, we obtain

$$f(\beta) = -\frac{u(\zeta e^{-\psi}/\omega_p)}{2\sinh\psi\sqrt{\beta^2+\omega_p^2}}\left\{e^{a+\zeta}\left[C_+ + (a_+\cosh\psi + \beta/\omega_p)Je_0(a_+,\zeta)\right]\right.$$

$$\left. - \; e^{a-\zeta}\left[C_- + (a_-\cosh\psi + \beta/\omega_p)Je_0(a_-,\zeta)\right]\right\}, \tag{3.19}$$

where the incomplete Lipschitz-Hankel integral (ILHI) of the first kind is defined as [9]

$$Je_n(a,\zeta) = \int_0^{\zeta} e^{-a\tau}\tau^n J_n(\tau)d\tau. \tag{3.20}$$

The undetermined constants, $C_{\pm}$, depend on the initial conditions of $f(\beta)$ and $\frac{\partial f(\beta)}{\partial \zeta}$ as $\zeta \to 0$. From the definition in (3.6), $f(\beta)$ may be rewritten as

$$f(\beta) = -\frac{1}{2\pi j}\int_0^{\infty}\int_{c-j\infty}^{c+j\infty} e^{-\lambda(u+\beta)}\frac{\exp\left[\zeta\left(\frac{u}{\omega_p}\cosh\psi - \sinh\psi\sqrt{\frac{u^2}{\omega_p^2}+1}\right)\right]}{\sqrt{u^2+\omega_p^2}}dud\lambda. \quad (3.21)$$

Using the first initial condition $\zeta \to 0$, we find that

$$\lim_{\zeta\to 0} f(\beta) = \int_0^{\infty} e^{-\beta\lambda}d\lambda \left[-\frac{1}{2\pi j}\int_{c-j\infty}^{c+j\infty}\frac{e^{(-\lambda)u}}{\sqrt{u^2+\omega_p^2}}du\right]. \quad (3.22)$$

When comparing the term in the square brackets in (3.22) with (3.8), we find that

$$\lim_{\zeta\to 0} f(\beta) = -\int_0^{\infty} e^{-\beta\lambda}u(-t')J_0(\omega_p\lambda)d\lambda = 0. \quad (3.23)$$

Thus, after letting $\zeta \to 0$ in (3.19) and setting the result equal to 0, we find that

$$C_+ = C_-. \quad (3.24)$$

Next we use the initial condition on the derivative of the function. If we perform the derivative of (3.21) first and then let $\zeta \to 0$, we have

$$\lim_{\zeta\to 0}\frac{\partial f(\beta)}{\partial\zeta} = -\frac{1}{2\pi j}\int_0^{\infty}\int_{c-j\infty}^{c+j\infty}\left(\frac{u}{\omega_p}\cosh\psi - \sinh\psi\sqrt{\frac{u^2}{\omega_p^2}+1}\right)\frac{e^{-\lambda(u+\beta)}}{\sqrt{u^2+\omega_p^2}}dudt'$$

$$= -\frac{1}{2\pi j}\frac{1}{\omega_p}\int_0^{\infty} e^{-\lambda\beta}d\lambda\left[\int_{c-j\infty}^{c+j\infty}\frac{e^{(-\lambda)u}u\cosh\psi}{\sqrt{u^2+\omega_p^2}}du - \int_{c-j\infty}^{c+j\infty}e^{(-\lambda)u}\sinh\psi du\right]$$

$$= \int_0^{\infty}\frac{e^{-\lambda\beta}}{\omega_p}\left[\sinh\psi\,\delta(\lambda) + \cosh\psi\frac{\partial}{\partial\lambda}\frac{1}{2\pi j}\int_{c-j\infty}^{c+j\infty}\frac{e^{-u\lambda}}{\sqrt{u^2+\omega_p^2}}du\right]d\lambda$$

$$= \int_0^{\infty}\frac{e^{-\lambda\alpha}}{\omega_p}\left[\sinh\psi\,\delta(\lambda) + \cosh\psi\frac{\partial}{\partial\lambda}u(-\lambda)J_0(\omega_p t')\right]d\lambda. \quad (3.25)$$

Applying integration by parts to the second term in the square bracket in (3.25), we obtain

$$\lim_{\zeta \to 0} \frac{\partial f(\beta)}{\partial \zeta} = -\frac{e^{-\psi}}{\omega_p}. \tag{3.26}$$

Since this must be equal to the derivative of (3.19), i.e.,

$$\lim_{\zeta \to 0} \frac{\partial f(\beta)}{\partial \zeta} = -\frac{u(0)}{2 \sinh \psi \omega_p \sqrt{\beta^2 + \omega_p^2}} [(a_+ - a_-)c_+ + (a_+ - a_-) \cos \psi], \tag{3.27}$$

we find that

$$C_+ = C_- = -\sinh \psi. \tag{3.28}$$

When taken together with the results in (3.19) and (3.28), we obtain the solution for the differential equation in (3.10):

$$f(\beta) = -\frac{u\left(\frac{\zeta e^{\psi}}{\omega_p}\right)}{2 \sinh \psi \sqrt{\beta^2 + \omega_p^2}} \left\{ e^{a_+ \zeta} \left[ -\sinh \psi + \left( \frac{\beta}{\omega_p} + a_+ \cosh \psi \right) Je_0(a_+, \zeta) \right] \right.$$

$$\left. - \; e^{a_- \zeta} \left[ -\sinh \psi + \left( \frac{\beta}{\omega_p} + a_- \cosh \psi \right) Je_0(a_-, \zeta) \right] \right\}$$

$$= \frac{u(t' - \frac{z}{\hat{v}} \cos \hat{\theta}_t)}{\sqrt{\beta^2 + \omega_p^2}} \left\{ e^{-\beta t'} \sinh \left( \frac{z}{\hat{v}} \cos \hat{\theta}_t \sqrt{\beta^2 + \omega_p^2} \right) + \frac{1}{2\omega_p \sqrt{t'^2 - \frac{z^2}{\hat{v}^2} \cos^2 \hat{\theta}_t}} \left[ \left( \frac{\beta z}{\hat{v}} \cos \hat{\theta}_t \right. \right. \right.$$

$$\left. \left. \left. - \; t' \sqrt{\beta^2 + \omega_p^2} \right) e^{a_+ \zeta} Je_0(a_+, \zeta) - \left( \frac{\beta z}{\hat{v}} \cos \hat{\theta}_t + t' \sqrt{\alpha^2 + \omega_p^2} \right) e^{a_- \zeta} Je_0(a_-, \zeta) \right] \right\}. \tag{3.29}$$

In order to obtain an expression for $e(\beta)$, we substitute (3.29) into (3.9):

$$e(\beta) = u\left(t' - \frac{z}{\hat{v}} \cos \hat{\theta}_t\right) \left\{ e^{-\beta t'} \cosh \left( \frac{z}{\hat{v}} \cos \hat{\theta}_t \sqrt{\beta^2 + \omega_p^2} \right) \right.$$

$$+ \quad \frac{1}{2\omega_p\sqrt{t'^2 - \frac{z^2}{\hat{v}^2}\cos^2\hat{\theta}_t}}\left[\left(\frac{\beta z}{\hat{v}}\cos\hat{\theta}_t - t'\sqrt{\beta^2+\omega_p^2}\right)e^{a_+\zeta}Je_0(a_+,\zeta)\right.$$

$$\left. + \quad \left(\frac{\beta z}{\hat{v}}\cos\hat{\theta}_t + t'\sqrt{\beta^2+\omega_p^2}\right)e^{a_-\zeta}Je_0(a_-,\zeta)\right]\Bigg\}. \tag{3.30}$$

The canonical integrals $e(\beta)$ and $f(\beta)$ will be used in a closed-form solution for the transient fields in the following chapters.

# CHAPTER 4

## Derivation of the Transient Fields (TE Case)

Having obtained expressions for the transmitted and reflected fields in the Laplace domain in Chapter 2, we can now derive the transient field response by applying an inverse Laplace transform. We make use of the mathematical tools we developed in Chapter 3. In this chapter, we will only consider the TE case and leave the TM case for the next chapter.

In this chapter, we first derive integral representations for the transient transmitted field by inverse Laplace transforming the previously derived results. We next show that the transient transmitted field can be expressed in terms of two canonical integrals, $f(\beta)$ and $e(\beta)$, which were represented in closed-form in the last chapter. We claim that this expression is an exact, closed-form solution since only elementary functions and readily computable special functions are present, and no approximations are employed. We then use the convolution theorem to determine a closed-form solution for the reflected field. Finally, we use the closed-form solutions to study this important canonical problem.

## 4.1 Transient Transmitted Field

Based on the results obtained in Chapter 2, the field $\tilde{E}_y^{(t)}(x,z,s)$ depends on the source spectrum $\tilde{E}_0(s)$. We employ two types of sources in this dissertation: a unit-step and a double-exponential pulse. These two sources are handled separately.

### 4.1.1 Transient Transmitted Field Associated with a Unit-Step Function Source

For the unit-step function input, i.e.

$$E_0(t) = u(t) = \begin{cases} 1, & t \geq 0 \\ \\ 0, & t < 0, \end{cases} \tag{4.1}$$

the amplitude spectrum is

$$\tilde{E}_0(s) = \frac{1}{s}. \tag{4.2}$$

The transmitted field for the TE case is given by (2.18) together with the transmission coefficient $T_e$ in (2.33). As stated in Chapter 2, the transient field response can be obtained by invoking the inverse Laplace transform (2.3),

$$E_y^{(t)}(x,z,t) = \frac{1}{2\pi j}\int_{\xi-j\infty}^{\xi+j\infty} \frac{2}{s + b_e\sqrt{s^2+2as}} e^{st - \frac{x}{v}s\sin\hat{\theta}_t - \frac{z}{v}\cos\hat{\theta}_t\sqrt{s^2+2as}}\, ds. \tag{4.3}$$

After multiplying the denominator as well as the numerator of (4.3) by $b_e\sqrt{s^2+2as}$ $-s$, which corresponds to the numerator of the reflection coefficient $R_e$, we obtain

$$E_y^{(t)}(x,z,t) = \frac{1}{2\pi j}\int_{\xi-j\infty}^{\xi+j\infty} \frac{2b_e s e^{s(t-\frac{x}{v}\sin\hat{\theta}_t) - \frac{z}{v}\cos\hat{\theta}_t\sqrt{s^2+2as}}}{(b_e^2-1)\sqrt{s^2+2as}\left(s + \frac{2ab_e^2}{b_e^2-1}\right)} ds$$

$$+ \frac{1}{2\pi j}\int_{\xi-j\infty}^{\xi+j\infty} \frac{4ab_e e^{s(t-\frac{x}{v}\sin\hat{\theta}_t)-\frac{z}{v}\cos\hat{\theta}_t\sqrt{s^2+2as}}}{(b_e^2-1)\sqrt{s^2+2as}\left(s+\frac{2ab_e^2}{b_e^2-1}\right)}\,ds$$

$$- \frac{1}{2\pi j}\int_{\xi-j\infty}^{\xi+j\infty} \frac{2e^{s(t-\frac{x}{v}\sin\hat{\theta}_t)-\frac{z}{v}\cos\hat{\theta}_t\sqrt{s^2+2as}}}{(b_e^2-1)\left(s+\frac{2ab^2}{b_e^2-1}\right)}\,ds$$

$$= \frac{1}{2\pi j}\int_{\xi-j\infty}^{\xi+j\infty} \frac{2b_e(s+a)e^{s(t-\frac{x}{v}\sin\hat{\theta}_t)-\frac{z}{v}\cos\hat{\theta}_t\sqrt{(s+a)^2-a^2}}}{(b_e^2-1)\sqrt{(s+a)^2-a^2}\left[(s+a)+\left(\frac{2ab_e^2}{b_e^2-1}-a\right)\right]}\,ds$$

$$+ \frac{1}{2\pi j}\int_{\xi-j\infty}^{\xi+j\infty} \frac{2ab_e e^{s(t-\frac{x}{v}\sin\hat{\theta}_t)-\frac{z}{v}\cos\hat{\theta}_t\sqrt{(s+a)^2-a^2}}}{(b_e^2-1)\sqrt{(s+a)^2-a^2}\left[(s+a)+\left(\frac{2ab_e^2}{b_e^2-1}-a\right)\right]}\,ds$$

$$- \frac{1}{2\pi j}\int_{\xi-j\infty}^{\xi+j\infty} \frac{2e^{s(t-\frac{x}{v}\sin\hat{\theta}_t)-\frac{z}{v}\cos\hat{\theta}_t\sqrt{(s+a)^2-a^2}}}{(b_e^2-1)\left[(s+a)+\left(\frac{2ab_e^2}{b_e^2-1}-a\right)\right]}\,ds. \tag{4.4}$$

After making the change of variables,

$$\left.\begin{aligned} u &= s+a \\ \beta_0 &= \tfrac{2ab_e^2}{b_e^2-1}-a \\ t' &= t-\tfrac{x}{v}\sin\hat{\theta}_t \\ \omega_p &= ja \end{aligned}\right\}, \tag{4.5}$$

we find that the transient electric field associated with the unit-step input has the following integral representation:

$$E_y^{(t)}(x,z,t) = \frac{2e^{-at'}}{b_e^2-1}\left[\frac{1}{2\pi j}\int_{\xi-j\infty}^{\xi+j\infty} \frac{b_e e^{ut'-\frac{z}{v}\cos\hat{\theta}_t\sqrt{u^2+\omega_p^2}}}{\sqrt{u^2+\omega_p^2}}\,du\right.$$

$$+ \quad \frac{1}{2\pi j}\int_{\xi-j\infty}^{\xi+j\infty} \frac{b_e(a-\beta_0)e^{ut'-\frac{z}{\hat{v}}\cos\hat{\theta}_t\sqrt{u^2+\omega_p^2}}}{\sqrt{u^2+\omega_p^2}(u+\beta_0)}\,du$$

$$- \quad \frac{1}{2\pi j}\int_{\xi-j\infty}^{\xi+j\infty} \frac{e^{ut'-\frac{z}{\hat{v}}\cos\hat{\theta}_t\sqrt{u^2+\omega_p^2}}}{u+\beta_0}\,du\Bigg]. \tag{4.6}$$

The first term in (4.6) can be handled using the Laplace transform pair in (3.8). The second and third terms in (4.6) have the general form of the canonical integrals $f(\beta_0)$ and $e(\beta_0)$. Thus, the transient field can be expressed in closed-form as

$$\begin{aligned} E_y^{(t)}(x,z,t) &= \frac{2e^{-at'}}{b_e^2-1}\left[b_e J_0\left(\omega_p\sqrt{t'^2-\frac{z^2}{\hat{v}^2}\cos^2\hat{\theta}_t}\right)u\left(t'-\frac{z}{\hat{v}}\cos\hat{\theta}_t\right)\right. \\ &+ \left. b_e(\beta_0-a)f(\beta_0)-e(\beta_0)\right]. \end{aligned} \tag{4.7}$$

Similar techniques can be used to find the transient magnetic fields. Using (2.30) and (2.33), the $x$-component of the time domain transmitted magnetic field is

$$\tilde{H}_x^{(t)}(x,z,s) = -\frac{2\cos\hat{\theta}_t}{\mu\hat{v}}\frac{\sqrt{s^2+2as}e^{-\frac{x}{\hat{v}}\sin\hat{\theta}_t-\frac{z}{\hat{v}}\cos\hat{\theta}_t\sqrt{s^2+2as}}}{s(s+b_e\sqrt{s^2+2as})}. \tag{4.8}$$

Multiplying the denominator as well as the numerator of (4.8) by $b_e\sqrt{s^2+2as}-s$ yields

$$\tilde{H}_x^{(t)}(x,z,s) = -\frac{2\cos\hat{\theta}_t}{\mu\hat{v}(b_e^2-1)}\frac{b_e(s+2a)-\sqrt{s^2+2as}}{s\left(s+\frac{2ab_e^2}{b_e^2-1}\right)}e^{-\frac{x}{\hat{v}}\sin\hat{\theta}_t-\frac{z}{\hat{v}}\cos\hat{\theta}_t\sqrt{s^2+2as}}$$

$$= -\frac{2\cos\hat{\theta}_t}{\mu\hat{v}(b_e^2-1)}\frac{b_e(s+2a)-\sqrt{s^2+2as}}{s(s+\alpha_0)}e^{-\frac{x}{\hat{v}}\sin\hat{\theta}_t-\frac{z}{\hat{v}}\cos\hat{\theta}_t\sqrt{s^2+2as}}, \tag{4.9}$$

where

$$\alpha_0 = \frac{2ab_e^2}{b_e^2-1}. \tag{4.10}$$

After employing the partial fraction expansion method [33], we rewrite (4.9) as

$$\tilde{H}_x^{(t)}(x,z,s) = \frac{2\cos\hat{\theta}_t}{\mu\hat{v}\alpha_0(b_e^2-1)}\left[\frac{b_e(s+2a)-\sqrt{s^2+2as}}{(s+\alpha_0)}\right.$$

$$\left. - \frac{b_e(s+2a)-\sqrt{s^2+2as}}{s}\right] e^{-\frac{x}{\hat{v}}\sin\hat{\theta}_t - \frac{z}{\hat{v}}\cos\hat{\theta}_t\sqrt{s^2+2as}}. \tag{4.11}$$

Application of the inverse Laplace transform results in the following expressions for the transient magnetic field:

$$\begin{aligned} H_x^{(t)}(x,z,t) &= \frac{2\cos\hat{\theta}_t}{\mu\hat{v}\alpha_0(b_e^2-1)}\left[\frac{1}{2\pi j}\int_{\xi-j\infty}^{\xi+j\infty}\frac{b_e(2a-\alpha_0)}{s+\alpha_0}e^{st-(\frac{x}{\hat{v}}\sin\hat{\theta}_t+\frac{z}{\hat{v}}\cos\hat{\theta}_t\sqrt{s^2+2as})}\,ds\right. \\ &+ \frac{1}{2\pi j}\int_{\xi-j\infty}^{\xi+j\infty}\frac{\alpha_0}{\sqrt{s^2+2as}}e^{st-(\frac{x}{\hat{v}}\sin\hat{\theta}_t+\frac{z}{\hat{v}}\cos\hat{\theta}_t\sqrt{s^2+2as})}\,ds \\ &- \frac{1}{2\pi j}\int_{\xi-j\infty}^{\xi+j\infty}\frac{\alpha_0(2a-\alpha_0)}{\sqrt{s^2+2as}(s+\alpha_0)}e^{st-(\frac{x}{\hat{v}}\sin\hat{\theta}_t+\frac{z}{\hat{v}}\cos\hat{\theta}_t\sqrt{s^2+2as})}\,ds \\ &\left.- \frac{1}{2\pi j}\int_{\xi-j\infty}^{\xi+j\infty}\frac{2ab_e}{s}e^{st-(\frac{x}{\hat{v}}\sin\hat{\theta}_t+\frac{z}{\hat{v}}\cos\hat{\theta}_t\sqrt{s^2+2as})}\,ds\right]. \end{aligned} \tag{4.12}$$

Application of the change of variables defined in (4.5) puts the integrand in the general canonical form:

$$\begin{aligned} H_x^{(t)}(x,z,t) &= \frac{2\cos\hat{\theta}_t e^{-at'}}{\mu\hat{v}\alpha_0(b_e^2-1)}\left[\frac{1}{2\pi j}\int_{\xi-j\infty}^{\xi+j\infty}\frac{b_e(a-\beta_0)}{u+\beta_0}e^{ut'-\frac{z}{\hat{v}}\cos\hat{\theta}_t\sqrt{u^2+\omega_p^2}}\,du\right. \\ &\left.+ \frac{1}{2\pi j}\int_{\xi-j\infty}^{\xi+j\infty}\frac{\alpha_0}{\sqrt{u^2+\omega_p^2}}e^{ut'-\frac{z}{\hat{v}}\cos\hat{\theta}_t\sqrt{u^2+\omega^2}}\,du\right. \end{aligned}$$

$$- \frac{1}{2\pi j}\int_{\xi-j\infty}^{\xi+j\infty} \frac{\alpha_0(a-\beta_0)}{\sqrt{u^2+\omega_p^2}(u+\beta_0)} e^{ut'-\frac{z}{\hat{v}}\cos\hat{\theta}_t\sqrt{u^2+\omega_p^2})}\, du$$

$$- \frac{1}{2\pi j}\int_{\xi-j\infty}^{\xi+j\infty} \frac{2ab_e}{u-a} e^{ut'-\frac{z}{\hat{v}}\cos\hat{\theta}_t\sqrt{u^2+\omega^2}}\, du\Bigg]. \tag{4.13}$$

Thus, reference to (3.1) and (3.2) allows us to rewrite the transient magnetic field in closed-form as:

$$H_x^{(t)}(x,z,t) = \frac{2\cos\hat{\theta}_t e^{-at'}}{(b_e^2-1)\alpha_0\mu\hat{v}}\Bigg[b_e(a-\beta_0)e(\beta_0) + \alpha_0 J_0\left(\omega_p\sqrt{t'^2-\frac{z^2}{\hat{v}^2}\cos^2\hat{\theta}_t}\right)$$

$$\times u\left(t'-\frac{z}{\hat{v}}\cos\hat{\theta}_t\right) + \alpha_0(a-\beta_0)f(\beta_0) - 2ab_e e(-a)\Bigg]. \tag{4.14}$$

Since $\tilde{H}_z$ is directly proportional to $\tilde{E}_y$ (see (2.18) and (2.31)), i.e.,

$$\tilde{H}_z^{(t)}(x,z,s) = \frac{\sin\theta_i}{\mu c}\tilde{E}_y^{(t)}(x,z,s), \tag{4.15}$$

the $z$-component of transient magnetic field can be represented as

$$H_z^{(t)}(x,z,t) = \frac{\sin\theta_i}{\mu c}E_y^{(t)}(x,z,t). \tag{4.16}$$

### 4.1.2 Transient Transmitted Field Associated with a Double-Exponential Source Excitation

In the last subsection, we solved for the transient transmitted fields associated with unit-step excitation. In this subsection, we investigate a normalized double-exponential pulse excitation, i.e.,

$$E_0(t) = A(e^{-\alpha_1 t} - e^{-\alpha_2 t})u(t), \tag{4.17}$$

where $A$ is a normalization factor chosen such that the peak amplitude of the pulse is unity for all $t > 0$ and $\alpha_1, \alpha_2 > 0$. Since $E_0(t)$ has only one local maximum at $t = t_m$, we can find $A$ and $t_m$ by applying simple rules of calculus. In order to find the maximum, we set the derivative of $E_0(t) = 0$ at $t = t_m$, viz.:

$$\left.\frac{dE_0}{dt}\right|_{t=t_m} = A(-\alpha_1 e^{-\alpha_1 t_m} + \alpha_2 e^{-\alpha_2 t_m}) = 0. \tag{4.18}$$

If $A \neq 0$ then

$$\frac{\alpha_2}{\alpha_1} e^{-\alpha_2 t_m} = e^{-\alpha_1 t_m} \tag{4.19}$$

or

$$\ln \frac{\alpha_2}{\alpha_1} - \alpha_2 t_m = -\alpha_1 t_m, \tag{4.20}$$

which can be solved for $t_m$ to give

$$t_m = \frac{1}{\alpha_2 - \alpha_1} \ln \frac{\alpha_2}{\alpha_1}. \tag{4.21}$$

We now find $A$ by setting the maximum value of $E_0(t)$ to one, i.e.,

$$E_0(t_m) = A(e^{-\alpha_1 t_m} - e^{-\alpha_2 t_m}) = 1, \tag{4.22}$$

and solve for $A$ to obtain

$$A = \frac{1}{e^{-\alpha_1 t_m} - e^{-\alpha_2 t_m}}. \tag{4.23}$$

After we perform the Laplace transform of $E_0(t)$, we find that the spectral representation for the double-exponential pulse is

$$\tilde{E}_0(s) = A\left(\frac{1}{s+\alpha_1} - \frac{1}{s+\alpha_2}\right). \tag{4.24}$$

Figures 4.1 and 4.2 are plots of the normalized double-exponential pulse function and its spectral response, respectively.

Some advantages of choosing a double-exponential pulse excitation as the input signal include:

(1) The waveform can be used to model finite rise time and fall time requirements. The rise time and fall time are determined by $\alpha_1$ and $\alpha_2$ since we often need to change the width of the pulse.

(2) As we will show, this source allows closed-form expressions to be derived for the transient fields. The closed-form solution provides physical insight which is difficult to obtain from purely numerical solutions.

Reference to (2.18), (2.22), (2.23), and (2.33) show that the transient transmitted electric field associated with a double-exponential pulse is given by the following inverse Laplace transform:

$$E_y^{(t)}(x,z,t) = \frac{1}{2\pi j}\int_{\xi-j\infty}^{\xi+j\infty} \frac{2sA}{(s+\alpha_1)(s+b_e\sqrt{s^2+2as})} e^{st-\frac{x}{v}s\sin\hat{\theta}_t-\frac{z}{v}\cos\hat{\theta}_t\sqrt{s^2+2as}}\,ds$$

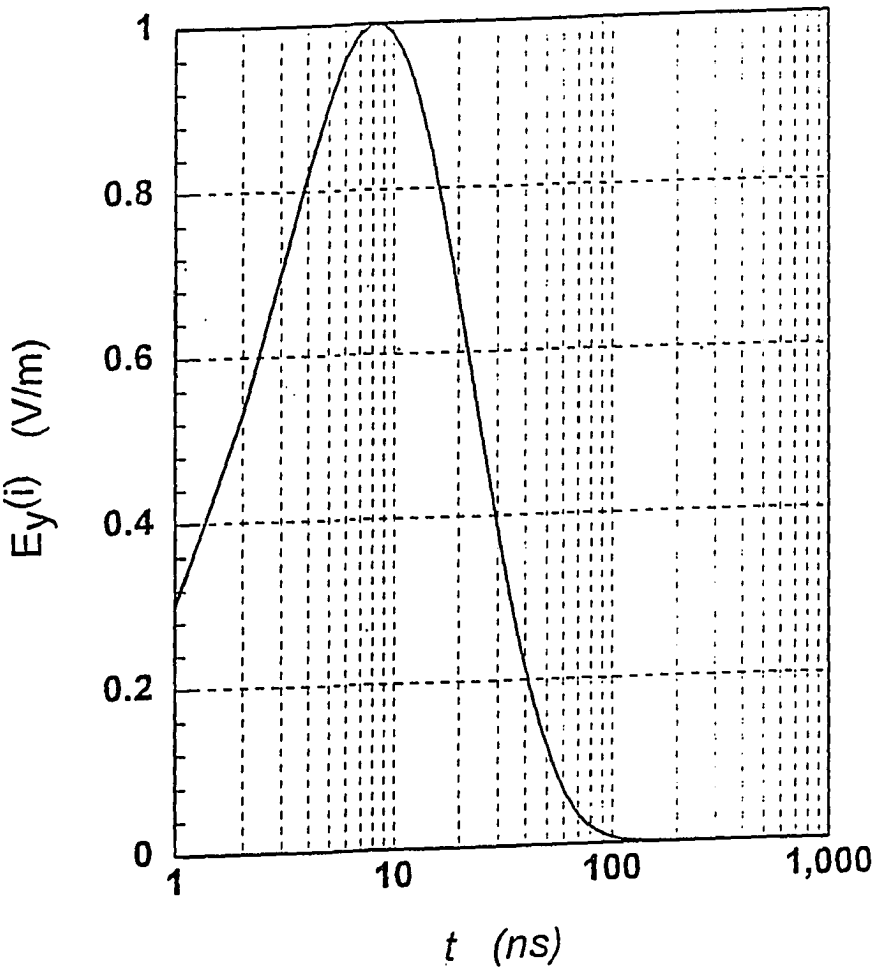


Figure 4.1: A graph of the double-exponential input pulse waveform. The parameters are defined as $\alpha_1 = 5.9 \times 10^7 sec^{-1}$ and $\alpha_2 = 2.1 \times 10^8 sec^{-1}$.

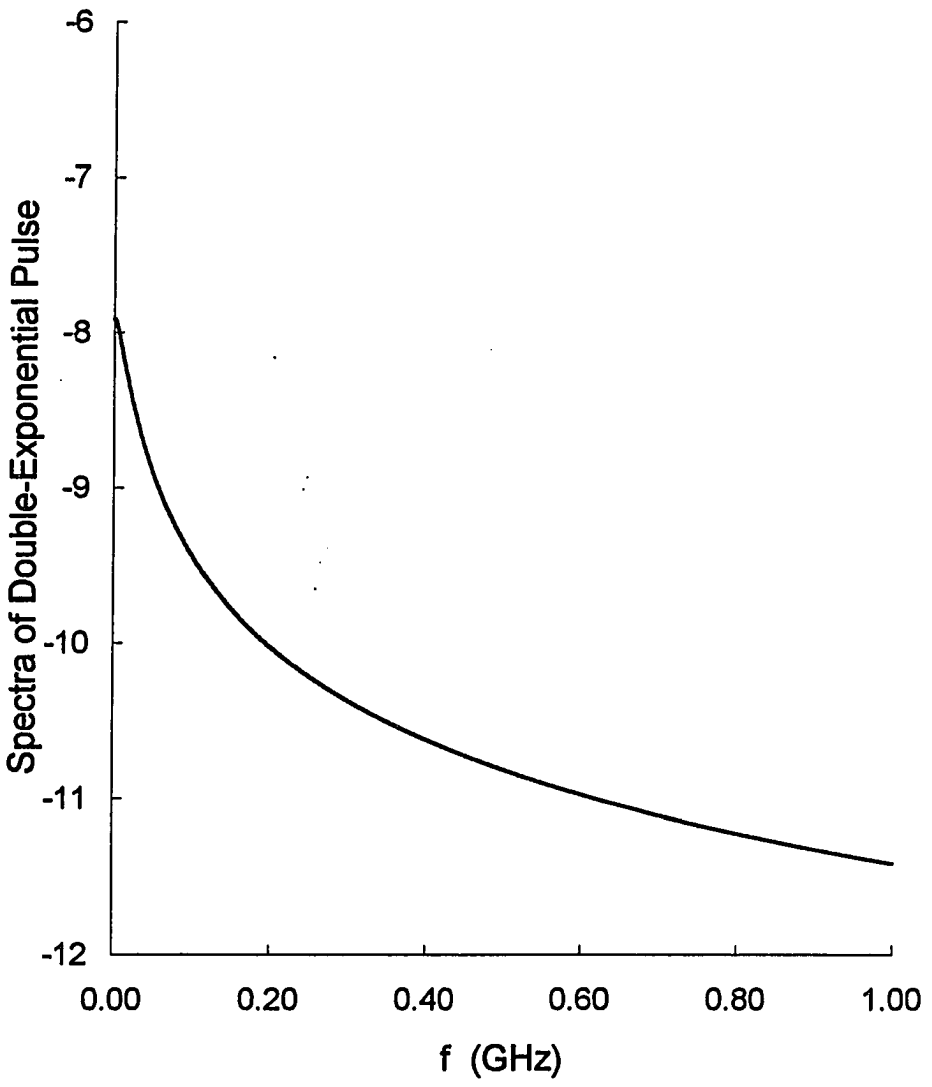


Figure 4.2: A graph of the spectral function of the double-exponential pulse waveform with the parameters $\alpha_1 = 5.9 \times 10^7 sec^{-1}$ and $\alpha_2 = 2.1 \times 10^8 sec^{-1}$.

$$- \frac{1}{2\pi j}\int_{\xi-j\infty}^{\xi+j\infty} \frac{2sA}{(s+\alpha_2)(s+b_e\sqrt{s^2+2as})} e^{st-\frac{x}{v}s\sin\hat{\theta}_t-\frac{z}{v}\cos\hat{\theta}_t\sqrt{s^2+2as}}\, ds. \qquad (4.25)$$

Next we rewrite this integral in terms of the canonical integrals in (3.1) and (3.2). As before, we multiply the denominator and the numerator of (4.25) by $b_e\sqrt{s^2+2as}-s$:

$$E_y^{(t)}(x,z,t) = \frac{2A}{b_e^2-1}\left[\frac{1}{2\pi j}\int_{\xi-j\infty}^{\xi+j\infty} \frac{b_e\sqrt{s^2+2as}-s}{(s+\alpha_1)(s+\alpha_0)} e^{st-\frac{x}{v}s\sin\hat{\theta}_t-\frac{z}{v}\cos\hat{\theta}_t\sqrt{s^2+2as}}\, ds\right.$$

$$\left. - \frac{1}{2\pi j}\int_{\xi-j\infty}^{\xi+j\infty} \frac{b_e\sqrt{s^2+2as}-s}{(s+\alpha_2)(s+\alpha_2)} e^{st-\frac{x}{v}s\sin\hat{\theta}_t-\frac{z}{v}\cos\hat{\theta}_t\sqrt{s^2+2as}}\, ds\right]$$

$$= \frac{2A}{b_e^2-1}\left[\frac{1}{2\pi j}\int_{\xi-j\infty}^{\xi+j\infty} \frac{s(b_es+2ab_e-\sqrt{s^2+2as})}{(s+\alpha_1)(s+\alpha_0)\sqrt{s^2+2as}} e^{st-\frac{x}{v}s\sin\hat{\theta}_t-\frac{z}{v}\cos\hat{\theta}_t\sqrt{s^2+2as}}\, ds\right.$$

$$\left. - \frac{1}{2\pi j}\int_{\xi-j\infty}^{\xi+j\infty} \frac{s(b_es+2ab_e-\sqrt{s^2+2as})}{(s+\alpha_2)(s+\alpha_2)\sqrt{s^2+2as}} e^{st-\frac{x}{v}s\sin\hat{\theta}_t-\frac{z}{v}\cos\hat{\theta}_t\sqrt{s^2+2as}}\, ds\right]. \qquad (4.26)$$

Employing the partial fraction expansion again [33], we have

$$E_y^{(t)}(x,z,t) = \frac{2A}{b_e^2-1}\left[\frac{\alpha_0(\alpha_1-\alpha_2)}{(\alpha_0-\alpha_1)(\alpha_0-\alpha_2)}\frac{1}{2\pi j}\int_{\xi-j\infty}^{\xi+j\infty} \frac{b_es+2ab_e-\sqrt{s^2+2as}}{\sqrt{s^2+2as}(s+\alpha_0)}\right.$$

$$\times\ e^{st-\frac{x}{v}s\sin\hat{\theta}_t-\frac{z}{v}\cos\hat{\theta}_t\sqrt{s^2+2as}}\, ds$$

$$\left. + \frac{\alpha_1}{\alpha_1-\alpha_0}\frac{1}{2\pi j}\int_{\xi-j\infty}^{\xi+j\infty} \frac{b_es+2ab_e-\sqrt{s^2+2as}}{\sqrt{s^2+2as}(s+\alpha_1)} e^{st-\frac{x}{v}s\sin\hat{\theta}_t-\frac{z}{v}\cos\hat{\theta}_t\sqrt{s^2+2as}}\, ds\right.$$

$$- \quad \frac{\alpha_2}{\alpha_2-\alpha_0}\frac{1}{2\pi j}\int_{\xi-j\infty}^{\xi+j\infty}\frac{b_e s+2ab_e-\sqrt{s^2+2as}}{\sqrt{s^2+2as}(s+\alpha_2)}e^{st-\frac{x}{v}s\sin\hat{\theta}_t-\frac{z}{v}\cos\hat{\theta}_t\sqrt{s^2+2as}}\,ds$$

$$= \quad \frac{2Ae^{-a(t-\frac{x}{v}a\sin\hat{\theta}_t)}}{b_e^2-1}\left\{\frac{\alpha_0(\alpha_1-\alpha_2)}{(\alpha_0-\alpha_1)(\alpha_0-\alpha_2)}\right.$$

$$\times \quad \frac{1}{2\pi j}\int_{\xi-j\infty}^{\xi+j\infty}\frac{b_e(s+a)+ab_e-\sqrt{(s+a)^2-a^2}}{\sqrt{(s+a)^2-a^2}[(s+a)+\alpha_0-a)]}$$

$$\times \quad e^{(s+a)t-\frac{x}{v}(s+a)\sin\hat{\theta}_t-\frac{z}{v}\cos\hat{\theta}_t\sqrt{(s+a)^2-a^2}}\,ds$$

$$+ \quad \frac{\alpha_1}{\alpha_1-\alpha_0}\frac{1}{2\pi j}\int_{\xi-j\infty}^{\xi+j\infty}\frac{b_e(s+a)+ab_e-\sqrt{(s+a)^2-a^2}}{\sqrt{(s+a)^2-a^2}[(s+a)+\alpha_1-a)]}$$

$$\times \quad e^{(s+a)t-\frac{x}{v}(s+a)\sin\hat{\theta}_t-\frac{z}{v}\cos\hat{\theta}_t\sqrt{(s+a)^2-a^2}}\,ds$$

$$- \quad \frac{\alpha_2}{\alpha_2-\alpha_0}\frac{1}{2\pi j}\int_{\xi-j\infty}^{\xi+j\infty}\frac{b_e(s+a)+ab_e-\sqrt{(s+a)^2-a^2}}{\sqrt{(s+a)^2-a^2}[(s+a)+\alpha_1-a)]}$$

$$\times \quad e^{(s+a)t-\frac{x}{v}(s+a)\sin\hat{\theta}_t-\frac{z}{v}\cos\hat{\theta}_t\sqrt{(s+a)^2-a^2}}\,ds\Bigg\}. \qquad (4.27)$$

After changing the variables as in (4.5), $E_y^{(t)}$ can be rewritten as:

$$E_y^{(t)}(x,z,t) = \frac{2Ae^{-at'}}{b_e^2-1}\left\{\frac{\alpha_0(\alpha_1-\alpha_2)}{(\alpha_0-\alpha_1)(\alpha_0-\alpha_2)}\left[b_e(a-\beta_0)\right.\right.$$

$$\times \quad \frac{1}{2\pi j}\int_{\xi-j\infty}^{\xi+j\infty} \frac{e^{ut'-\frac{z}{v}\cos\hat{\theta}_t\sqrt{u^2+\omega_p^2}}}{\sqrt{u^2+\omega_p^2}(u+\beta_0)}\,du - \frac{1}{2\pi j}\int_{\xi-j\infty}^{\xi+j\infty} \frac{e^{ut'-\frac{z}{v}\cos\hat{\theta}_t\sqrt{u^2+\omega_p^2}}}{u+\beta_0}\,du\Bigg]$$

$$+ \quad \frac{\alpha_1}{\alpha_1-\alpha_0}\Bigg[b_e(a-\beta_1)\frac{1}{2\pi j}\int_{\xi-j\infty}^{\xi+j\infty} \frac{e^{ut'-\frac{z}{v}\cos\hat{\theta}_t\sqrt{u^2+\omega_p^2}}}{\sqrt{u^2+\omega_p^2}(u+\beta_1)}\,du$$

$$- \quad \frac{1}{2\pi j}\int_{\xi-j\infty}^{\xi+j\infty} \frac{e^{ut'-\frac{z}{v}\cos\hat{\theta}_t\sqrt{u^2+\omega_p^2}}}{u+\beta_1}\,du\Bigg]$$

$$- \quad \frac{\alpha_2}{\alpha_2-\alpha_0}\Bigg[b_e(a-\beta_2)\frac{1}{2\pi j}\int_{\xi-j\infty}^{\xi+j\infty} \frac{e^{ut'-\frac{z}{v}\cos\hat{\theta}_t\sqrt{u^2+\omega_p^2}}}{\sqrt{u^2+\omega_p^2}(u+\beta_2)}\,du$$

$$- \quad \frac{1}{2\pi j}\int_{\xi-j\infty}^{\xi+j\infty} \frac{e^{ut'-\frac{z}{v}\cos\hat{\theta}_t\sqrt{u^2+\omega_p^2}}}{u+\beta_2}\,du\Bigg]\Bigg\}, \tag{4.28}$$

where the additional constants are defined as

$$\beta_i = \alpha_i - a, \qquad i = 1, 2. \tag{4.29}$$

Since all the terms in (4.28) have the form of either $f(\beta_i)$ or $e(\beta_i)$,

$$E_y^{(t)}(x,z,t) = \frac{2Ae^{-at'}}{b^2-1}\Bigg\{\frac{\alpha_0(\alpha_1-\alpha_2)}{(\alpha_0-\alpha_1)(\alpha_0-\alpha_2)}[b(\beta_0-a)f(\beta_0)-e(\beta_0)]$$

$$+ \quad \frac{\alpha_1}{\alpha_1-\alpha_0}[b(\beta_1-a)f(\beta_1)-e(\beta_1)] - \frac{\alpha_2}{\alpha_2-\alpha_0}[b(\beta_2-a)f(\beta_2)-e(\beta_2)]\Bigg\}. \tag{4.30}$$

In a similar manner, equations (2.30) and (2.33) can be used to show that the $x$-component of the magnetic field associated with the double-exponential excitation

is given by

$$\tilde{H}_x^{(t)}(x,z,s) = -\frac{\cos\hat{\theta}_t}{\mu\hat{v}}\frac{\sqrt{s^2+2as}}{s}\frac{2sA}{s+b_e\sqrt{s^2+2as}}\left(\frac{1}{s+\alpha_1}-\frac{1}{s+\alpha_2}\right)$$

$$\times \quad e^{-\frac{x}{\hat{v}}s\sin\hat{\theta}_t-\frac{z}{\hat{v}}\cos\hat{\theta}_t\sqrt{s^2+2as}}$$

$$= \quad -\frac{2A\cos\hat{\theta}_t}{\mu\hat{v}}\frac{\sqrt{s^2+2as}}{s+b_e\sqrt{s^2+2as}}\left(\frac{1}{s+\alpha_1}-\frac{1}{s+\alpha_2}\right)$$

$$\times \quad e^{-\frac{x}{\hat{v}}s\sin\hat{\theta}_t-\frac{z}{\hat{v}}\cos\hat{\theta}_t\sqrt{s^2+2as}}. \tag{4.31}$$

Multiplying the denominator as well as the numerator of (4.8) by $b_e\sqrt{s^2+2as}-s$, yields

$$\tilde{H}_x^{(t)}(x,z,s) = -\frac{2A\cos\hat{\theta}_t}{\mu\hat{v}(b_e^2-1)}(b_es+2ab_e-\sqrt{s^2+2as})\left[\frac{1}{(s+\alpha_0)(s+\alpha_1)}\right.$$

$$\left. - \quad \frac{1}{(s+\alpha_0)(s+\alpha_2)}\right] e^{-\frac{x}{\hat{v}}s\sin\hat{\theta}_t-\frac{z}{\hat{v}}\cos\hat{\theta}_t\sqrt{s^2+2as}}. \tag{4.32}$$

After applying the partial fraction expansion method [33] and taking an inverse Laplace transform, we obtain the integral representation for the $x$-component of the transient transmitted magnetic field:

$$H_x^{(t)}(x,z,t) = -\frac{2A\cos\hat{\theta}_t}{\mu\hat{v}(b_e^2-1)}\left\{\frac{1}{\alpha_1-\alpha_0}\right.$$

$$\times \quad \frac{1}{2\pi j}\int_{\xi-j\infty}^{\xi+j\infty} \frac{b_e s + 2ab_e - \sqrt{s^2+2as}}{s+\alpha_0} e^{st-\frac{x}{v}s\sin\hat{\theta}_t - \frac{z}{v}\cos\hat{\theta}_t\sqrt{s^2+2as}}\, ds$$

$$+ \quad \frac{1}{\alpha_0-\alpha_1}\frac{1}{2\pi j}\int_{\xi-j\infty}^{\xi+j\infty} \frac{b_e s + 2ab_e - \sqrt{s^2+2as}}{s+\alpha_1} e^{st-\frac{x}{v}s\sin\hat{\theta}_t - \frac{z}{v}\cos\hat{\theta}_t\sqrt{s^2+2as}}\, ds$$

$$- \quad \frac{1}{\alpha_2-\alpha_0}\frac{1}{2\pi j}\int_{\xi-j\infty}^{\xi+j\infty} \frac{b_e s + 2ab_e - \sqrt{s^2+2as}}{s+\alpha_0} e^{st-\frac{x}{v}s\sin\hat{\theta}_t - \frac{z}{v}\cos\hat{\theta}_t\sqrt{s^2+2as}}\, ds$$

$$- \quad \frac{1}{\alpha_0-\alpha_2}\frac{1}{2\pi j}\int_{\xi-j\infty}^{\xi+j\infty} \frac{b_e s + 2ab_e - \sqrt{s^2+2as}}{s+\alpha_2} e^{st-\frac{x}{v}s\sin\hat{\theta}_t - \frac{z}{v}\cos\hat{\theta}_t\sqrt{s^2+2as}}\, ds \Bigg\}$$

$$= \quad -\frac{2A\cos\hat{\theta}_t}{\mu\hat{v}(b_e^2-1)} \Bigg\{ \frac{\alpha_2-\alpha_1}{(\alpha_1-\alpha_0)(\alpha_2-\alpha_0)}$$

$$\times \quad \frac{1}{2\pi j}\int_{\xi-j\infty}^{\xi+j\infty} \frac{b_e s + 2ab_e - \sqrt{s^2+2as}}{s+\alpha_0} e^{st-\frac{x}{v}s\sin\hat{\theta}_t - \frac{z}{v}\cos\hat{\theta}_t\sqrt{s^2+2as}}\, ds$$

$$+ \quad \frac{1}{\alpha_0-\alpha_1}\frac{1}{2\pi j}\int_{\xi-j\infty}^{\xi+j\infty} \frac{b_e s + 2ab_e - \sqrt{s^2+2as}}{s+\alpha_1} e^{st-\frac{x}{v}s\sin\hat{\theta}_t - \frac{z}{v}\cos\hat{\theta}_t\sqrt{s^2+2as}}\, ds$$

$$- \quad \frac{1}{\alpha_0-\alpha_2}\frac{1}{2\pi j}\int_{\xi-j\infty}^{\xi+j\infty} \frac{b_e s + 2ab_e - \sqrt{s^2+2as}}{s+\alpha_2}$$

$$\times \quad e^{st-\frac{x}{v}s\sin\hat{\theta}_t - \frac{z}{v}\cos\hat{\theta}_t\sqrt{s^2+2as}}\, ds\}. \tag{4.33}$$

A change of variables, as defined in (4.5) and (4.29), allows $H_x^{(t)}(x,z,t)$ to be rewritten as

$$H_x^{(t)}(x,z,t) = -\frac{2A\cos\hat{\theta}_t e^{-at'}}{\mu\hat{v}(b_e^2-1)}\left\{\frac{\alpha_2-\alpha_1}{(\alpha_1-\alpha_0)(\alpha_2-\alpha_0)}\left[b_e(2a-\alpha_0)\right.\right.$$

$$\times\ \left.\frac{1}{2\pi j}\int_{\xi-j\infty}^{\xi+j\infty}\frac{e^{ut'-\frac{z}{\hat{v}}\cos\hat{\theta}_t\sqrt{u^2+\omega_p^2}}}{u+\beta_0}\,du-(\alpha_0^2-2a\alpha_0)\frac{1}{2\pi j}\int_{\xi-j\infty}^{\xi+j\infty}\frac{e^{ut'-\frac{z}{\hat{v}}\cos\hat{\theta}_t\sqrt{u^2+\omega_p^2}}}{(u+\beta_0)\sqrt{u^2+\omega_p^2}}\,du\right]$$

$$+\ \frac{1}{\alpha_0-\alpha_1}\left[b_e(2a-\alpha_1)\frac{1}{2\pi j}\int_{\xi-j\infty}^{\xi+j\infty}\frac{e^{ut'-\frac{z}{\hat{v}}\cos\hat{\theta}_t\sqrt{u^2+\omega_p^2}}}{u+\beta_1}\,du\right.$$

$$-\ \left.(\alpha_1^2-2a\alpha_1)\frac{1}{2\pi j}\int_{\xi-j\infty}^{\xi+j\infty}\frac{e^{ut'-\frac{z}{\hat{v}}\cos\hat{\theta}_t\sqrt{u^2+\omega_p^2}}}{(u+\beta_1)\sqrt{u^2+\omega_p^2}}\,du\right]$$

$$-\ \frac{1}{\alpha_0-\alpha_2}\left[b_e(2a-\alpha_2)\frac{1}{2\pi j}\int_{\xi-j\infty}^{\xi+j\infty}\frac{e^{ut'-\frac{z}{\hat{v}}\cos\hat{\theta}_t\sqrt{u^2+\omega_p^2}}}{u+\beta_2}\,du\right.$$

$$-\ \left.\left.(\alpha_2^2-2a\alpha_2)\frac{1}{2\pi j}\int_{\xi-j\infty}^{\xi+j\infty}\frac{e^{ut'-\frac{z}{\hat{v}}\cos\hat{\theta}_t\sqrt{u^2+\omega_p^2}}}{(u+\beta_2)\sqrt{u^2+\omega_p^2}}\,du\right]\right\}. \tag{4.34}$$

All the terms in (4.34) have the exact form of either $f(\beta_i)$ or $e(\beta_i)$; therefore,

$$H_x^{(t)}(x,z,t) = -\frac{2A\cos\hat{\theta}_t e^{-at'}}{(b_e^2-1)\mu\hat{v}}\left\{\frac{\alpha_2-\alpha_1}{(\alpha_1-\alpha_0)(\alpha_2-\alpha_0)}\left[b_e(2a-\alpha_0)e(\beta_0)\right.\right.$$

$$+\ \left.(\alpha_0^2-2a\alpha_0)f(\beta_0)\right]+\frac{1}{\alpha_0-\alpha_1}\left[b_e(2a-\alpha_1)e(\beta_1)+(\alpha_1^2-2a\alpha_1)f(\beta_1)\right]$$

$$-\ \left.\frac{1}{\alpha_0-\alpha_2}\left[b_e(2a-\alpha_2)e(\beta_2)+(\alpha_2^2-2a\alpha_2)f(\beta_2)\right]\right\}. \tag{4.35}$$

Once again, the $z$-component of the transient transmitted magnetic field is directly proportional to the electric field,

$$H_z^{(t)}(x,z,t) = \frac{\sin\theta_i}{\mu c} E_y^{(t)}(x,z,t). \tag{4.36}$$

Notice that the canonical functions $f(\beta)$ and $e(\beta)$ (i.e. (3.29) and (3.30)) express the retarded time for the transmitted pulse as $\frac{x}{\hat{v}}\sin\hat{\theta}_t + \frac{z}{\hat{v}}\cos\hat{\theta}_t$. This shows that in the dispersive medium, the early-time behavior results from a wave that propagates at the speed of light for the lossless medium, i.e., $\hat{v} = \frac{1}{\sqrt{\mu\epsilon}}$. We interpret this phenomenon as follows: The early-time portion of the signal is associated with the high frequency components. Therefore, as expected, $v \to \hat{v}$ as $\omega \to \infty$ (see (2.65) in chapter 2).

## 4.2 Transient Reflected Field

In the last section, we obtained closed-form expressions for the transient transmitted fields associated with two types of excitations, a unit-step function and a double-exponential pulse. Instead of using the same procedure to solve for the transient reflected field, we develop a simple method whereby the transmitted field results developed in last section are used to find the reflected fields.

By invoking the boundary conditions at $z = 0$, we obtain the following relationship between the transmission coefficient and the reflection coefficient [17]:

$$R_e = T_e - 1. \tag{4.37}$$

After substituting (4.37) into (2.17), we find that

$$\tilde{E}_y^{(r)}(x,z,s) = \tilde{E}_0(s)T_e e^{-\frac{s}{c}(x\sin\theta_i - z\cos\theta_i)} - \tilde{E}_0(s)e^{-\frac{s}{c}(x\sin\theta_i - z\cos\theta_i)}. \tag{4.38}$$

The inverse Laplace transforms for each term of (4.38) are given below:

$$\tilde{E}_0(s) \overset{\mathcal{L}}{\longleftrightarrow} E_0(t), \tag{4.39}$$

which is the input waveform,

$$\tilde{E}_0(s)T_e \overset{\mathcal{L}}{\longleftrightarrow} E_y^{(t)}(0,0,t), \tag{4.40}$$

is the transmitted field at the interface, and

$$e^{-\frac{s}{c}(x\sin\theta_i - z\cos\theta_i)} \overset{\mathcal{L}}{\longleftrightarrow} \delta\left(t - \frac{x}{c}\sin\theta_i + \frac{z}{c}\cos\theta_i\right), \tag{4.41}$$

is just a time delay term by the delay theorem for the Laplace transform [55]. The convolution theorem for the Laplace transform states that the Laplace transform of the convolution of two signals is equal to the product of their respective Laplace transforms [55]. Employing the convolution theorem and time delay theorem, we find that the transient reflected field is given by

$$\begin{aligned} E_y^{(r)}(x,z,t) &= E_y^{(t)}(0,0,t) * \delta\left(t - \frac{x}{c}\sin\theta_i + \frac{z}{c}\cos\theta_i\right) \\ &- E_0(t) * \delta\left(t - \frac{x}{c}\sin\theta_i + \frac{z}{c}\cos\theta_i\right) \\ &= E_y^{(t)}\left(0,0,t - \frac{x}{c}\sin\theta_i + \frac{z}{c}\cos\theta_i\right) - E_0\left(t - \frac{x}{c}\sin\theta_i + \frac{z}{c}\cos\theta_i\right). \end{aligned} \tag{4.42}$$

The above relationship shows that the transient reflected field is the difference between the transient transmitted field at the interface and the incident field adjusted by the proper time delay. The expression $t - \frac{x}{c}\sin\theta_i + \frac{z}{c}\cos\theta_i$ denotes the retarded time in the free space region.

Using Faraday law, we solve for the transient magnetic fields:

$$H_x^{(r)}(x,z,t) = \frac{\cos\theta_i}{c\mu_0} E_y^{(r)}(x,z,t), \tag{4.43}$$

$$H_z^{(r)}(x,z,t) = \frac{\sin\theta_i}{c\mu_0} E_y^{(r)}(x,z,t). \tag{4.44}$$

The reflected fields associated with the two different source excitations are given below:

Unit-step input:

$$E_y^{(r)}(x,z,t) = E_y^{(t)}\left(0,0,t - \frac{x}{c}\sin\theta_i + \frac{z}{c}\cos\theta_i\right) - u\left(t - \frac{x}{c}\sin\theta_i + \frac{z}{c}\cos\theta_i\right). \tag{4.45}$$

Double-exponential excitation:

$$\begin{aligned} E_y^{(r)}(x,z,t) &= E_y^{(t)}\left(0,0,t - \frac{x}{c}\sin\theta_i + \frac{z}{c}\cos\theta_i\right) - e^{-\alpha_1\left(t-\frac{x}{c}\sin\theta_i+\frac{z}{c}\cos\theta_i\right)} \\ &+ e^{-\alpha_2\left(t-\frac{x}{c}\sin\theta_i+\frac{z}{c}\cos\theta_i\right)}. \end{aligned} \tag{4.46}$$

The magnetic fields are then obtained from (4.43) and (4.44).

## 4.3 Numerical Results

In this section, numerical results are presented for both the transmitted and reflected transient TE plane waves associated with pulses that are obliquely incident

on a dispersive half space. We investigate both unit-step and double-exponential excitations.

### 4.3.1 Unit-Step Excitation

First, we investigate the transient field associated with a unit-step input. In order to allow for comparisons, we employ the same parameters that were used in [21], i.e., we assume that $\epsilon = 9\epsilon_0$, $\mu = \mu_0$, $\sigma = 1 \times 10^{-3}\mho/m$, and $\theta_i = 0$. The time histories of the transient transmitted fields for different values of $z$ are plotted in Fig. 4.3. The incidence angle $\theta_i$ is chosen to be zero. This figure clearly shows a number of interesting physical phenomenon. First, it illustrates that the wave requires a finite amount of time to propagate into the material. Furthermore, the high-frequency components propagate faster than the low-frequency components (see (2.65)). Since the early-time portion of the signal decays faster than the late-time signal, the high-frequency components experience more attenuation than the low-frequency components. This observation agrees with (2.63). It is also interesting to look at the early- and late-time transmission coefficients, i.e.,

$$\lim_{\omega\to\infty} T = \left.\frac{2}{1+b_e}\right|_{\theta_i=0} = 0.5 \tag{4.47}$$

and

$$\lim_{\omega\to 0} T = 0.0, \tag{4.48}$$

respectively. The early-time behavior is clearly illustrated by the $z = 0$ case in Fig. 4.3. The late-time transmission coefficient indicates that the $z = 0$ curve tends towards zero as $at' \to \infty$.

Fig. 4.4 shows the behavior of the transmitted transient fields for different incidence angles $\theta_i$. The results are plotted for the case $z = 0$. Observe that the amplitude of the transmitted field decays as $\theta_i$ becomes larger. The early-time behavior is dictated by (4.47), e.g.,

$$\lim_{\omega \to \infty} T|_{\theta_i = 80^\circ} = 0.13. \tag{4.49}$$

The late-time signals all tend to zero.

Fig. 4.5 shows the reflected field as the function of normalized time $at'$ for $z = 0$. The early- and late-time behaviors of this curve are predicted by

$$\lim_{\omega \to \infty} R = -0.5 \tag{4.50}$$

and

$$\lim_{\omega \to 0} R = -1.0, \tag{4.51}$$

respectively. A visual comparison between Figs. 4.3-4.5 and the figures in [21] demonstrates that the closed-form expressions yield the correct results. The results obtained using (4.7) were also checked using numerical integration (see Appendix A for a formulation of the convolution integrals). For the numerical integration, we employed a general purpose, adaptive integration algorithm (D01AKF) from the Numerical Algorithm Group FORTRAN library [31]. This algorithm uses Gauss 30-point and

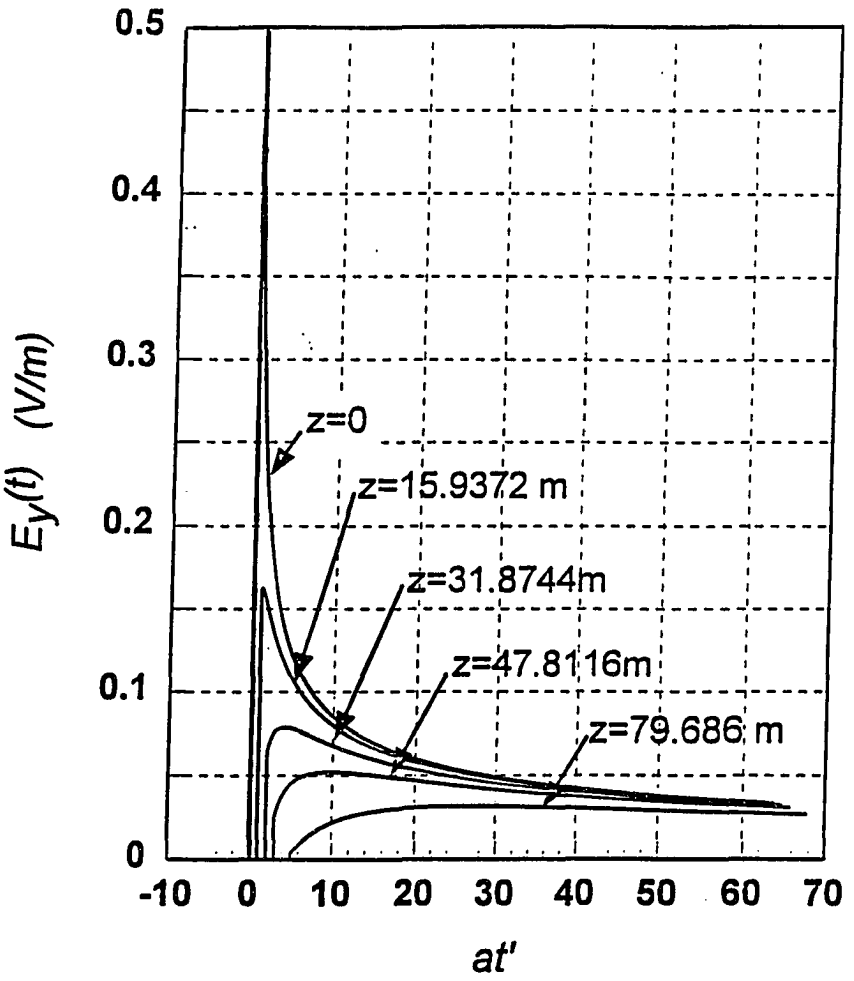


Figure 4.3: The transient transmitted electric field associated with a unit-step input as a function of normalized time $at'$ for different values of $z$. The parameters are defined as $\epsilon = 9\epsilon_0$, $\mu = \mu_0$, $\sigma = 1 \times 10^{-3}\mho/m$, and $\theta_i = 0$.

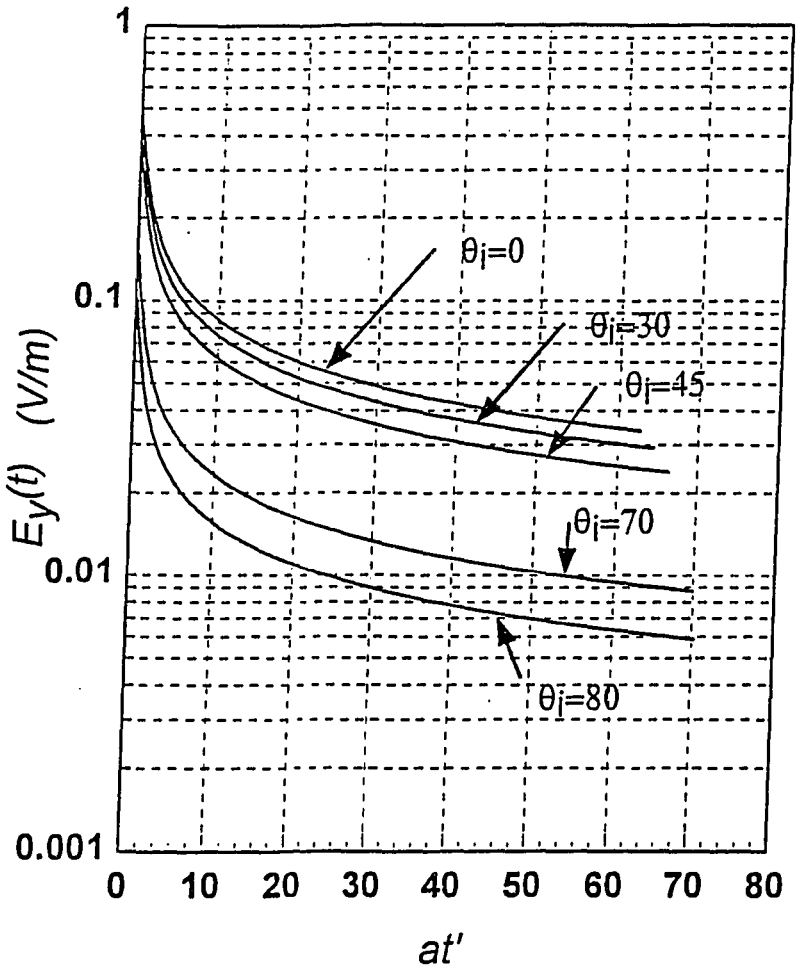


Figure 4.4: The transient transmitted electric field associated with a unit-step input as a function of normalized time $at'$ for different incidence angles $\theta_i$. The parameters are defined as $\epsilon = 9\epsilon_0$, $\mu = \mu_0$, $\sigma = 1 \times 10^{-3}\mho/m$, $z = 0$.

Kronrod 61-point rules. Our studies showed excellent agreement between the closed-form expressions and numerical integration results, i.e., we obtained at least five significant digits of accuracy in all cases we tested. Due to the singularity at $s = 0$, the FFT cannot be directly applied to carry out the inverse transform in (4.3). This singularity results from the source being left on until $t = \infty$.

### 4.3.2 Double-Exponential Pulse Excitation

In this subsection, we provide numerical results for a double-exponential pulse excitation. We employ the same parameters as were used in [8] and [34], i.e., $\epsilon = 10\epsilon_0$, $\mu = \mu_0$, $\alpha_1 = 5.9 \times 10^7 sec^{-1}$, and $\alpha_2 = 2.1 \times 10^8 sec^{-1}$. Fig. 4.6 presents the transient field for different values of $z$. The angle of incidence for the input pulse has been chosen as $\theta_i = 45°$. The pulse is clearly losing energy as it propagates through the lossy medium.

Fig. 4.7 shows the transmitted transient electric field at $z = 10\ cm$ for different incidence angles $\theta_i$. As was the case with the unit-step function, the transmitted field amplitude decreases as $\theta_i$ increases. The time histories contain both positive and negative values. In fact, $\int_0^\infty E_y(t)dt = 0$ for each of the transient curves in Fig. 4.7 since the transmitted field associated with the double-exponential pulse contains no DC component (see (4.25)).

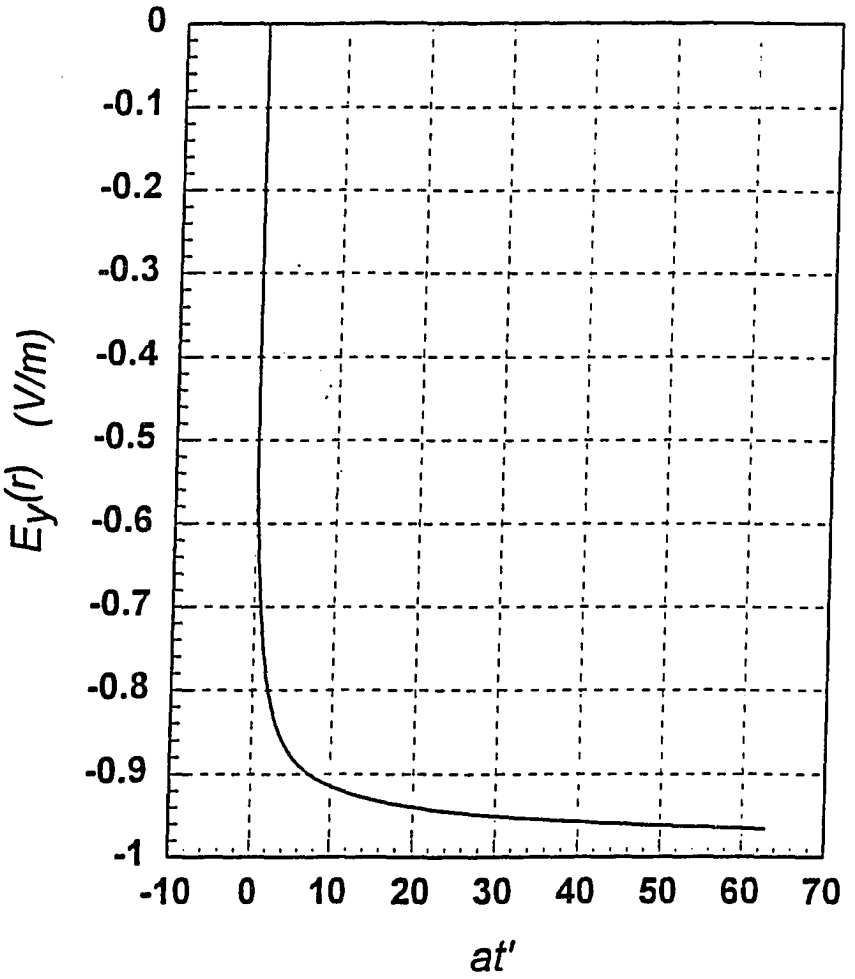


Figure 4.5: The transient reflected electric field associated with a unit-step input plotted as a function of normalized time $at'$. The parameters are defined as $\epsilon = 9\epsilon_0$, $\mu = \mu_0$, $\sigma = 1 \times 10^{-3}\mho/m$, $\theta_i = 0$, $z = 0$.

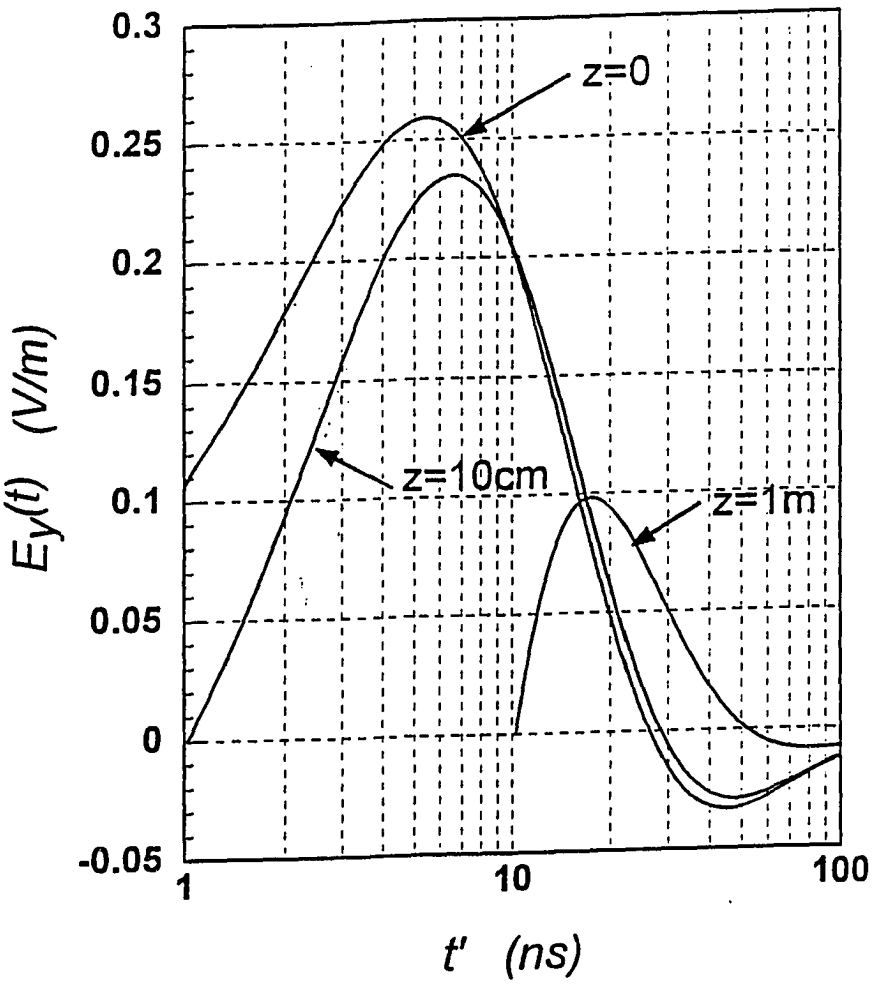


Figure 4.6: The transient transmitted electric fields associated with double-exponential excitations plotted as a function of $t'$ for various values of $z$. The parameters are defined as $\sigma = 2 \times 10^{-2} \mho/m$, $\epsilon = 10\epsilon_0$, $\mu = \mu_0$, $\theta_i = 45°$, $\alpha_1 = 5.9 \times 10^7 sec^{-1}$, and $\alpha_2 = 2.1 \times 10^8 sec^{-1}$.

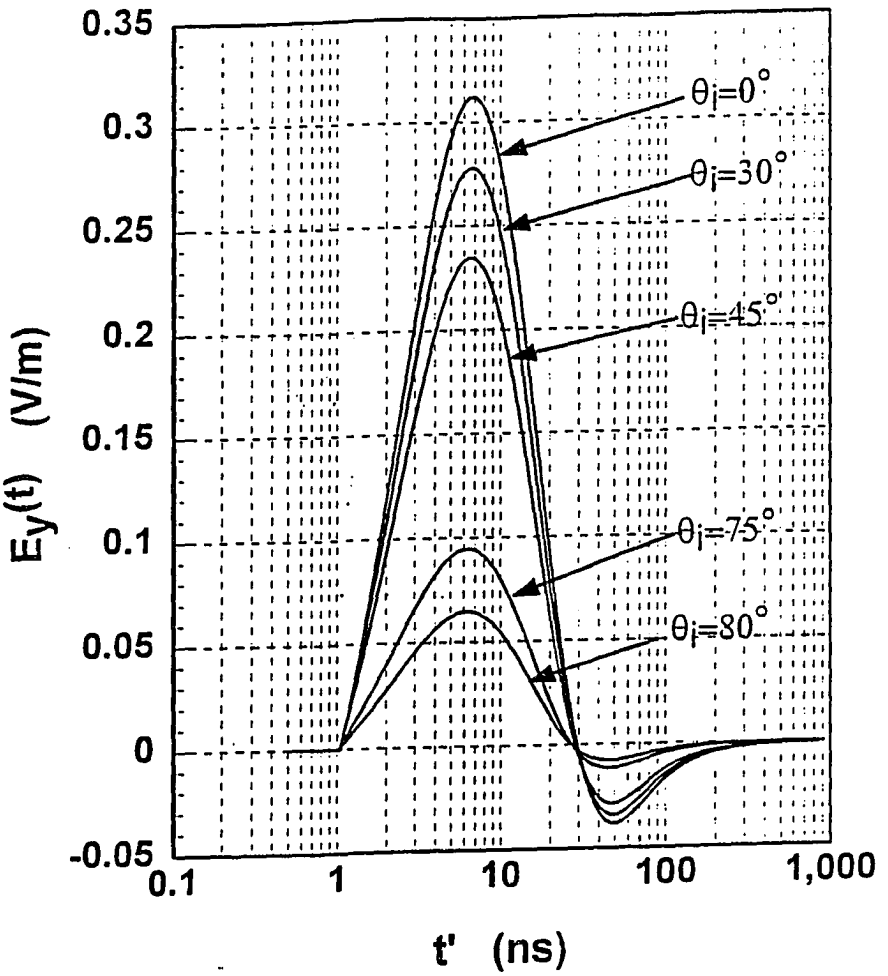


Figure 4.7: The transient transmitted electric fields associated with double-exponential excitations plotted as a function of $t'$ for various incidence angles of $\theta_i$. The parameters are defined as $\sigma = 2 \times 10^{-2} \mho/m$, $\epsilon = 10\epsilon_0$, $\mu = \mu_0$, $z = 10cm$, $\alpha_1 = 5.9 \times 10^7 sec^{-1}$, and $\alpha_2 = 2.1 \times 10^8 sec^{-1}$.

Fig. 4.8 shows how the transmitted field is affected by changing the conductivity $\sigma$. It shows that the conductivity strongly influences the rate of decay for the signal. It also shows that the retarded time is independent of $\sigma$.

Fig. 4.9 shows the reflected transient electric field associated with the double-exponential excitation at the interface $z = 0$. Note that the reflected field experiences a sign reversal and most of the field is reflected when the angle of incidence is near grazing. It should noted that the data at the interface is sufficient to determine the fields at any arbitrary height above the interface (in air) since one only needs to insert the appropriate time delay (4.46). The results in Figs. 4.6-4.9, obtained using the closed-form expression (4.30), once again show excellent agreement with those found in the existing literature [8], and [34]. Furthermore, once again we found that the closed-form results match very well with those produced by the numerical integration algorithm (see Appendix A for the formulation of the convolution integrals). Even though both the closed-form expression and the numerical integration algorithm produce very accurate results, our numerical tests have shown that the closed-form expressions require approximately one-fifth the computation time as compared with the numerical integration algorithm. Since $\zeta$ in $Je_0(a_\pm, \zeta)$ is purely imaginary (see (3.5) and (4.5)) and $Je_0(a_\pm, \zeta) = -jIe_0(-ja_\pm, j\zeta)$, the efficiency of the closed-form expression could be further improved by employing modified ILHIs of the first kind since this would require computing a series of modified Bessel functions of the first kind with real arguments instead of Bessel functions with complex

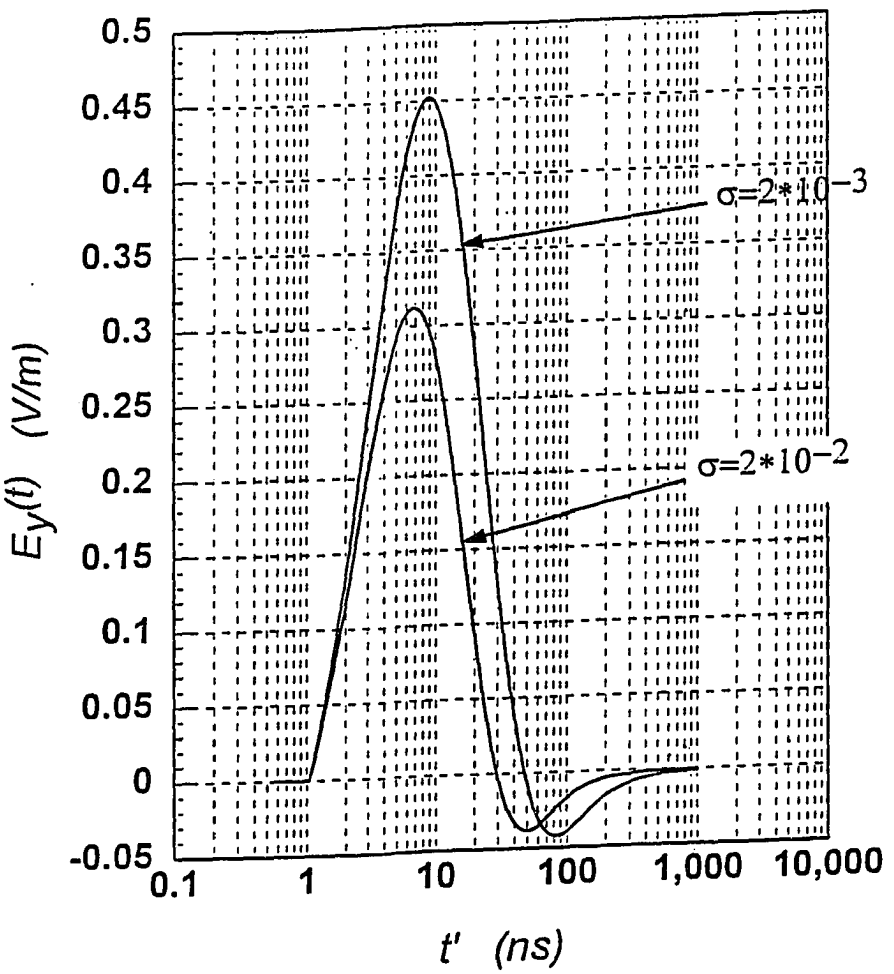


Figure 4.8: The transient transmitted electric fields associated with double-exponential excitations plotted as a function of $t'$ for two values of conductivity $\sigma$. The parameters are defined as $\epsilon = 10\epsilon_0$, $\mu = \mu_0$, $z = 10cm$, $\theta_i = 0$, $\alpha_1 = 5.9 \times 10^7 sec^{-1}$, and $\alpha_2 = 2.1 \times 10^8 sec^{-1}$.

arguments. We anticipate that this modification would lead to an additional factor of two improvement in efficiency.

An FFT algorithm [35] was also used to compute the transient fields for the double-exponential excitation. The FFT allows for the direct inversion of (4.25). Figs. 4.10 and 4.11 show a comparison between the results produced by the closed-form representation (4.30) and an FFT algorithm for the early- and late-time portions of the signal, respectively. The number of sample points in the FFT has been varied in order to demonstrate the accuracy of the FFT. We can see that aliasing and truncation errors can still be observed in the FFT results associated with 16,384 sample points. This clearly illustrates that a very large number of sample points are required to obtain an accurate time history using a FFT algorithm. This is due in part to the requirement that the data be uniformly sampled in the frequency and time domains. If the frequency spectrum is sampled out to $f_{max} = 2.0$ GHz then an FFT with 8,192 points yields results which are indistinguishable from the results plotted in Figure 4.6 provided they are plotted on the same scale. However, closer inspection shows that even with this large number of sample points, the FFT results are aliased. In Figure 4.10, we increase both the maximum sample frequency and the number of sample points by a factor of two in order to better model the high frequency content of the signal. These increases lead to more accurate results, but there is still substantial aliasing in the early-time signal. In order to investigate aliasing in the late-time results, we sample the spectrum finer at low frequencies

by holding the maximum sample frequency constant while increasing the number of sample points. The use of 16,384 sample points reduces the aliasing in the late-time response. However, in contrast, only 100 data points, uniformly distributed on a logarithmic scale, were required to produce each curve in Fig. 4.6 using the closed-form representation (4.30). Due to the large differences in the number of data points, thirty-two times less CPU time was required to compute the data in Fig. 4.6 using the closed-form representation as compared to the FFT algorithm. This demonstrates that the closed-form representation is more efficient, and more accurate than the FFT algorithm for this problem. In addition, the closed-form representation is much easier to use since one does not have to worry about aliasing errors. Similar observations were also made in [12].

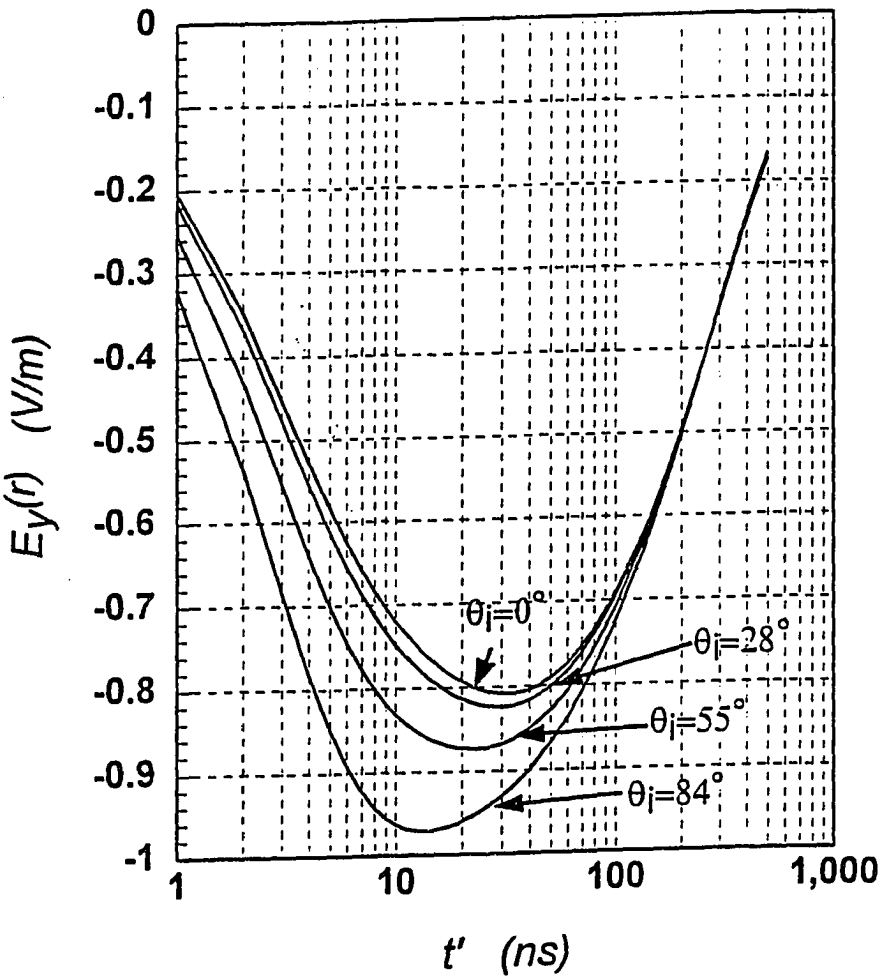


Figure 4.9: The transient reflected electric fields associated with double-exponential excitations as a function of $t'$ for four arrival angle $\theta_i$. The parameters are defined as $\sigma = 2 \times 10^{-2} \mho/m$, $\epsilon = 15\epsilon_0$, $\mu = \mu_0$, $z = 0$, $\alpha_1 = 5.9 \times 10^7 sec^{-1}$, and $\alpha_2 = 2.1 \times 10^8 sec^{-1}$.

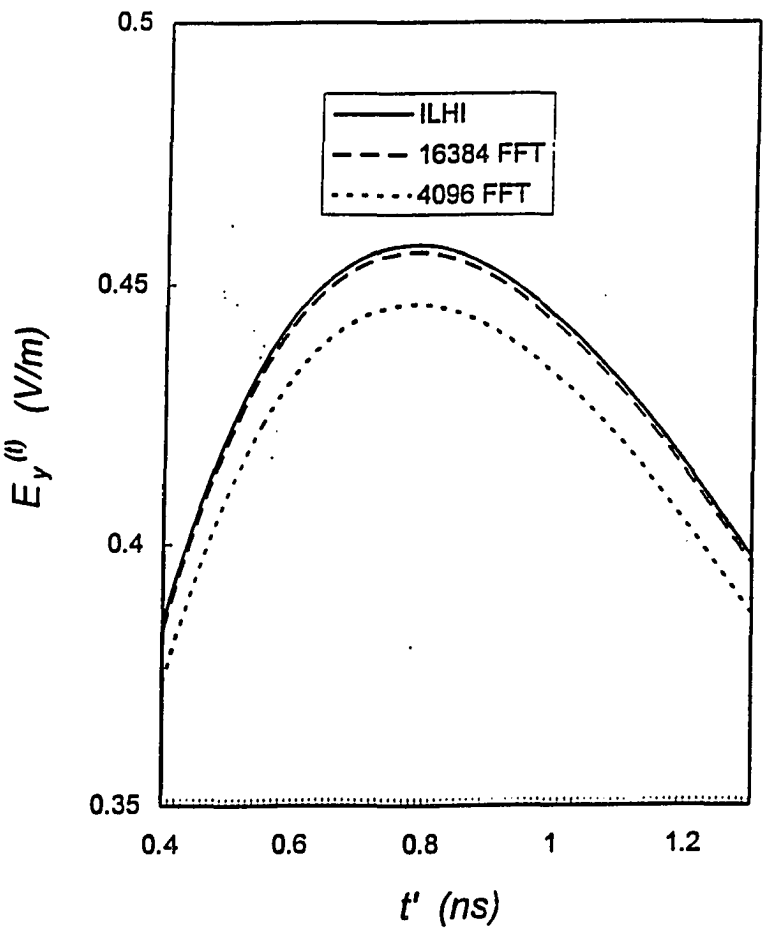


Figure 4.10: A comparison between the early-time double-exponential waveforms computed using the closed-form expression and an FFT algorithm. The parameters are defined as $\sigma = 2 \times 10^{-2} \mho/m$, $\epsilon = 10\epsilon_0$, $\mu = \mu_0$, $\theta_i = 45°$, $z = 0$, $\alpha_1 = 5.9 \times 10^7 sec^{-1}$, and $\alpha_2 = 2.1 \times 10^8 sec^{-1}$.

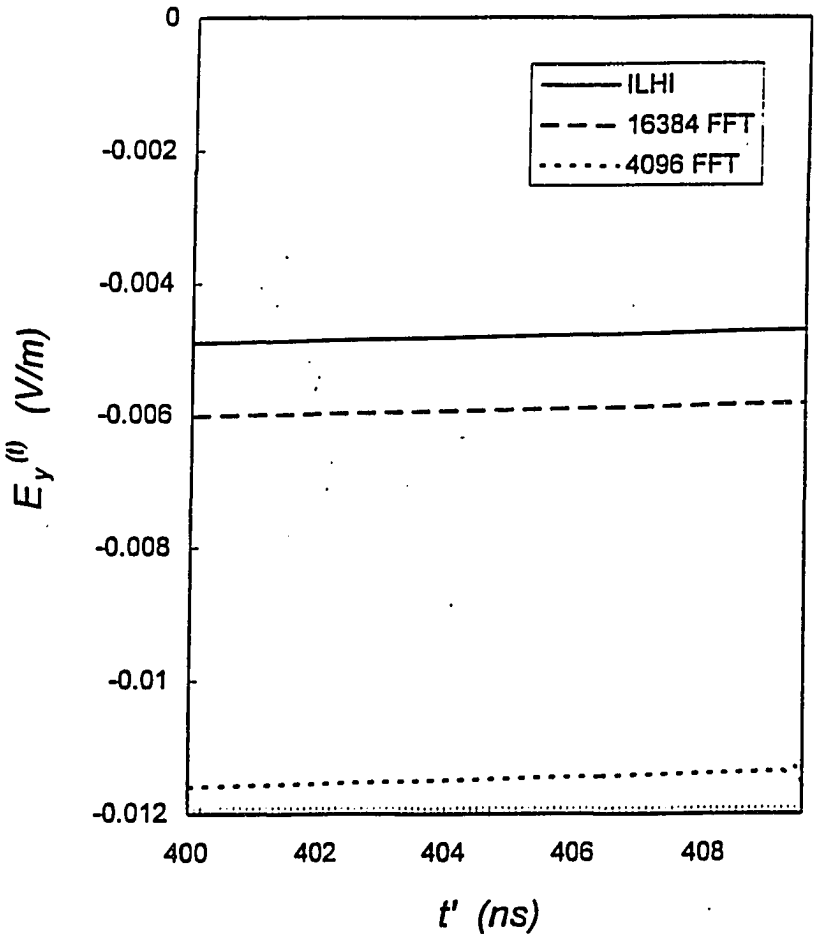


Figure 4.11: A comparison between the late-time double-exponential waveforms computed using the closed-form expression and an FFT algorithm. The parameters are defined as $\sigma = 2 \times 10^{-2} \mho/m$, $\epsilon = 10\epsilon_0$, $\mu = \mu_0$, $\theta_i = 45°$, $z = 0$, $\alpha_1 = 5.9 \times 10^7 sec^{-1}$, and $\alpha_2 = 2.1 \times 10^8 sec^{-1}$.

# CHAPTER 5

## Derivation of the Transient Fields (TM Case)

In this chapter, we obtain closed-form field expressions for the TM case. We first use Laplace transforms to derive integral representations for the transient transmitted fields. We then show that these fields can be written in terms of the same canonical integrals as in the TE case. The reflected field is then obtained from the transmitted field by using the convolution theorem. Finally, these results are used to numerically study this important canonical problem. The TM case is more complicated then the TE case since the TM transmission and reflection coefficients contain second-order poles.

### 5.1 Transient Transmitted Field

In Chapter 2, we demonstrated that the principle field for TM case is $\tilde{H}_y^{(t)}(x, z, s)$. We only consider a double-exponential excitation in the TM case.

Starting with (2.44) and (2.54), we find that the transmitted magnetic field is given by

$$\tilde{H}_y^{(t)}(x, z, s) = \frac{2(s+\rho)}{(s+\rho) + b_h\sqrt{s^2+2as}} \tilde{H}_0(s) e^{-(\frac{x}{v} s \sin\hat{\theta}_t + \frac{z}{v}\cos\hat{\theta}_t \sqrt{s^2+2as})}. \tag{5.1}$$

We multiply the denominator as well as the numerator of (5.1) by $b_h\sqrt{s^2+2as}-(s+\rho)$, which is the numerator of the reflection coefficient $R_h$, so that

$$\tilde{H}_y^{(t)}(x,z,s)=\frac{2(s+\rho)[b_h\sqrt{s^2+2as}-(s+\rho)]}{(b_h^2-1)s^2+2(ab_h^2-\rho)s-\rho^2}\tilde{H}_0(s)e^{-(\frac{x}{v}s\sin\hat{\theta}_t+\frac{z}{v}\cos\hat{\theta}_t\sqrt{s^2+2as})}. \quad (5.2)$$

For the case $b_h \neq 1$, the poles of the transmitted magnetic field, which are the roots of the polynomial

$$(b_h^2-1)s^2+2(ab_h^2-\rho)s-\rho^2=0 \quad (5.3)$$

are given by

$$\left.\begin{aligned} s_1 &= -\tfrac{a}{b_h^2-1}(b_h^2-2\cos^2\hat{\theta}_t-b_h\sqrt{b_h^2-\sin^2 2\hat{\theta}_t}) \\ s_2 &= -\tfrac{a}{b_h^2-1}(b_h^2-2\cos^2\hat{\theta}_t+b_h\sqrt{b_h^2-\sin^2 2\hat{\theta}_t}) \end{aligned}\right\};\quad b_h\neq 1. \quad (5.4)$$

It can be shown that the term under the square root in $s_1$ and $s_2$ is always larger than or equal to zero. Therefore, $s_1$ and $s_2$ are always real valued.

After factorizing the polynomial in the denominator, we rewrite the transmitted magnetic field as

$$\tilde{H}_y^{(t)}(x,z,s) = \frac{\tilde{H}_0}{b_h^2-1}\left[\frac{2(s+\rho)b_h(s^2+2as)}{(s-s_1)(s-s_2)\sqrt{s^2+2as}}-\frac{2(s+\rho)^2}{(s-s_1)(s-s_2)}\right]$$

$$\times\ e^{-(\frac{x}{v}s\sin\hat{\theta}_t+\frac{z}{v}\cos\hat{\theta}_t\sqrt{s^2+2as})}. \quad (5.5)$$

Using the spectral representation for the double-exponential pulse,

$$\tilde{H}_0(s)=A\left(\frac{1}{s+\alpha_1}-\frac{1}{s+\alpha_2}\right), \quad (5.6)$$

we find that the time-domain transmitted field is given by the following inverse Laplace transform representation:

$$H_y^{(t)}(x,z,t) = \frac{1}{2\pi j}\int_{\xi-j\infty}^{\xi+j\infty} \frac{2A(s+\rho)b_h(s^2+2as)e^{st-\frac{x}{v}s\sin\hat{\theta}_t-\frac{z}{v}\cos\hat{\theta}_t\sqrt{s^2+2as}}}{(b_h^2-1)(s-s_1)(s-s_2)(s+\alpha_1)\sqrt{s^2+2as}}\,ds$$

$$- \frac{1}{2\pi j}\int_{\xi-j\infty}^{\xi+j\infty} \frac{2A(s+\rho)b_h(s^2+2as)e^{st-\frac{x}{v}s\sin\hat{\theta}_t-\frac{z}{v}\cos\hat{\theta}_t\sqrt{s^2+2as}}}{(b_h^2-1)(s-s_1)(s-s_2)(s+\alpha_2)\sqrt{s^2+2as}}\,ds$$

$$- \frac{1}{2\pi j}\int_{\xi-j\infty}^{\xi+j\infty} \frac{2A(s+\rho)^2e^{st-\frac{x}{v}s\sin\hat{\theta}_t-\frac{z}{v}\cos\hat{\theta}_t\sqrt{s^2+2as}}}{(b_h^2-1)(s-s_1)(s-s_2)(s+\alpha_1)}\,ds$$

$$+ \frac{1}{2\pi j}\int_{\xi-j\infty}^{\xi+j\infty} \frac{2A(s+\rho)^2e^{st-\frac{x}{v}s\sin\hat{\theta}_t-\frac{z}{v}\cos\hat{\theta}_t\sqrt{s^2+2as}}}{(b_h^2-1)(s-s_1)(s-s_2)(s+\alpha_2)}\,ds. \tag{5.7}$$

Following the procedure we previously developed for the TE case, we find that the partial fraction expansion technique can be used to express the time-domain transmitted magnetic field as:

$$H_y^{(t)}(x,z,t) = \frac{2A}{b_h^2-1}\left[(B_{11}-B_{21})b_h\frac{1}{2\pi j}\int_{\xi-j\infty}^{\xi+j\infty} \frac{e^{st-\frac{x}{v}s\sin\hat{\theta}_t-\frac{z}{v}\cos\hat{\theta}_t\sqrt{s^2+2as}}}{(s-s_1)\sqrt{s^2+2as}}\,ds\right.$$

$$+ (B_{22}-B_{12})b_h\frac{1}{2\pi j}\int_{\xi-j\infty}^{\xi+j\infty} \frac{e^{st-\frac{x}{v}s\sin\hat{\theta}_t-\frac{z}{v}\cos\hat{\theta}_t\sqrt{s^2+2as}}}{(s-s_2)\sqrt{s^2+2as}}\,ds$$

$$+ C_1b_h\frac{1}{2\pi j}\int_{\xi-j\infty}^{\xi+j\infty} \frac{e^{st-\frac{x}{v}s\sin\hat{\theta}_t-\frac{z}{v}\cos\hat{\theta}_t\sqrt{s^2+2as}}}{(s+\alpha_1)\sqrt{s^2+2as}}\,ds$$

$$\left. - C_2b_h\frac{1}{2\pi j}\int_{\xi-j\infty}^{\xi+j\infty} \frac{e^{st-\frac{x}{v}s\sin\hat{\theta}_t-\frac{z}{v}\cos\hat{\theta}_t\sqrt{s^2+2as}}}{(s+\alpha_2)\sqrt{s^2+2as}}\,ds\right.$$

$$+ \quad (D_{21} - D_{11})\frac{1}{2\pi j}\int_{\xi-j\infty}^{\xi+j\infty} \frac{e^{st-\frac{x}{v}s\sin\hat{\theta}_t-\frac{z}{v}\cos\hat{\theta}_t\sqrt{s^2+2as}}}{s-s_1}\,ds$$

$$+ \quad (D_{12} - D_{22})\frac{1}{2\pi j}\int_{\xi-j\infty}^{\xi+j\infty} \frac{e^{st-\frac{x}{v}s\sin\hat{\theta}_t-\frac{z}{v}\cos\hat{\theta}_t\sqrt{s^2+2as}}}{s-s_2}\,ds$$

$$- \quad E_1\frac{1}{2\pi j}\int_{\xi-j\infty}^{\xi+j\infty} \frac{e^{st-\frac{x}{v}s\sin\hat{\theta}_t-\frac{z}{v}\cos\hat{\theta}_t\sqrt{s^2+2as}}}{s+\alpha_1}\,ds$$

$$+ \quad E_2\frac{1}{2\pi j}\int_{\xi-j\infty}^{\xi+j\infty} \frac{e^{st-\frac{x}{v}s\sin\hat{\theta}_t-\frac{z}{v}\cos\hat{\theta}_t\sqrt{s^2+2as}}}{s+\alpha_2}\,ds\Bigg]$$

$$= \quad \frac{2Ae^{-a(t-\frac{x}{v}\sin\hat{\theta}_t)}}{b_h^2-1}\Bigg\{(B_{11} - B_{21})b_h\frac{1}{2\pi j}\int_{\xi-j\infty}^{\xi+j\infty} \frac{e^{(s+a)(t-\frac{x}{v}\sin\hat{\theta}_t)-\frac{z}{v}\cos\hat{\theta}_t\sqrt{(s+a)^2-a^2}}}{[(s+a)-s_1-a]\sqrt{(s+a)^2-a^2}}\,ds$$

$$+ \quad (B_{22} - B_{12})b_h\frac{1}{2\pi j}\int_{\xi-j\infty}^{\xi+j\infty} \frac{e^{(s+a)(t-\frac{x}{v}\sin\hat{\theta}_t)-\frac{z}{v}\cos\hat{\theta}_t\sqrt{(s+a)^2-a^2}}}{[(s+a)-s_2-a]\sqrt{(s+a)^2-a^2}}\,ds$$

$$+ \quad C_1 b_h\frac{1}{2\pi j}\int_{\xi-j\infty}^{\xi+j\infty} \frac{e^{(s+a)(t-\frac{x}{v}\sin\hat{\theta}_t)-\frac{z}{v}\cos\hat{\theta}_t\sqrt{(s+a)^2-a^2}}}{[(s+a)+\alpha_1-a]\sqrt{(s+a)^2-a^2}}\,ds$$

$$- \quad C_2 b_h\frac{1}{2\pi j}\int_{\xi-j\infty}^{\xi+j\infty} \frac{e^{(s+a)(t-\frac{x}{v}\sin\hat{\theta}_t)-\frac{z}{v}\cos\hat{\theta}_t\sqrt{(s+a)^2-a^2}}}{[(s+a)+\alpha_2-a]\sqrt{(s+a)^2-a^2}}\,ds$$

$$+ \quad (D_{21} - D_{11})\frac{1}{2\pi j}\int_{\xi-j\infty}^{\xi+j\infty} \frac{e^{(s+a)(t-\frac{x}{v}\sin\hat{\theta}_t)-\frac{z}{v}\cos\hat{\theta}_t\sqrt{(s+a)^2-a^2}}}{(s+a)-s_1-a}\,ds$$

$$+ \quad (D_{12} - D_{22}) \frac{1}{2\pi j} \int_{\xi - j\infty}^{\xi + j\infty} \frac{e^{(s+a)(t - \frac{x}{v}\sin\hat{\theta}_t) - \frac{z}{v}\cos\hat{\theta}_t \sqrt{(s+a)^2 - a^2}}}{(s+a) - s_2 - a} \, ds$$

$$- \quad E_1 \frac{1}{2\pi j} \int_{\xi - j\infty}^{\xi + j\infty} \frac{e^{(s+a)(t - \frac{x}{v}\sin\hat{\theta}_t) - \frac{z}{v}\cos\hat{\theta}_t \sqrt{(s+a)^2 - a^2}}}{(s+a) + \alpha_1 - a} \, ds$$

$$+ \quad E_2 \frac{1}{2\pi j} \int_{\xi - j\infty}^{\xi + j\infty} \frac{e^{(s+a)(t - \frac{x}{v}\sin\hat{\theta}_t) - \frac{z}{v}\cos\hat{\theta}_t \sqrt{(s+a)^2 - a^2}}}{(s+a) + \alpha_2 - a} \, ds \Bigg\}, \tag{5.8}$$

where the constants which appear in the above expressions are defined by

$$\left.\begin{aligned} B_{mn} &= \frac{(2a+\rho-\alpha_m+s_1+s_2)s_n^2 + (2a\rho - s_1 s_2 + \alpha_m s_n)s_n}{(s_1 - s_2)(s_n + \alpha_m)} \\ C_m &= \frac{(2a+\rho-\alpha_m+s_1+s_2)\alpha_m^2 - (2a\rho + s_1\alpha_m + s_2\alpha_m)\alpha_m}{(s_1+\alpha_m)(s_2+\alpha_m)} \\ D_{mn} &= \frac{(s_n+\rho)^2}{(s_1-s_2)(s_n+\alpha_m)} \\ E_m &= \frac{(\alpha_m - \rho)^2}{(s_1+\alpha_m)(s_2+\alpha_m)} \end{aligned}\right\}. \quad m, n = 1, 2. \tag{5.9}$$

Following the TE case, we make the changes of the variables in (4.5) and (4.29), as well as

$$\left.\begin{aligned} \beta_3 &= -s_1 - a \\ \beta_4 &= -s_2 - a \end{aligned}\right\}. \tag{5.10}$$

This leads to a new expression which only involves the canonical integrals $e(\beta)$ and $f(\beta)$:

$$H_y^{(t)}(x, z, t) = \frac{2Ae^{-at'}}{b_h^2 - 1} \left[ (B_{11} - B_{21}) b_h \frac{1}{2\pi j} \int_{\xi - j\infty}^{\xi + j\infty} \frac{e^{ut' - \frac{z}{v}\cos\hat{\theta}_t \sqrt{u^2 + \omega_p^2}}}{(u + \beta_3)\sqrt{u^2 + \omega_p^2}} \, du \right.$$

$$+ \quad (B_{22}-B_{12})b_h\frac{1}{2\pi j}\int_{\xi-j\infty}^{\xi+j\infty}\frac{e^{ut'-\frac{z}{\hat{v}}\cos\hat{\theta}_t\sqrt{u^2+\omega_p^2}}}{(u+\beta_4)\sqrt{u^2+\omega_p^2}}\,du$$

$$+ \quad C_1b_h\frac{1}{2\pi j}\int_{\xi-j\infty}^{\xi+j\infty}\frac{e^{ut'-\frac{z}{\hat{v}}\cos\hat{\theta}_t\sqrt{u^2+\omega_p^2}}}{(u+\beta_1)\sqrt{u^2+\omega_p^2}}\,du - C_2b_h\frac{1}{2\pi j}\int_{\xi-j\infty}^{\xi+j\infty}\frac{e^{ut'-\frac{z}{\hat{v}}\cos\hat{\theta}_t\sqrt{u^2+\omega_p^2}}}{(u+\beta_2)\sqrt{u^2+\omega_p^2}}\,du$$

$$+ \quad (D_{21}-D_{11})\frac{1}{2\pi j}\int_{\xi-j\infty}^{\xi+j\infty}\frac{e^{ut'-\frac{z}{\hat{v}}\cos\hat{\theta}_t\sqrt{u^2+\omega_p^2}}}{(u+\beta_3)}\,du$$

$$+ \quad (D_{12}-D_{22})\frac{1}{2\pi j}\int_{\xi-j\infty}^{\xi+j\infty}\frac{e^{ut'-\frac{z}{\hat{v}}\cos\hat{\theta}_t\sqrt{u^2+\omega_p^2}}}{(u+\beta_4)}\,du$$

$$- \quad E_1\frac{1}{2\pi j}\int_{\xi-j\infty}^{\xi+j\infty}\frac{e^{ut'-\frac{z}{\hat{v}}\cos\hat{\theta}_t\sqrt{u^2+\omega_p^2}}}{(u+\beta_1)}\,du + E_2\frac{1}{2\pi j}\int_{\xi-j\infty}^{\xi+j\infty}\frac{e^{ut'-\frac{z}{\hat{v}}\cos\hat{\theta}_t\sqrt{u^2+\omega_p^2}}}{(u+\beta_2)}\,du \tag{5.11}$$

Reference to (3.1) and (3.2) shows that the desired closed-form canonical solution for the transient transmitted magnetic field is given by ($b_h \neq 1$),

$$H_y^{(t)}(x,z,t) = \frac{2Ae^{-at'}}{b_h^2-1}\left[(B_{21}-B_{11})b_hf(\beta_3) + (B_{12}-B_{22})b_hf(\beta_4) - C_1b_hf(\beta_1)\right.$$
$$\left. + \quad C_2b_hf(\beta_2) + (D_{21}-D_{11})e(\beta_3) + (D_{12}-D_{22})e(\beta_4) - E_1e(\beta_1) + E_2e(\beta_2)\right]. \tag{5.12}$$

Employing Ampere's law, we find that the $x$-component of the electric field associated with a double-exponential pulse excitation is given by:

$$E_x^{(t)}(x,z,s) = \frac{T_hA}{\sigma+s\epsilon}\frac{\cos\hat{\theta}_t}{\hat{v}}\sqrt{s^2+2as}\left(\frac{1}{s+\alpha_1}-\frac{1}{s+\alpha_2}\right)$$

$$\times \quad e^{-(\frac{x}{v}s\sin\hat{\theta}_t+\frac{z}{v}\cos\hat{\theta}_t\sqrt{s^2+2as})}$$

$$= \frac{2A\sqrt{s^2+2as}\cos\hat{\theta}_t}{\hat{v}\epsilon[(s+\rho)+b_h\sqrt{s^2+2as}]}\left(\frac{1}{s+\alpha_1}-\frac{1}{s+\alpha_2}\right)e^{-(\frac{x}{v}s\sin\hat{\theta}_t+\frac{z}{v}\cos\hat{\theta}_t\sqrt{s^2+2as})} \quad (5.13)$$

Multiplying the denominator as well as the numerator of (5.13) by $b_h\sqrt{s^2+2as}-(s+\rho)$, we obtain

$$E_x^{(t)}(x,z,s) = \frac{2A[b_h\sqrt{s^2+2as}-(s+\rho)]\sqrt{s^2+2as}\cos\hat{\theta}_t}{\hat{v}\epsilon[(b_h^2-1)s^2-2(ab_h^2-\rho)s-\rho^2]}\left(\frac{1}{s+\alpha_1}-\frac{1}{s+\alpha_2}\right)$$

$$\times \quad e^{-(\frac{x}{v}s\sin\hat{\theta}_t+\frac{z}{v}\cos\hat{\theta}_t\sqrt{s^2+2as})}$$

$$= \frac{2A[b_h(s^2+2as)-(s+\rho)\sqrt{s^2+2as}]\cos\hat{\theta}_t}{\hat{v}\epsilon(b_h^2-1)(s-s_1)(s-s_2)}\left(\frac{1}{s+\alpha_1}-\frac{1}{s+\alpha_2}\right)$$

$$\times \quad e^{-(\frac{x}{v}s\sin\hat{\theta}_t+\frac{z}{v}\cos\hat{\theta}_t\sqrt{s^2+2as})}$$

$$= \frac{2A\eta\cos\hat{\theta}_t}{b_h^2-1}\left[\frac{b_h(s^2+2as)}{(s-s_1)(s-s_2)(s+\alpha_1)}-\frac{b_h(s^2+2as)}{(s-s_1)(s-s_2)(s+\alpha_2)}\right.$$

$$\left.-\frac{(s+\rho)(s^2+2as)}{(s-s_1)(s-s_2)(s+\alpha_1)\sqrt{s^2+2as}}+\frac{(s+\rho)(s^2+2as)}{(s-s_1)(s-s_2)(s+\alpha_2)\sqrt{s^2+2as}}\right]$$

$$\times \quad e^{-(\frac{x}{v}s\sin\hat{\theta}_t+\frac{z}{v}\cos\hat{\theta}_t\sqrt{s^2+2as})}. \quad (5.14)$$

Using the partial fraction expansion technique and inverse Laplace transform again, we find that the time-domain $E_x^{(t)}$ is given by

$$E_x^{(t)}(x,z,t) = \frac{2A\eta\cos\hat{\theta}_t}{b_h^2-1}\left[G_{11}b_h\frac{1}{2\pi j}\int_{\xi-j\infty}^{\xi+j\infty}\frac{e^{st-\frac{x}{v}s\sin\hat{\theta}_t-\frac{z}{v}\cos\hat{\theta}_t\sqrt{s^2+2as}}}{s-s_1}\,ds\right.$$

$$-\ G_{12}b_h\frac{1}{2\pi j}\int_{\xi-j\infty}^{\xi+j\infty}\frac{e^{st-\frac{x}{v}s\sin\hat{\theta}_t-\frac{z}{v}\cos\hat{\theta}_t\sqrt{s^2+2as}}}{s-s_2}\,ds$$

$$+\ H_1b_h\frac{1}{2\pi j}\int_{\xi-j\infty}^{\xi+j\infty}\frac{e^{st-\frac{x}{v}s\sin\hat{\theta}_t-\frac{z}{v}\cos\hat{\theta}_t\sqrt{s^2+2as}}}{s+\alpha_1}\,ds$$

$$-\ G_{21}b_h\frac{1}{2\pi j}\int_{\xi-j\infty}^{\xi+j\infty}\frac{e^{st-\frac{x}{v}s\sin\hat{\theta}_t-\frac{z}{v}\cos\hat{\theta}_t\sqrt{s^2+2as}}}{s-s_1}\,ds$$

$$+\ G_{22}b_h\frac{1}{2\pi j}\int_{\xi-j\infty}^{\xi+j\infty}\frac{e^{st-\frac{x}{v}s\sin\hat{\theta}_t-\frac{z}{v}\cos\hat{\theta}_t\sqrt{s^2+2as}}}{s-s_2}\,ds$$

$$-\ H_2b_h\frac{1}{2\pi j}\int_{\xi-j\infty}^{\xi+j\infty}\frac{e^{st-\frac{x}{v}s\sin\hat{\theta}_t-\frac{z}{v}\cos\hat{\theta}_t\sqrt{s^2+2as}}}{s+\alpha_2}\,ds$$

$$-\ B_{11}\frac{1}{2\pi j}\int_{\xi-j\infty}^{\xi+j\infty}\frac{e^{st-\frac{x}{v}s\sin\hat{\theta}_t-\frac{z}{v}\cos\hat{\theta}_t\sqrt{s^2+2as}}}{(s-s_1)\sqrt{s^2+2as}}\,ds$$

$$+\ B_{12}\frac{1}{2\pi j}\int_{\xi-j\infty}^{\xi+j\infty}\frac{e^{st-\frac{x}{v}s\sin\hat{\theta}_t-\frac{z}{v}\cos\hat{\theta}_t\sqrt{s^2+2as}}}{(s-s_2)\sqrt{s^2+2as}}\,ds$$

$$-\ C_1\frac{1}{2\pi j}\int_{\xi-j\infty}^{\xi+j\infty}\frac{e^{st-\frac{x}{v}s\sin\hat{\theta}_t-\frac{z}{v}\cos\hat{\theta}_t\sqrt{s^2+2as}}}{(s+\alpha_1)\sqrt{s^2+2as}}\,ds$$

$$+ \quad B_{21}\frac{1}{2\pi j}\int_{\xi-j\infty}^{\xi+j\infty}\frac{e^{st-\frac{x}{v}s\sin\hat{\theta}_t-\frac{z}{v}\cos\hat{\theta}_t\sqrt{s^2+2as}}}{(s-s_1)\sqrt{s^2+2as}}\,ds$$

$$- \quad B_{22}\frac{1}{2\pi j}\int_{\xi-j\infty}^{\xi+j\infty}\frac{e^{st-\frac{x}{v}s\sin\hat{\theta}_t-\frac{z}{v}\cos\hat{\theta}_t\sqrt{s^2+2as}}}{(s-s_2)\sqrt{s^2+2as}}\,ds$$

$$+ \quad C_2\frac{1}{2\pi j}\int_{\xi-j\infty}^{\xi+j\infty}\frac{e^{st-\frac{x}{v}s\sin\hat{\theta}_t-\frac{z}{v}\cos\hat{\theta}_t\sqrt{s^2+2as}}}{(s+\alpha_2)\sqrt{s^2+2as}}\,ds\Bigg], \tag{5.15}$$

where the constants are defined as

$$\left.\begin{aligned} G_{mn} &= \tfrac{(2a+s_n)s_n}{(s_1-s_2)(s_n+\alpha_m)} \\ H_m &= \tfrac{(\alpha_m-2a)\alpha_m}{(s_1+\alpha_m)(s_2+\alpha_m)} \end{aligned}\right\}, \quad m,n=1,2. \tag{5.16}$$

Following the same procedure that was used to derive $H_y^{(t)}$, we find that

$$E_x^{(t)}(x,z,t) = \frac{2A\eta\cos\hat{\theta}_t e^{-at'}}{b^2-1}[(G_{11}-G_{21})b_h e(\beta_3)+(G_{22}-G_{12})b_h e(\beta_4)$$

$$+ \quad H_1 b_h e(\beta_1) - H_2 b_h e(\beta_2) + (B_{11}-B_{21})f(\beta_3) + (B_{22}-B_{12})f(\beta_4)$$

$$+ \quad C_1 f(\beta_1) - C_2 f(\beta_2)]. \tag{5.17}$$

Similarly, the canonical solution for the $z$-component of the transient electric field can be expressed as

$$E_z^{(t)}(x,z,t) = \frac{2A\sin\theta_i e^{-at'}}{c\epsilon(b_h^2-1)}[(F_{11}-F_{21})e(\beta_3)+(F_{22}-F_{12})e(\beta_4)+I_1 e(\beta_1)$$

$$- \quad I_2 e(\beta_2) + (s_1G_{11}-s_1G_{21})b_h f(\beta_3) + (s_2G_{12}-s_2G_{22})b_h f(\beta_4)$$

$$+ \quad \alpha_1 H_1 b_h f(\beta_1) - \alpha_2 H_2 b_h f(\beta_2)], \tag{5.18}$$

where

$$\left.\begin{aligned} F_{mn} &= \frac{s_n^2+\rho s_n}{(s_1-s_2)(s_n+\alpha_m)} \\ I_m &= \frac{\alpha_m^2+\rho\alpha_m}{(s_1+\alpha_m)(s_2+\alpha_m)} \end{aligned}\right\}, \quad m,n = 1,2. \tag{5.19}$$

Reference to (2.55) and (2.72) shows that $\theta_i$ equals the Brewster angle when the conditions $b_h = 1$ and $\mu = \mu_0$ are satisfied. As indicated in Chapter 2, Brewster's angle occurs only in the lossless case [37]; therefore, the solutions of the transient response for $b_h = 1$ case will not be considered.

## 5.2 Reflected Fields

Similar to the TE case, we obtain the relationship between the transmission and reflection coefficients by invoking the boundary conditions at $z = 0$,

$$R_h = T_h - 1. \tag{5.20}$$

Application of the convolution theorem results in the following expressions for the transient reflected fields:

$$\begin{aligned} H_y^{(r)}(x,z,t) &= H_y^{(t)}\left(0,0,t-\frac{x}{c}\sin\theta_i+\frac{z}{c}\cos\theta_i\right) - e^{-\alpha_1(t-\frac{x}{c}\sin\theta_i+\frac{z}{c}\cos\theta_i)} \\ &+ e^{-\alpha_2(t-\frac{x}{c}\sin\theta_i+\frac{z}{c}\cos\theta_i)}, \end{aligned} \tag{5.21}$$

and

$$E_x^{(r)}(x,z,t) = -\frac{\cos\theta_i}{c\epsilon_0} H_y^{(r)}(x,z,t), \tag{5.22}$$

$$E_z^{(r)}(x,z,t) = -\frac{\sin\theta_i}{c\epsilon_0} H_y^{(r)}(x,z,t). \tag{5.23}$$

The expression $t - \frac{x}{c}\sin\theta_i + \frac{z}{c}\cos\theta_i$ denotes the retarded time in the free space region.

## 5.3 Numerical Results

In this section, we validate the closed-form expression in (5.12). The ILHI's in (5.12) are calculated via a call to a FORTRAN subroutine which has been developed for their computation [9]. We compare the results computed using (5.12) against "exact" results which are obtained by numerical integration. We employ the general purpose, adaptive integration algorithm (D01AKF) from the Numerical Algorithm Group Library [31]. Following the procedure in Appendix A, we apply the convolution theorem to (5.7) in order to derive real-valued integrals that possess finite integration ranges.

In all cases tested, we obtained at least six significant digits of accuracy in the closed-form results. However, the CPU time required by the numerical integration algorithm was at least ten times more than that required for the closed-form expressions. A visual comparison was made between the closed-form results and previously published results [8, 34], and we are convinced that the closed-form results are correct. We also compare the closed-form results with those obtained by applying a FFT to (5.7), which we will discuss later.

In this section, numerical results are presented for both the transmitted and reflected transient TM plane waves associated with a double-exponential pulse that is obliquely incident on a conductive half-space. We assume that $\epsilon = 10\epsilon_0$, $\mu = \mu_0$, and $\sigma = 2 \times 10^{-2}\mho/m$ in all computations. We use the same input waveform as the TE case which is show in 4.1.

Fig. 5.1 shows the transient field at different depths $z_0$. The angle of incidence for the input pulse has been chosen as $\theta_i = 45°$ in this case. The pulse is clearly losing energy as it propagates through the lossy medium. Note that only 44% of the peak value of the signal at the surface penetrates below one meter. Furthermore, the tangential magnetic field at the interface has a peak magnitude that is greater than unity because the incident and reflected fields add constructively.

Fig. 5.2 shows the behavior of the transmitted transient field for different angles of incidence $\theta_i$. The results are plotted at a depth of $z = 10cm$. The amplitude of the transmitted fields decreases as $\theta_i$ increases. This is primarily due to additional decay associated with the longer propagation paths for the larger angles of incidence.

Reflected transient fields for different incident angles are plotted in Fig. 5.3. Note that the reflected field for $\theta_i = 85°$ changes sign once as a function of time. We attribute this phenomenon to a pseudo-Brewster angle, as was discussed in Chapter 2. In the high frequency limit, the reflection coefficient (2.78) reduces to the lossless

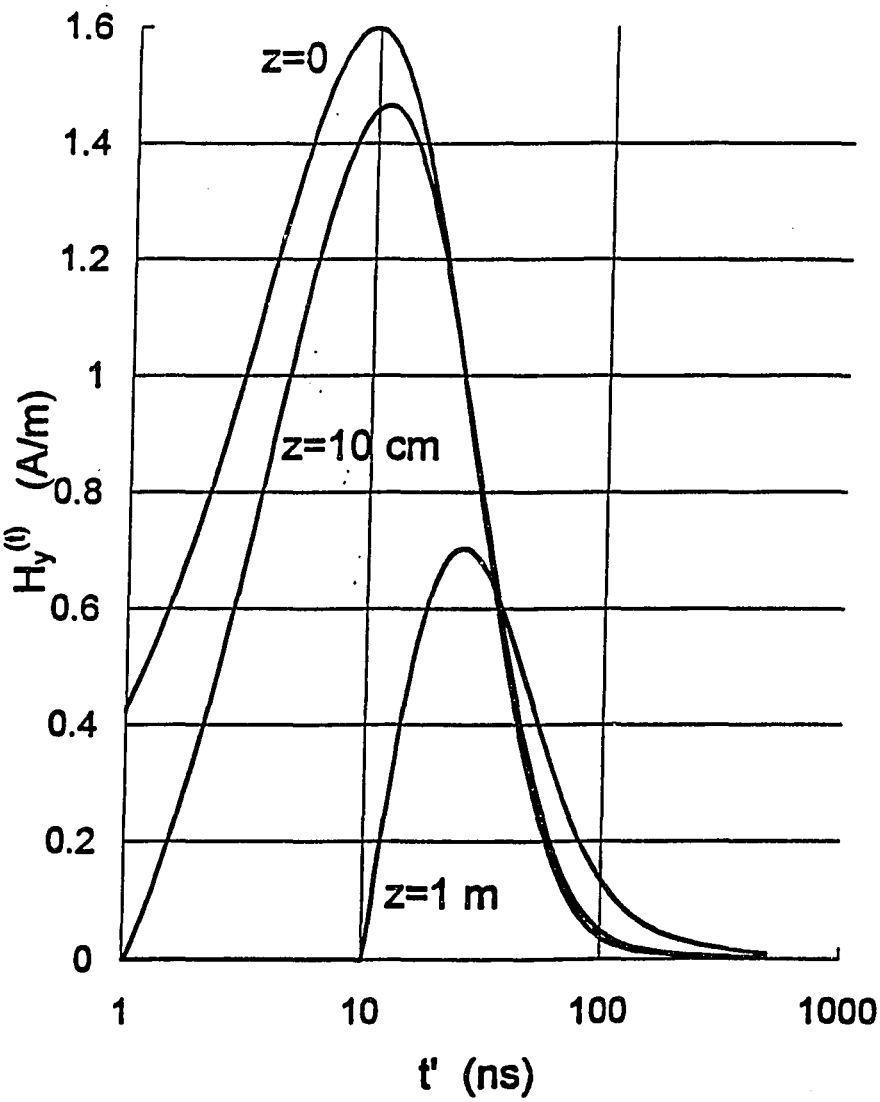


Figure 5.1: The transient transmitted magnetic fields associated with double-exponential excitations plotted as a function of $t'$ for various values of $z$. The parameters are defined as $\sigma = 2 \times 10^{-2} \mho/m$, $\epsilon = 10\epsilon_0$, $\mu = \mu_0$, $\theta_i = 45°$, $\alpha_1 = 5.9 \times 10^7 sec^{-1}$, and $\alpha_2 = 2.1 \times 10^8 sec^{-1}$.

case

$$\lim_{\omega\to\infty} R_h = \frac{\epsilon_r - \frac{1}{\cos\theta_i}\sqrt{\mu_r\epsilon_r - \sin^2\theta_i}}{\epsilon_r + \frac{1}{\cos\theta_i}\sqrt{\mu_r\epsilon_r - \sin^2\theta_i}}. \tag{5.24}$$

It can be shown that the reflection coefficient in (5.24) possesses the opposite signs depending on whether the angle of incidence is greater or smaller than Brewster's angle (2.72). Since the early-time response is associated with the high-frequency components, the early-time field changes sign as the incident angle passes Brewster's angle. In contrast, since the late-time response is associated with the low-frequency components, which experience little of the pseudo-Brewster's angle effect, the field does not change sign when the angle of incidence passes Brewster's angle. The 85° case in Fig. 5.3 shows this effect.

FFT techniques are often employed to evaluate inverse Fourier transforms similar to the one in (5.5). Application of FFT techniques to this example illustrates the problems which are encountered when FFT techniques are used to compute the transmitted transient field. Because of the large signal spread in both the frequency and time domains, a large number of sample points must be employed when using an FFT in order to minimize aliasing. Fig. 5.4 shows the comparison between the closed-form expression and the FFT results for the late-time portion of the transient transmitted field. This figure shows that the FFT results are converging to the closed-form results as the number of sample points is increased. However, an FFT with 32,768 points yields results which are still alised and distinguishable from the closed-form ILHI result. However, ten times more CPU time is required to carry

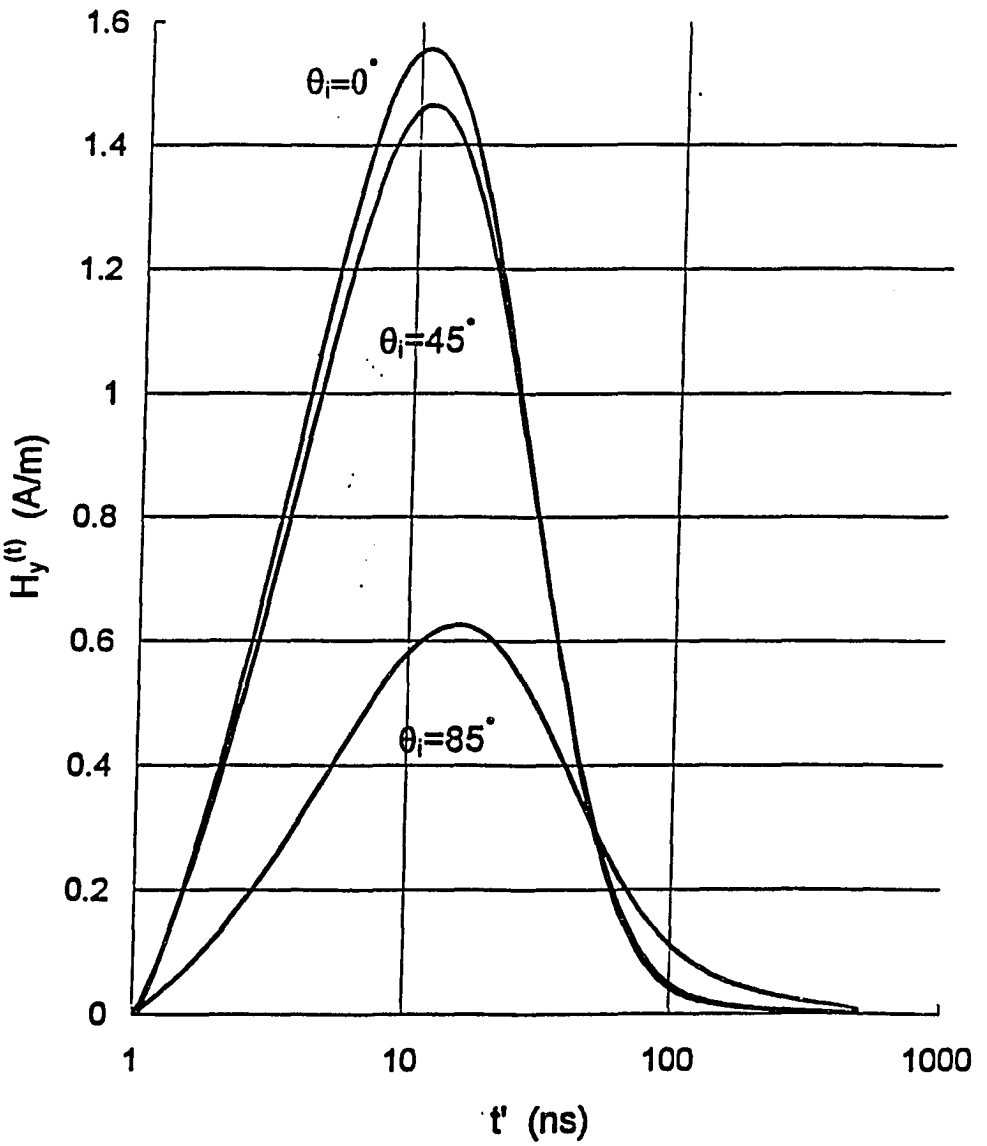


Figure 5.2: The transient transmitted magnetic fields associated with double-exponential excitations plotted as a function of $t'$ for various incidence angles of $\theta_i$. The parameters are defined as $\sigma = 2 \times 10^{-2} \mho/m$, $\epsilon = 10\epsilon_0$, $\mu = \mu_0$, $z = 10cm$, $\alpha_1 = 5.9 \times 10^7 sec^{-1}$, and $\alpha_2 = 2.1 \times 10^8 sec^{-1}$.

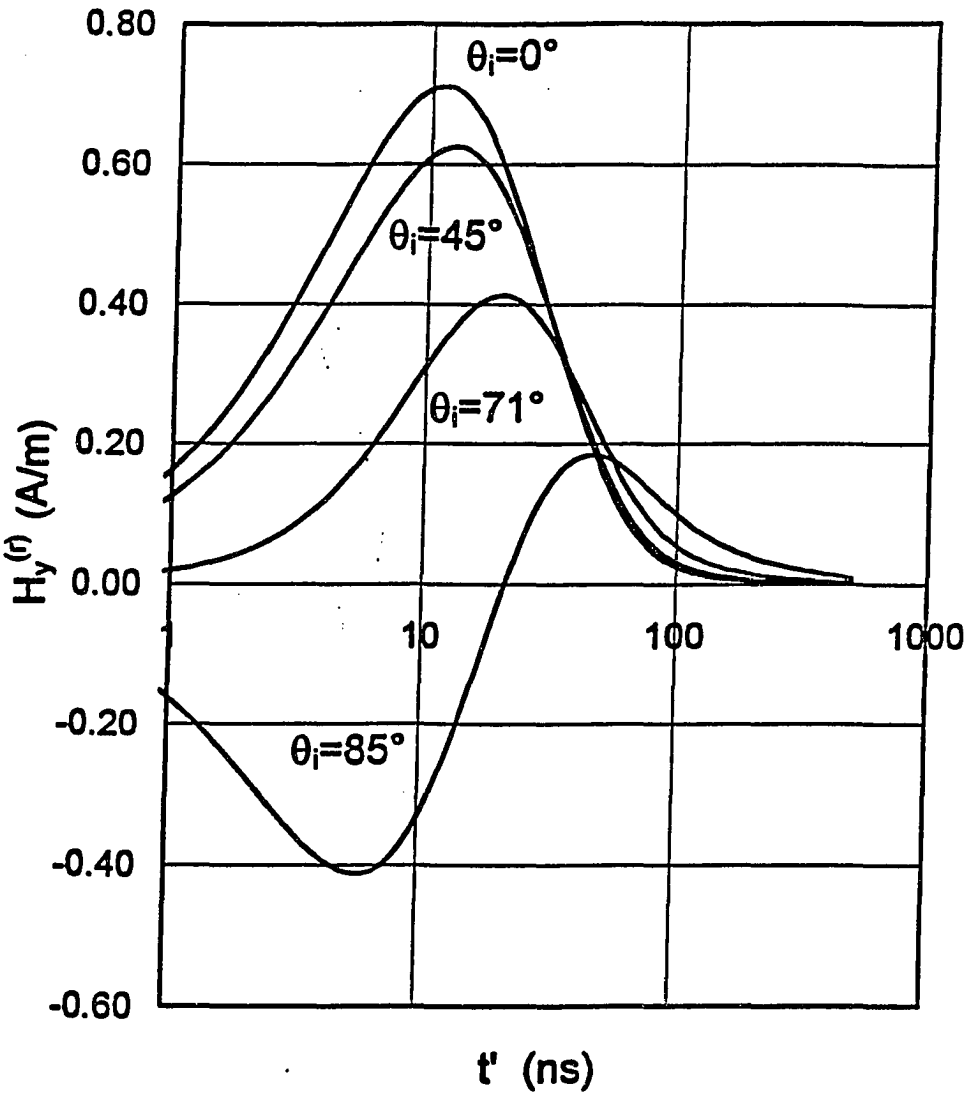


Figure 5.3: The transient reflected magnetic fields associated with double-exponential excitations as a function of $t'$ for four arrival angle $\theta_i$. The parameters are defined as $\sigma = 2 \times 10^{-2}\mho/m$, $\epsilon = 10\epsilon_0$, $\mu = \mu_0$, $z = 0$, $\alpha_1 = 5.9 \times 10^7 sec^{-1}$, and $\alpha_2 = 2.1 \times 10^8 sec^{-1}$.

out a 32,768 point FFT than is that required by the ILHI's. Furthermore, the FFT algorithm requires much more computer memory.

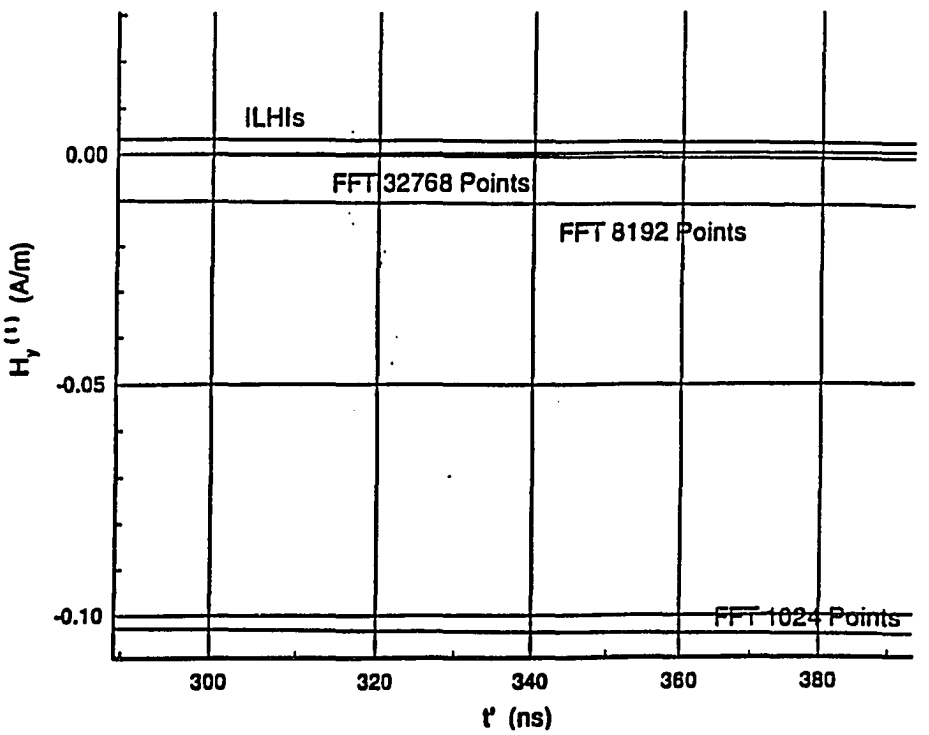


Figure 5.4: A comparison between the late-time double-exponential waveforms computed using the closed-form expression and an FFT algorithm. The parameters are defined as $\sigma = 2 \times 10^{-2} \mho/m$, $\epsilon = 10\epsilon_0$, $\mu = \mu_0$, $\theta_i = 45°$, $z = 0$, $\alpha_1 = 5.9 \times 10^7 sec^{-1}$, and $\alpha_2 = 2.1 \times 10^8 sec^{-1}$.

# CHAPTER 6

## Late-Time Response

We have obtained exact, closed-form solutions for the canonical problem of a transient electromagnetic plane wave incident on a conductive half-space in the previous chapters. In this chapter, we now derive a relatively simple, approximate late-time response by directly employing the closed-form results derived in the previous chapters.

As was demonstrated in [12], the asymptotic factorial-Neumann series expansion for the ILHI [9]

$$J_{e0}^{M}(a,z) = \frac{1}{\sqrt{a^2+1}} + \frac{e^{-az}}{\Gamma\left(\frac{1}{2}\right)(a^2+1)} \sum_{k=0}^{M-1} \left[\frac{2}{z(a^2+1)}\right]^k \Gamma\left(k+\frac{1}{2}\right)\left[J_{k+1}(z) - aJ_k(z)\right] \tag{6.1}$$

can be used to obtain an approximate expression for the late-time response. It is clear that only the first few terms are required in the summation in (6.1) when $z \gg 1$. Comparing the asymptotic factorial-Neumann series expansion for the ILHI with the expressions for the canonical integrals $f(\beta)$ and $e(\beta)$, we find that $a$ and $z$ in (6.1) are the same as $a_{\pm}$ and $\zeta$ in $f(\beta)$ and $e(\beta)$. Therefore, the condition required for the late-time approximation is

$$t' \gg \max\left(\frac{z}{\hat{v}}\cos\hat{\theta}_t,\ \left|\frac{\omega_p}{\sqrt{\beta^2+\omega_p^2}}\right|\right). \tag{6.2}$$

In order to employ the asymptotic factorial-Neumann series expansion, we must first determine the sign of $\sqrt{a_{\pm}^2+1}$. If we let

$$\sqrt{a_{\pm}^2+1} = s_{\pm}\frac{-\beta\frac{z}{\hat{v}}\cos\hat{\theta}_t \pm t'\sqrt{\beta^2+\omega_p^2}}{\omega_p\sqrt{t'^2-\left(\frac{z}{\hat{v}}\cos\hat{\theta}_t\right)^2}} = s_{\pm}j\frac{\beta\frac{z}{\hat{v}}\cos\hat{\theta}_t \mp t'\sqrt{\beta^2-a^2}}{a\sqrt{t'^2-\left(\frac{z}{\hat{v}}\cos\hat{\theta}_t\right)^2}}, \tag{6.3}$$

where $s_{\pm}$ equals +1 or -1, then the sign of (6.3) is determined by the branch cut chosen for $\sqrt{a_{\pm}^2+1}$.

The study conducted by Dvorak and Kuester [9] has shown that the branch cut for the asymptotic factorial-Neumann series expansion for $J_{e0}(a_{\pm},\zeta)$ is shown in Fig. 6.1. This branch cut can be defined analytically by

$$\begin{aligned} &\Re\sqrt{a_{\pm}^2+1} < 0; \quad a_{\pm} \in \{\Re(a_{\pm}) < 0\} \cap \{|\Im(a_{\pm})|\} > 1, \\ &\Re\sqrt{a_{\pm}^2+1} \geq 0; \quad \text{otherwise.} \end{aligned} \tag{6.4}$$

From the results of the previous chapters, in order to choose $s_{\pm}$, we must first determine where $a_{\pm}$ lies in the complex $a_{\pm}$-plane.

$$a_{\pm} = \frac{-\beta t' \pm \frac{z}{\hat{v}}\cos\hat{\theta}_t\sqrt{\beta^2+\omega_p^2}}{\omega_p\sqrt{t'^2-\frac{z^2}{\hat{v}^2}\cos^2\hat{\theta}_t}} = j\frac{\beta t' \mp \frac{z}{\hat{v}}\cos\hat{\theta}_t\sqrt{\beta^2-a^2}}{a\sqrt{t'^2-\frac{z^2}{\hat{v}^2}\cos^2\hat{\theta}_t}}. \tag{6.5}$$

It can be shown that the modulus of $a_{\pm}$ are always greater than 1,

$$|a_{\pm}| > 1. \tag{6.6}$$

Furthermore, in order to have a non-zero causal response,

$$t' > \frac{z}{\hat{v}}\cos\hat{\theta}_t. \tag{6.7}$$

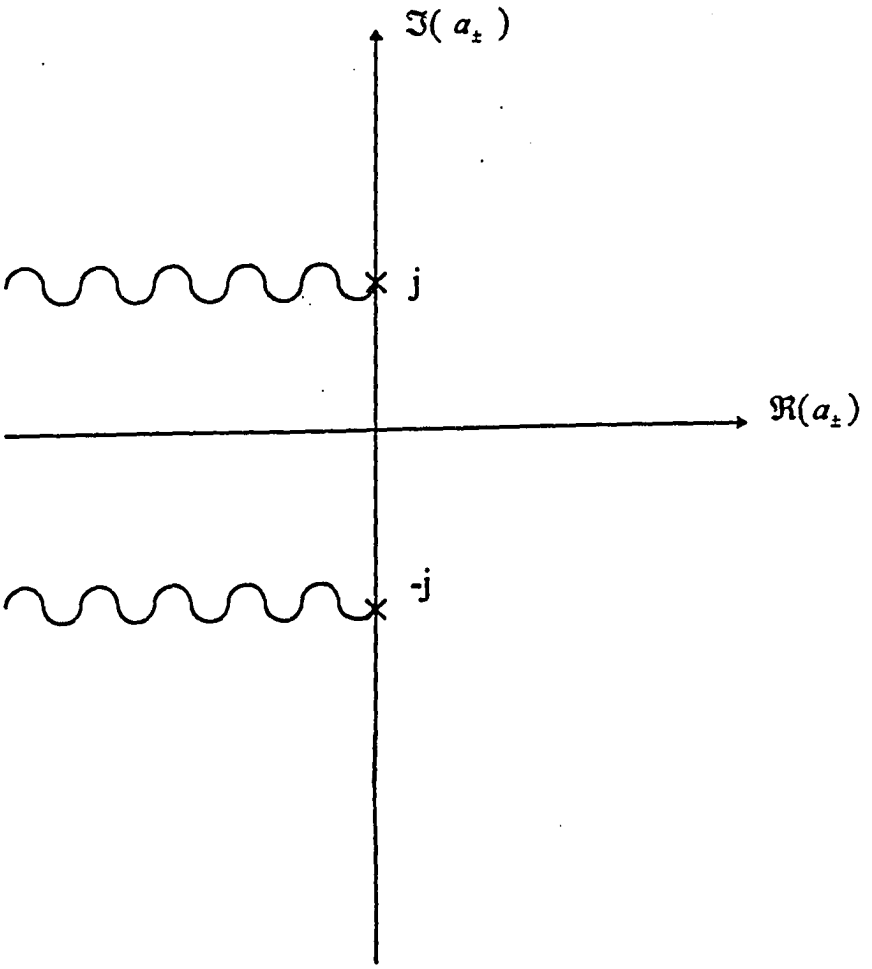


Figure 6.1: Branch cut for the asymptotic factorial-Neumann series expansion for $J_{e0}(a_\pm, \zeta)$.

Recall from previous chapters, $\beta$ is always real valued (4.29), (5.10). Therefore, we only need to consider three cases: $\beta < a$, $\beta > a$, and $\beta = a$.

We consider the $\beta < a$ case first. For this case

$$a_{\pm} = j\frac{\beta t' \mp j\frac{z}{\hat{v}}\cos\hat{\theta}_t\sqrt{a^2-\beta^2}}{a\sqrt{t'^2-\frac{z^2}{\hat{v}^2}\cos^2\hat{\theta}_t}} = \frac{\pm\frac{z}{\hat{v}}\cos\hat{\theta}_t\sqrt{a^2-\beta^2}+j\beta t'}{a\sqrt{t'^2-\frac{z^2}{\hat{v}^2}\cos^2\hat{\theta}_t}}. \tag{6.8}$$

Therefore $\Re(a_+) > 0$, $\Re(a_-) < 0$, and $\Im(a_-) < 1$. Reference to the definition of the branch cut (6.4) shows that $\Re\sqrt{a_+^2+1} \geq 0$, and $\Re\sqrt{a_-^2+1} \geq 0$, or $s_+ = +1$ and $s_- = -1$ in (6.3).

Substitution of the asymptotic factorial-Neumann series expansion expression into $e(\beta)$, we have

$$\begin{aligned} e(\beta) = u\left(t' - \frac{z}{\hat{v}}\cos\hat{\theta}_t\right)\Bigg\{ & \frac{e^{a+\zeta}}{2} - \frac{-\beta\frac{z}{\hat{v}}\cos\hat{\theta}_t + t'\sqrt{\beta^2+\omega_p^2}}{2\omega_p\sqrt{t'^2-\left(\frac{z}{\hat{v}}\cos\hat{\theta}_t\right)^2}}\Bigg[\frac{e^{a+\zeta}}{\sqrt{a_+^2+1}} \\ & + \frac{1}{\Gamma\left(\frac{1}{2}\right)(a_+^2+1)}\sum_{k=0}^{M-1}\left[\frac{2}{\zeta(a_+^2+1)}\right]^k\Gamma\left(k+\frac{1}{2}\right)\left[J_{k+1}(\zeta)-a_+J_k(\zeta)\right]\Bigg] + \frac{e^{a-\zeta}}{2} \\ & - \frac{-\beta\frac{z}{\hat{v}}\cos\hat{\theta}_t - t'\sqrt{\beta^2+\omega_p^2}}{2\omega_p\sqrt{t'^2-\left(\frac{z}{\hat{v}}\cos\hat{\theta}_t\right)^2}}\Bigg[\frac{e^{a-\zeta}}{\sqrt{a_-^2+1}} + \frac{1}{\Gamma\left(\frac{1}{2}\right)(a_-^2+1)}\sum_{k=0}^{M-1}\left[\frac{2}{\zeta(a_-^2+1)}\right]^k \\ & \times \Gamma\left(k+\frac{1}{2}\right)\left[J_{k+1}(\zeta)-a_-J_k(\zeta)\right]\Bigg]\Bigg\}; \quad \beta < a. \end{aligned} \tag{6.9}$$

If we only keep one term in the series ($M = 1$) and use the result that $s_{\pm} = \pm 1$, then $e(\beta)$ can be approximated as

$$e(\beta) \approx u\left(t' - \frac{z}{\hat{v}}\cos\hat{\theta}_t\right)\left\{\frac{e^{a+\zeta}}{2} - \frac{e^{a+\zeta}}{2}\right.$$

$$+ \frac{\left(\beta\frac{z}{\hat{v}}\cos\hat{\theta}_t - t'\sqrt{\beta^2+\omega_p^2}\right)[J_1(\zeta) - a_+ J_0(\zeta)]}{2\omega_p\sqrt{t'^2 - \left(\frac{z}{\hat{v}}\cos\hat{\theta}_t\right)^2}(a_+^2+1)} + \frac{e^{a-\zeta}}{2} + \frac{e^{a-\zeta}}{2}$$

$$+ \frac{\left(\beta\frac{z}{\hat{v}}\cos\hat{\theta}_t + t'\sqrt{\beta^2+\omega_p^2}\right)[J_1(\zeta) - a_- J_0(\zeta)]}{2\omega_p\sqrt{t'^2 - \left(\frac{z}{\hat{v}}\cos\hat{\theta}_t\right)^2}(a_-^2+1)}\Bigg\} = u\left(t' - \frac{z}{\hat{v}}\cos\hat{\theta}_t\right)\Big\{e^{a-\zeta}$$

$$+ \frac{\left(\beta\frac{z}{\hat{v}}\cos\hat{\theta}_t - t'\sqrt{\beta^2+\omega_p^2}\right)[J_1(\zeta) - a_+ J_0(\zeta)]}{2\omega_p\sqrt{t'^2 - \left(\frac{z}{\hat{v}}\cos\hat{\theta}_t\right)^2}(a_+^2+1)}$$

$$+ \frac{\left(\beta\frac{z}{\hat{v}}\cos\hat{\theta}_t + t'\sqrt{\beta^2+\omega_p^2}\right)[J_1(\zeta) - a_- J_0(\zeta)]}{2\omega_p\sqrt{t'^2 - \left(\frac{z}{\hat{v}}\cos\hat{\theta}_t\right)^2}(a_-^2+1)}\Bigg\}; \quad \beta < a. \tag{6.10}$$

Inspecting (3.29), we observe that the second and third terms of $f(\beta)$ possess opposite signs. Therefore, two terms of the summation in (6.1) are required to approximate $f(\beta)$. Following the same procedure as was applied to obtain the late-time approximation of $e(\beta)$, we find that

$$f(\beta) \approx -\frac{u\left(t' - \frac{z}{\hat{v}}\cos\hat{\theta}_t\right)}{\sqrt{\alpha^2+\omega_p^2}}\Bigg\{e^{a-\zeta} + \frac{\left(\beta\frac{z}{\hat{v}}\cos\hat{\theta}_t - t'\sqrt{\beta^2+\omega_p^2}\right)[J_1(\zeta) - a_+ J_0(\zeta)]}{2\omega_p\sqrt{t'^2 - \left(\frac{z}{\hat{v}}\cos\hat{\theta}_t\right)^2}(a_+^2+1)}$$

$$- \frac{\left(\beta\frac{z}{\hat{v}}\cos\hat{\theta}_t + t'\sqrt{\beta^2+\omega_p^2}\right)[J_1(\zeta) - a_- J_0(\zeta)]}{2\omega_p\sqrt{t'^2 - \left(\frac{z}{\hat{v}}\cos\hat{\theta}_t\right)^2}(a_-^2+1)}\Bigg\}; \quad \beta < a. \tag{6.11}$$

Next we consider the case $\beta > a$, when

$$a_\pm = j\frac{\beta t' \mp \frac{z}{\hat{v}}\cos\hat{\theta}_t\sqrt{\beta^2 - a^2}}{a\sqrt{t'^2 - \frac{z^2}{\hat{v}^2}\cos^2\hat{\theta}_t}} \tag{6.12}$$

is purely imaginary. For this case, it is not clear how the branch cut is defined in (6.4). Complex variable analysis tells us that $a_\pm$ is located along the imaginary axis

in $a_\pm$-plane for this case. Furthermore, we conclude that $\Im(a_\pm) > 1$ ($|a_\pm| > 1$) and the late-time approximation condition $t' \gg \frac{z}{\hat{v}}\cos\hat{\theta}_t$. Therefore, the argument of $a_\pm$ is $\pi/2$. For the branch cut shown in 6.1, we find that the argument of the square root $\sqrt{a_\pm^2+1}$ must be $\pi/2$ as well. From (6.3), we choose $s_+ = -1$ and $s_- = +1$ in (6.3), which allows us to write

$$e(\beta) \approx u\left(t' - \frac{z}{\hat{v}}\cos\hat{\theta}_t\right)\left\{e^{a_+\zeta} + \frac{\left(\beta\frac{z}{\hat{v}}\cos\hat{\theta}_t - t'\sqrt{\beta^2+\omega_p^2}\right)[J_1(\zeta) - a_+J_0(\zeta)]}{2\omega_p\sqrt{t'^2 - \left(\frac{z}{\hat{v}}\cos\hat{\theta}_t\right)^2}(a_+^2+1)}\right.$$
$$\left. + \frac{\left(\beta\frac{z}{\hat{v}}\cos\hat{\theta}_t + t'\sqrt{\beta^2+\omega_p^2}\right)[J_1(\zeta) - a_-J_0(\zeta)]}{2\omega_p\sqrt{t'^2 - \left(\frac{z}{\hat{v}}\cos\hat{\theta}_t\right)^2}(a_-^2+1)}\right\}; \quad \beta > a, \tag{6.13}$$

and

$$f(\beta) \approx -\frac{u\left(t' - \frac{z}{\hat{v}}\cos\hat{\theta}_t\right)}{\sqrt{\alpha^2+\omega_p^2}}\left\{-e^{a_+\zeta} + \frac{\left(\beta\frac{z}{\hat{v}}\cos\hat{\theta}_t - t'\sqrt{\beta^2+\omega_p^2}\right)[J_1(\zeta) - a_+J_0(\zeta)]}{2\omega_p\sqrt{t'^2 - \left(\frac{z}{\hat{v}}\cos\hat{\theta}_t\right)^2}(a_+^2+1)}\right.$$
$$\left. - \frac{\left(\beta\frac{z}{\hat{v}}\cos\hat{\theta}_t + t'\sqrt{\beta^2+\omega_p^2}\right)[J_1(\zeta) - a_-J_0(\zeta)]}{2\omega_p\sqrt{t'^2 - \left(\frac{z}{\hat{v}}\cos\hat{\theta}_t\right)^2}(a_-^2+1)}\right\}; \quad \beta > a. \tag{6.14}$$

For the case $\beta = a$, we choose $s_\pm = +1$ in (6.3); therefore,

$$e(\beta) \approx u\left(t' - \frac{z}{\hat{v}}\cos\hat{\theta}_t\right)\left\{\frac{\left(\beta\frac{z}{\hat{v}}\cos\hat{\theta}_t - t'\sqrt{\beta^2+\omega_p^2}\right)[J_1(\zeta) - a_+J_0(\zeta)]}{2\omega_p\sqrt{t'^2 - \left(\frac{z}{\hat{v}}\cos\hat{\theta}_t\right)^2}(a_+^2+1)}\right.$$
$$\left. + \frac{\left(\beta\frac{z}{\hat{v}}\cos\hat{\theta}_t + t'\sqrt{\beta^2+\omega_p^2}\right)[J_1(\zeta) - a_-J_0(\zeta)]}{2\omega_p\sqrt{t'^2 - \left(\frac{z}{\hat{v}}\cos\hat{\theta}_t\right)^2}(a_-^2+1)}\right\}, \quad \beta = a, \tag{6.15}$$

and

$$f(\beta) \approx -\frac{u\left(t' - \frac{z}{\hat{v}}\cos\hat{\theta}_t\right)}{\sqrt{\alpha^2+\omega_p^2}}\left\{\frac{\left(\beta\frac{z}{\hat{v}}\cos\hat{\theta}_t - t'\sqrt{\beta^2+\omega_p^2}\right)[J_1(\zeta) - a_+J_0(\zeta)]}{2\omega_p\sqrt{t'^2 - \left(\frac{z}{\hat{v}}\cos\hat{\theta}_t\right)^2}(a_+^2+1)}\right.$$

$$- \left. \frac{\left(\beta\frac{z}{\hat{v}}\cos\hat{\theta}_t + t'\sqrt{\beta^2+\omega_p^2}\right)\left[J_1(\zeta) - a_- J_0(\zeta)\right]}{2\omega_p\sqrt{t'^2 - \left(\frac{z}{\hat{v}}\cos\hat{\theta}_t\right)^2}(a_-^2+1)} \right\}; \quad \beta = a. \tag{6.16}$$

In summary, the late-time approximations for $e(\beta)$ and $f(\beta)$ can be written as

$$\begin{aligned} e(\beta) \approx\ & u\left(t' - \frac{z}{\hat{v}}\cos\hat{\theta}_t\right)\left\{e^{a-\zeta}u(a-\beta) + e^{a+\zeta}u(\beta-a)\right. \\ & + \frac{\left(\beta\frac{z}{\hat{v}}\cos\hat{\theta}_t - t'\sqrt{\beta^2+\omega_p^2}\right)\left[J_1(\zeta) - a_+ J_0(\zeta)\right]}{2\omega_p\sqrt{t'^2 - \left(\frac{z}{\hat{v}}\cos\hat{\theta}_t\right)^2}(a_+^2+1)} \\ & \left. + \frac{\left(\beta\frac{z}{\hat{v}}\cos\hat{\theta}_t + t'\sqrt{\beta^2+\omega_p^2}\right)\left[J_1(\zeta) - a_- J_0(\zeta)\right]}{2\omega_p\sqrt{t'^2 - \left(\frac{z}{\hat{v}}\cos\hat{\theta}_t\right)^2}(a_-^2+1)} \right\}, \end{aligned} \tag{6.17}$$

and

$$\begin{aligned} f(\beta) \approx\ & -\frac{u\left(t' - \frac{z}{\hat{v}}\cos\hat{\theta}_t\right)}{\sqrt{\alpha^2+\omega_p^2}}\left\{e^{a-\zeta}u(a-\beta) - e^{a+\zeta}u(\beta-a)\right. \\ & + \frac{\left(\beta\frac{z}{\hat{v}}\cos\hat{\theta}_t - t'\sqrt{\beta^2+\omega_p^2}\right)\left[J_1(\zeta) - a_+ J_0(\zeta)\right]}{2\omega_p\sqrt{t'^2 - \left(\frac{z}{\hat{v}}\cos\hat{\theta}_t\right)^2}(a_+^2+1)} \\ & \left. - \frac{\left(\beta\frac{z}{\hat{v}}\cos\hat{\theta}_t + t'\sqrt{\beta^2+\omega_p^2}\right)\left[J_1(\zeta) - a_- J_0(\zeta)\right]}{2\omega_p\sqrt{t'^2 - \left(\frac{z}{\hat{v}}\cos\hat{\theta}_t\right)^2}(a_-^2+1)} \right\}. \end{aligned} \tag{6.18}$$

Note that the late-time expressions in (6.17) and (6.18) only consist of the zeroth and first order Bessel functions. Therefore, the late-time results are much easier to compute than the exact, closed-form transient field expressions.

Fig. 6.2 shows a comparison between the results produced by the exact, closed-form expression and the late-time approximations (6.17) and (6.18). As can been

seen, the late-time approximate results are accurate over a large portion of the waveform.

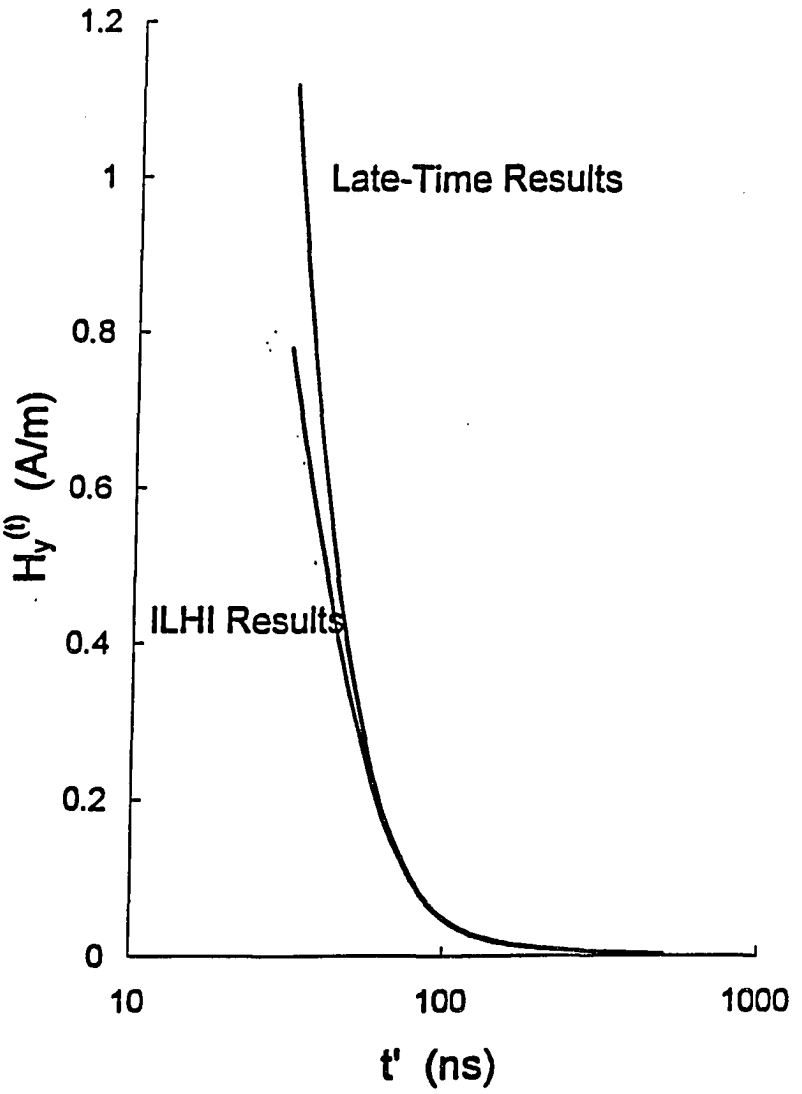


Figure 6.2: A comparison between the closed-form ILHI's expression, and the transmitted transient magnetic fields associated with double exponential excitations computed using the late-time approximation. The parameters are defined as $\sigma = 2 \times 10^{-2} \mho/m$, $\epsilon = 10\epsilon_0$, $\mu = \mu_0$, $z = 10cm$, $\alpha_1 = 5.9 \times 10^7 sec^{-1}$, and $\alpha_2 = 2.1 \times 10^8 sec^{-1}$.

# CHAPTER 7

## The Effects of Neglecting Displacement Currents when Studying Transient Wave Propagation in the Earth

There are many applications which can benefit from the results developed in the previous chapters. In this chapter, we present one example which investigates the effects of neglecting the displacement currents when studying transient plane wave propagation in the earth.

The transient response of an electromagnetic plane wave obliquely incident upon the earth has been of interest to scientists in exploration geophysics for some time [14, 48]. Since there previously was no analytical, closed-form solution (i.e., a solution consisting of readily computable special functions) available even for the problem of a transient plane wave obliquely incident on a conductive half-space, people often resorted to using a diffusion approximation, thereby allowing for the analytical computation of the required inverse Fourier or Laplace transform. In the diffusion approximation, the displacement current is neglected in the earth, thereby reducing the wave equation to the simpler diffusion equation [14]. We propose to use the previously developed analytical expressions to determine the error associated with the diffusion approximation.

## 7.1 Exact Transient Field Representations

We assume that the incident fields for the TE and TM polarizations are defined by

$$\left.\begin{array}{l} E_y^{(i)}(x,z,t) \\ \\ H_y^{(i)}(x,z,t) \end{array}\right\} = u\left(t - \frac{x}{c}\sin\theta_i - \frac{z}{c}\cos\theta_i\right). \tag{7.1}$$

Note that this incident plane wave arrives at the origin of the coordinate system at the time $t = 0$.

In Chapter 4, we demonstrated that the transmitted field for the TE polarization can be represented in closed-form as (4.7)

$$E_y^{(t)}(x,z,t) = \frac{2e^{-at'}}{b_e^2 - 1}\left[b_e J_0\left(\omega_p\sqrt{t'^2 - \frac{z^2}{\hat{v}^2}\cos^2\hat{\theta}_t}\right) u\left(t' - \frac{z}{\hat{v}}\cos\hat{\theta}_t\right)\right.$$

$$\left. + \; b_e(\beta_0 - a)f(\beta_0) - e(\beta_0)\right]. \tag{7.2}$$

Following the same procedure as in Chapter 5, we find that the exact, closed-form transmitted TM magnetic field associated with a unit-step input is given by

$$H_y^{(t)}(x,z,t) = \frac{2e^{-at'}}{b_h^2 - 1}\left\{b_h\left[J_0\left(\omega_p\sqrt{t'^2 - \frac{z^2}{\hat{v}^2}\cos^2\hat{\theta}_t}\right) u\left(t' - \frac{z}{\hat{v}}\cos\hat{\theta}_t\right)\right.\right.$$

$$\left. - \; \frac{(2a + \rho + s_1)s_1 + 2a\rho}{s(s_1 - s_2)}f(\beta_1) - \frac{(2a + \rho + s_2)s_2 + 2a\rho}{s(s_2 - s_1)}f(\beta_2)\right.$$

$$- \frac{\rho^2}{s_1 s_2} e(-a) - \frac{(s_1+\rho)^2}{s_1(s_1-s_2)} e(\beta_1) - \frac{(s_2+\rho)^2}{s_1(s_2-s_1)} e(\beta_2) \Bigg] \Bigg\}. \qquad (7.3)$$

Since the ILHIs in the expressions (7.2) and (7.3) can be efficiently computed using the asymptotic and convergent series expansions in [9] and [25], we use these expressions to compute the "exact" transient fields which are later employed to check the validity of the diffusion approximation.

## 7.2 Approximate Diffusion Representations

In this section, we solve for the transmitted diffusion fields by neglecting all displacement currents in the conductive half-space. We consider the TE case first.

We start with Maxwell's equations,

$$\left.\begin{aligned} \nabla \times \mathbf{E} + \tfrac{\partial \mathbf{B}}{\partial t} &= 0 \\ \nabla \cdot \mathbf{B} &= 0 \\ \nabla \times \mathbf{H} - \tfrac{\partial \mathbf{D}}{\partial t} &= \sigma \mathbf{E} \\ \nabla \cdot \mathbf{D} &= 0 \end{aligned}\right\}. \qquad (7.4)$$

In the air region, $\epsilon = \epsilon_0$, so the transient fields must satisfy the standard wave equation. In the conductive half-space, we allow the conduction currents to dominate,

which leads to the diffusion equation

$$\nabla^2 E_{yap} - \mu\sigma \frac{\partial E_{yap}}{\partial t} = 0, \tag{7.5}$$

where the subscript *yap* denotes the y-component of the approximate electric field. In order to eliminate the time derivative, we take the Laplace transform of both sides of (7.5), so that

$$(\nabla^2 - \gamma_{ap}^2)\tilde{\mathbf{E}}_{\mathbf{ap}}(x, z, s) = 0, \tag{7.6}$$

where

$$\gamma_{ap} = \sqrt{\mu\sigma s} \tag{7.7}$$

is the complex propagation constant assuming negligible displacement currents. The general solution of (7.6) is

$$\tilde{\mathbf{E}}_{\mathbf{ap}}(x, z, s) = \hat{\mathbf{y}}\tilde{E}_{yap} = \hat{\mathbf{y}}\tilde{E}_0(s)\exp(\mp\boldsymbol{\gamma}_{ap} \cdot \boldsymbol{r}), \tag{7.8}$$

where

$$\boldsymbol{\gamma}_{ap} = \gamma_{xap}\hat{\mathbf{x}} + \gamma_{zap}\hat{\mathbf{z}}. \tag{7.9}$$

Due to the phase matching condition, we know that $\gamma_{xap} = \frac{s}{c}\sin\theta_i$. Therefore,

$$\gamma_{zap} = \sqrt{\gamma_{ap}^2 - \gamma_{xap}^2} = \sqrt{\mu\sigma s - \frac{s^2}{c^2}\sin^2\theta_i} = \frac{1}{c}\sqrt{\mu\sigma c^2 s - s^2\sin^2\theta_t}. \tag{7.10}$$

The obliquely incidence electric field is given by

$$\tilde{E}_{yap}^{(i)}(x, z, s) = \tilde{E}_0 e^{-\frac{s}{c}(x\sin\theta_i + z\cos\theta_i)}, \tag{7.11}$$

where $\tilde{E}_0$ is the amplitude of the incident waveform. Likewise, the reflected and transmitted fields are given by

$$\tilde{E}^{(r)}_{yap}(x,z,s) = \tilde{E}_0 R^{TE}_{ap} e^{-\frac{s}{c}(x\sin\theta_r - z\cos\theta_r)} \tag{7.12}$$

and

$$\tilde{E}^{(t)}_{yap}(x,z,s) = \tilde{E}_0 T^{TE}_{ap} e^{-(\gamma_{xap}x + \gamma_{zap}z)}, \tag{7.13}$$

where $R^{TE}_{ap}$ and $T^{TE}_{ap}$ are the approximate TE reflection and transmission coefficients, respectively.

Employing Faraday law $\nabla \times \tilde{\mathbf{E}} = -s\mu\tilde{\mathbf{H}}$, we find that the corresponding magnetic fields are given by

$$\tilde{H}^{(i)}_{xap}(x,z,s) = -\frac{1}{c\mu_0}\cos\theta_i \tilde{E}_0 e^{-\frac{s}{c}(x\sin\theta_i + z\cos\theta_i)}, \tag{7.14}$$

$$\tilde{H}^{(r)}_{xap}(x,z,s) = \frac{R^{TE}_{ap}}{c\mu_0}\cos\theta_i \tilde{E}_0 e^{-\frac{s}{c}(x\sin\theta_i - z\cos\theta_i)}, \tag{7.15}$$

$$\tilde{H}^{(t)}_{xap}(x,z,s) = -\frac{T^{TE}_{ap}}{s\mu}\tilde{E}_0 \frac{\sqrt{\mu\sigma c^2 s - s^2\sin^2\theta_i}}{c} e^{-(\frac{x}{c}s\sin\theta_i + \frac{z}{c}\sqrt{\mu\sigma c^2 s - s^2\sin^2\theta_i})}. \tag{7.16}$$

After enforcing the boundary conditions (i.e., $\tilde{E}_{yap}$ and $\tilde{H}_{xap}$ continuous at $z = 0$), we find that

$$T^{TE}_{ap} = \frac{2\cos\theta_i s\mu}{\cos\theta_i s\mu + \mu_0\sqrt{\mu\sigma c^2 s - s^2\sin\theta_i}}. \tag{7.17}$$

In order to neglect the displacement currents in the earth, we have assumed that $\sigma \gg |s|\epsilon$. Since $\epsilon \geq \epsilon_0$, and $\sigma \gg |s|\epsilon_0$, we can further simplify the approximate field expressions as follows:

$$\tilde{E}^{(t)}_{yap}(x,z,s) = \frac{2\cos\theta_i\sqrt{\mu\epsilon_0}e^{-z\sqrt{\mu\sigma s}}}{\sqrt{\mu_0\sigma s}}. \tag{7.18}$$

The transient transmitted electric field is given by the inverse Laplace transform of (7.18). Employing the Laplace transform formula for (7.18), we have [1],

$$E_{yap}^{(t)}(x,z,t) = \frac{2\cos\theta_i\sqrt{\mu\epsilon_0}}{\sqrt{\mu_0\sigma}}\frac{e^{-\frac{z^2\mu\sigma}{4t}}}{\sqrt{\pi t}}u(t). \tag{7.19}$$

For the TM case, we once again start from Maxwell's equations and obtain the simplified wave equation

$$(\nabla^2 - \gamma_{ap}^2)\tilde{H}_{yap}(x,z,s) = 0. \tag{7.20}$$

Follow the same procedure used to derive $\tilde{E}_{yap}^{(t)}$, we find that the approximate TM transmission coefficient is given by

$$T_{ap}^{TM} = \frac{2\cos\theta_i\sigma}{\cos\theta_i\sigma + \epsilon_0\sqrt{\sigma\mu c^2 s - s^2\sin^2\theta_i}}. \tag{7.21}$$

Thus, the approximate transmitted magnetic field associated with a unit-step input can be written as

$$\tilde{H}_{yap}^{(t)}(x,z,s) = \frac{2\cos\theta_i\sqrt{\frac{\mu_0\sigma}{\epsilon_0}}e^{-z\sqrt{\mu\sigma s}}}{s\left(\sqrt{s} + \cos\theta_i\sqrt{\frac{\mu_0\sigma}{\epsilon_0}}\right)}. \tag{7.22}$$

Using the Laplace transform pair, the transient magnetic field associated with the unit-step input is found to be

$$\begin{aligned} H_{yap}^{(t)}(x,z,t) &= \left[\text{erfc}\left(\frac{z\sqrt{\mu\sigma}}{2\sqrt{t}}\right) - \exp\left(\cos\theta_i\sqrt{\frac{\mu_0\sigma}{\epsilon_0}}z\right)\exp\left(\frac{\cos^2\theta_i\sigma}{\mu}\sqrt{\frac{\mu_0}{\epsilon_0}}\right)\right. \\ &\times \left.\text{erfc}\left(\cos\theta_i\sqrt{\frac{\sigma\mu_0}{\epsilon_0\mu}}t + \frac{z\sqrt{\mu\sigma}}{2\sqrt{t}}\right)\right]u(t) \end{aligned} \tag{7.23}$$

where erfc(x) denotes the complementary error function [1]. It should be noted that using the late-time condition $t \gg \frac{z}{\hat{v}}\cos\hat{\theta}_t$ together with the condition that time is

much larger than the relaxation time $t \gg \epsilon/\sigma$, allows the diffusion results in (7.19) and (7.23) to be derived directly from the exact, closed-form solutions in (7.2) and (7.3). Thus, as previously noted by Wait [48], the diffusion approximations are valid when $t \gg \max\left(\frac{z}{\hat{v}}\cos\hat{\theta}_t, \epsilon/\sigma\right)$. It is also interesting to note that the approximate diffusion results in (7.19) and (7.23) have the same functional form as the expressions given in [48], after the typographical errors in [48] have been corrected.

## 7.3 Error Analysis

In this section, we use the exact Laplace transform domain field expressions to obtain a better understanding of the source for the errors in the diffusion expressions. Using the condition $\sigma \gg |s|\epsilon$, which was employed to obtain the approximate diffusion fields, we can approximate the exact TE solution (2.18) as follows:

$$\lim_{\frac{\sigma}{|s|\epsilon}\to\infty} \tilde{E}_y^{(t)}(x,z,s) = \tilde{E}_{yap}^{(t)}(x,z,s) + \Delta\tilde{E}_y^{(t)}(x,z,s), \tag{7.24}$$

where

$$\begin{aligned}\Delta\tilde{E}_y^{(t)}(x,z,s) \;\approx\; & \frac{2\cos\theta_i\sqrt{\mu\epsilon_0}e^{-z\sqrt{\mu\sigma s}}}{\sqrt{\mu_0\sigma s}}\left[-\frac{\epsilon s}{2\sigma}(1+z\sqrt{\mu\sigma s})\right. \\ & \left. -\;\frac{s\epsilon_0\mu}{\sigma\mu_0}\cos\theta_i + \frac{s\epsilon_0\mu_0}{\sigma\mu}\sin^2\theta_i(1+z\sqrt{\mu\sigma s})\right]\end{aligned} \tag{7.25}$$

is an approximation for the error between the exact solution and the diffusion field. Note that the diffusion field is the first-order term in the approximation, and the error field is represented by the next higher-order term in the series.

Similarly, for the TM case

$$\tilde{H}_y^{(t)}(x,z,s) = \tilde{H}_{yap}^{(t)}(x,z,s) + \Delta\tilde{H}_y^{(t)}(x,z,s), \tag{7.26}$$

where

$$\Delta\tilde{H}_y^{(t)}(x,z,s) \approx -\frac{2\cos\theta_i\sigma}{s(\cos\theta_i\sigma + c\epsilon_0\sqrt{\mu s\sigma})}\frac{\epsilon s}{2\sigma}\cos^2\hat{\theta}_t(1+z\sqrt{\mu\sigma s}). \tag{7.27}$$

We will use (7.25) and (7.27) to gain insight into the sources for errors in the diffusion approximations.

## 7.4 Numerical Results

Reference to (7.19) and (7.23) shows that the diffusion fields violate causality. This aspect was also noted in [14, 48]. Causality relates to the finite amount of time required for a wave to propagate from a source to the field point. This finite propagation time is taken into account by the unit-step function $u\left(t' - \frac{z}{v}\cos\hat{\theta}_t\right)$ which appears in the exact, closed-form expressions for the transient fields (7.2), (7.3), and the canonical integrals (3.29), (3.30). On the other hand, the diffusion results in equations (7.19) and (7.23) contain a unit-step function $u(t)$ which violates causality.

In order to demonstrate the accuracy of the diffusion solutions as a function of the variables in the problem, we plot the percentage relative error, which is defined as

$$\%\ \text{Relative Error} = \frac{|(\text{Exact Field}) - (\text{Diffusion Approximation})|}{|\max_t(\text{Exact Field})|}, \tag{7.28}$$

where $\max_t$ denotes the maximum field with respect to time.

In Figs. 7.1 and 7.2, we plot the time histories of the percentage relative errors for the TM and TE diffusion fields at various depths, $z$. These figures clearly demonstrate that the diffusion fields produce large errors when $t'$ is less than the retarded time, i.e., the diffusion approximation violates causality. For example, the time required for the plane wave to reach $z = 1m$ is about $10ns$. The $z = 1m$ curve shows a large error exists for $t' < 10ns$. In addition to the non-causal results, both the TE and TM diffusion approximations exhibit larger errors at early times than at late times. The initial and final value theorems for the Laplace transform [55], i.e.,

$$\lim_{s\to\infty} sX(s) = x(0^+) \tag{7.29}$$

and

$$\lim_{t\to\infty} x(t) = \lim_{s\to\infty} sX(s), \tag{7.30}$$

show that the early-time response corresponds to the high frequency components, while the late-time response corresponds to the low frequency components. Since the diffusion approximation is a low-frequency approximation (i.e., $\omega \ll \sigma/\epsilon$), the initial and final value theorems show that the largest errors should occur at early time. This is expected since we have previously shown that the diffusion approximation is valid only when $t \gg \max\left(\frac{z}{\hat{v}}\cos\hat{\theta}_t, \epsilon/\sigma\right)$. Since the reflected field is proportional to the field at the interface, the $z = 0$ curves in Figs. 7.1 and 7.2 show the amount of error in the reflected fields.

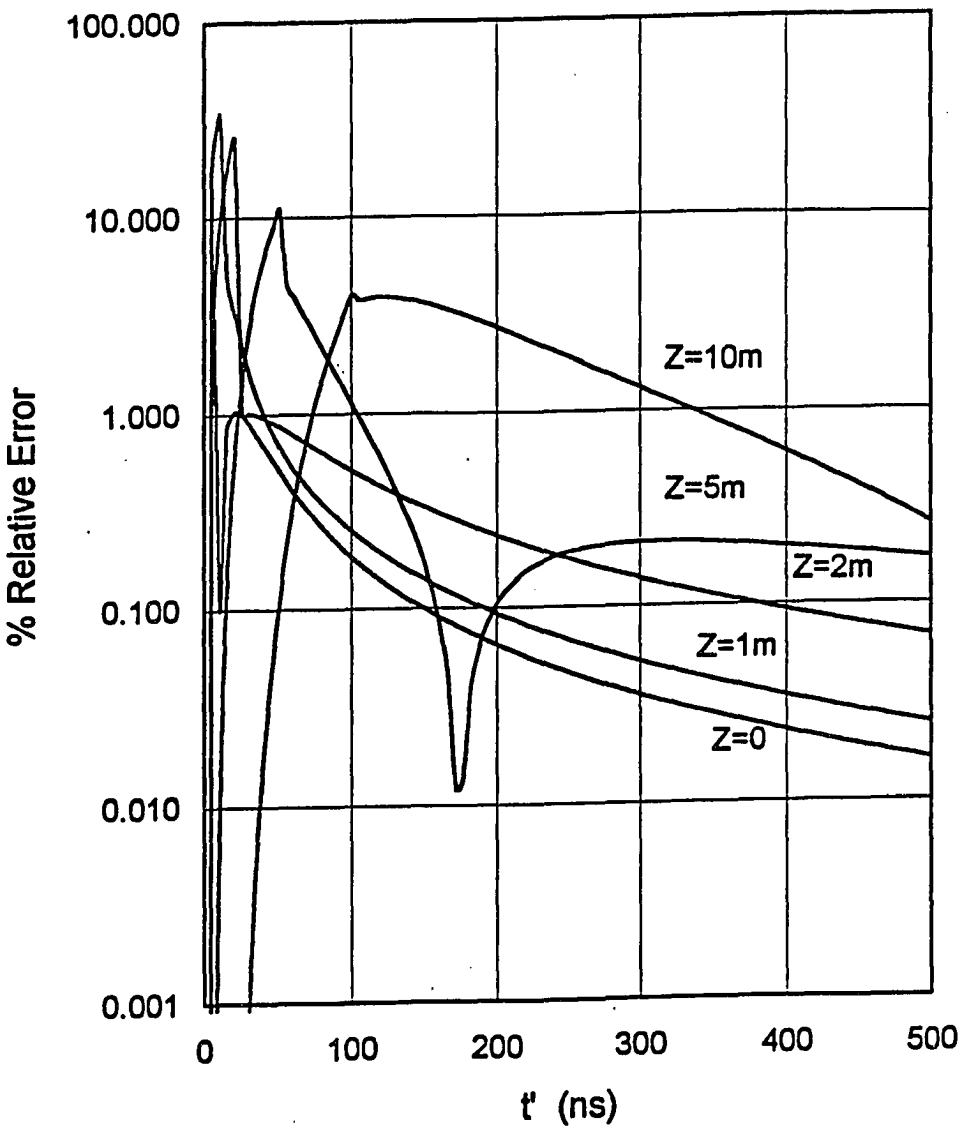


Figure 7.1: The time histories of the percentage relative errors in $H_y^{(t)}$ for different depths, $z$ (TM case). The parameters are defined as $\sigma = 2 \times 10^{-2} \mho/m$, $\epsilon = 10\epsilon_0$, $\mu = \mu_0$, $\theta_i = 45°$.

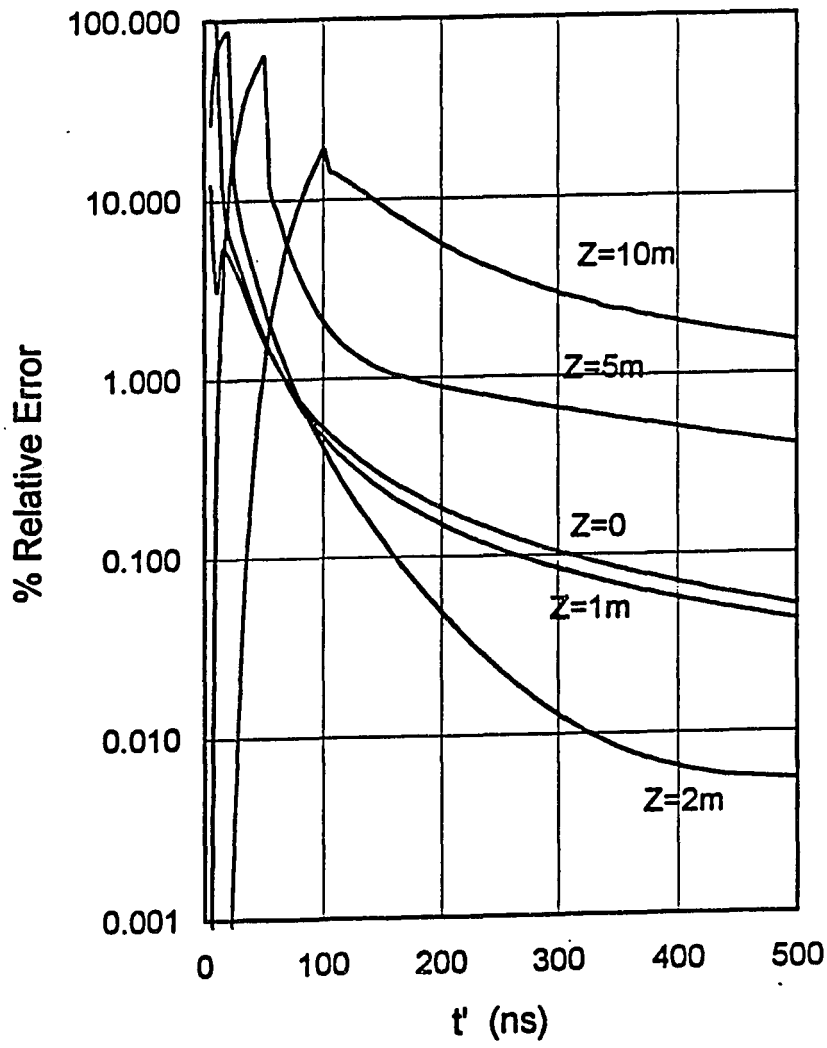


Figure 7.2: The time histories of the percentage relative errors in $E_y^{(t)}$ for different depths, $z$ (TE case). The parameters are defined as $\sigma = 2 \times 10^{-2}\mho/m$, $\epsilon = 10\epsilon_0$, $\mu = \mu_0$, $\theta_i = 45°$.

Fig. 7.3 gives the percentage relative errors plotted as a function of $z$ for $t' = 500ns$. This figure shows that the percentage relative error increases monotonically with increasing depth after a critical depth has been reached. We attribute this behavior to neglecting the higher-order terms, which depend on $z$, when deriving the diffusion approximation (see (7.25) and (7.27)). This behavior is related to the constraint $t \gg \max\left(\frac{z}{\tilde{v}}\cos\hat{\theta}_t, \epsilon/\sigma\right)$. As $z$ increases, $t'$ must also increases before this inequality is satisfied.

Figs. 7.4 and 7.5 present the time histories of the percentage relative errors for the TM and TE fields for different conductivities, $\sigma$. One expects an increase in the error as $\sigma$ becomes smaller since the diffusion fields are based on $\sigma \gg \omega\epsilon$ and $t \gg \max\left(\frac{z}{\tilde{v}}\cos\hat{\theta}_t, \epsilon/\sigma\right)$. This phenomenon is shown mathematically in the error expressions (7.25) and (7.27).

Figs. 7.6 and 7.7 show the time histories of the percentage relative errors for the TM and TE fields for different angles of incidence, $\theta_i$. For the TM case, we see that the error becomes larger as $\theta_i$ becomes smaller. This can be explained by the error terms in (7.27). As $\theta_i$ decreases, $\cos\hat{\theta}_t$ becomes larger, thereby resulting in a large error. For the TE case, the error becomes larger as $\theta_i$ either increases or decreases from $\theta_i = 45°$. Looking at the error terms in (7.25), we find that both $\cos\theta_i$ and $\sin\theta_i$ appear in this expression.

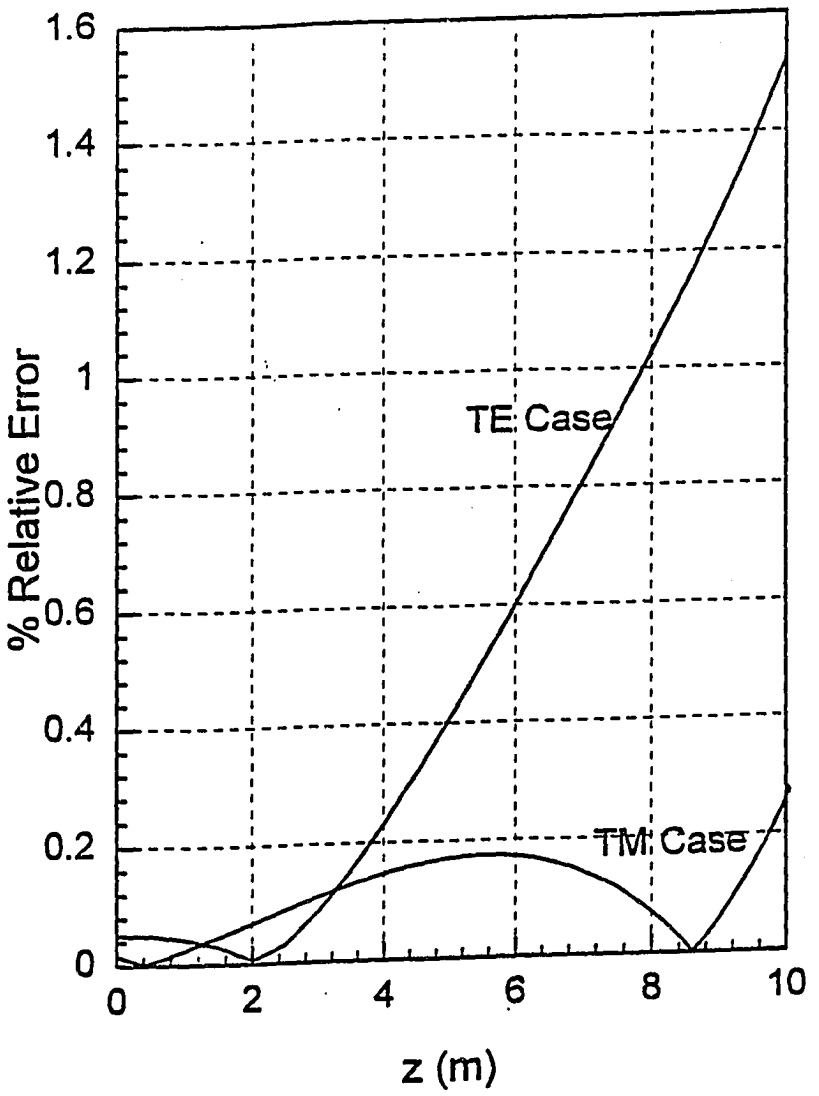


Figure 7.3: The percentage relative errors in $H_y^{(t)}$ and $E_y^{(t)}$ as a function of depth, $z$. The parameters are defined as $\sigma = 2 \times 10^{-2} \mho/m$, $\epsilon = 10\epsilon_0$, $\mu = \mu_0$, $\theta_i = 45°$, $t' = 500ns$.

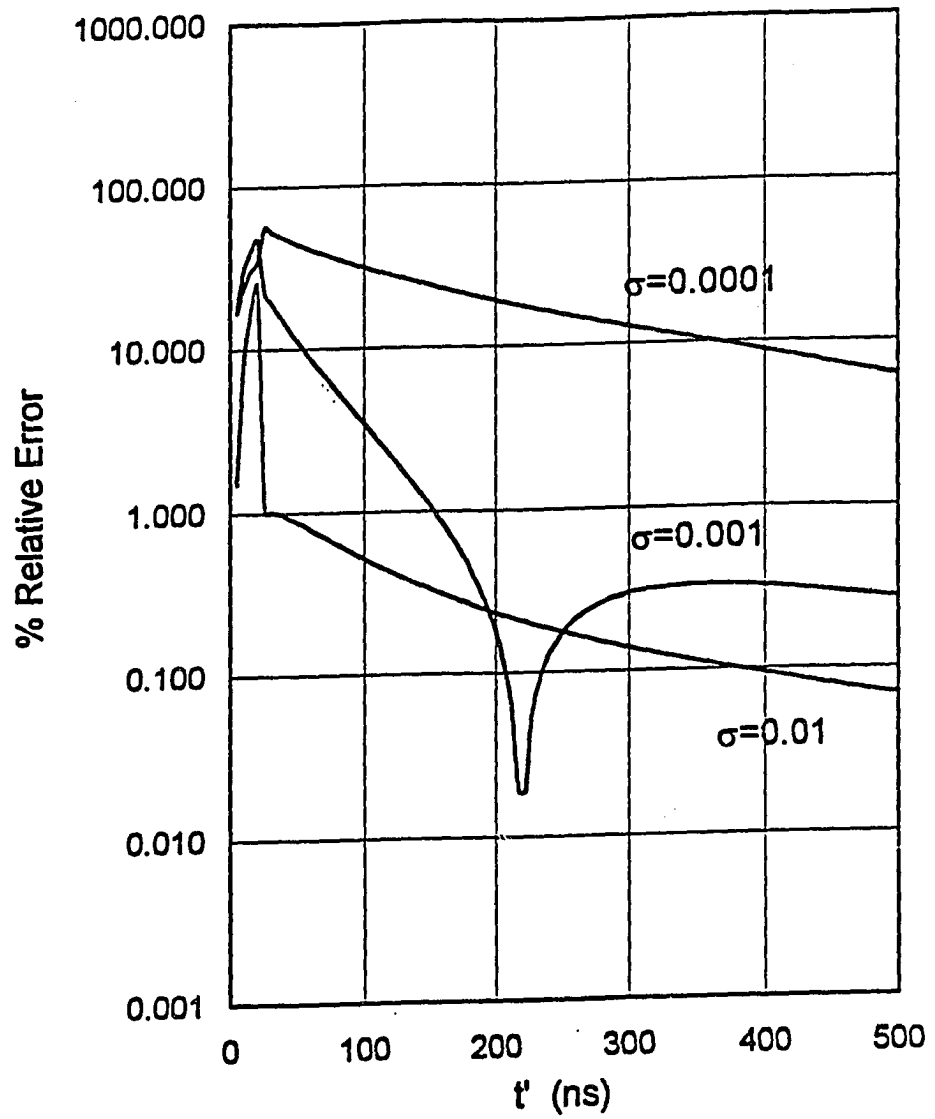


Figure 7.4: The time histories of the percentage relative errors in $H_y^{(t)}$ for different conductivities $\sigma$ (TM case). The parameters are defined as $z = 2m$, $\epsilon = 10\epsilon_0$, $\mu = \mu_0$, $\theta_i = 45°$.

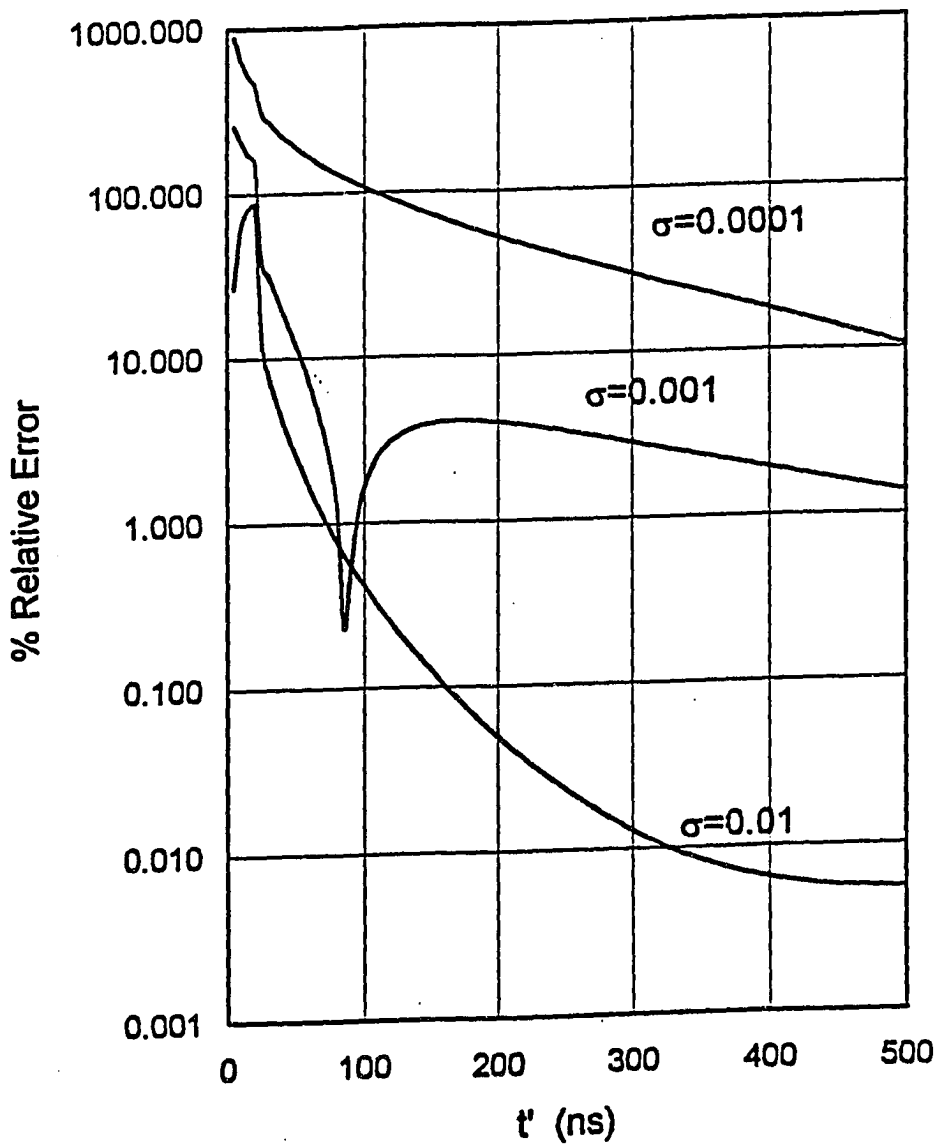


Figure 7.5: The time histories of the percentage relative errors in $E_y^{(t)}$ for different conductivities $\sigma$ (TE case). The parameters are defined as $z = 2m$, $\epsilon = 10\epsilon_0$, $\mu = \mu_0$, $\theta_i = 45°$.

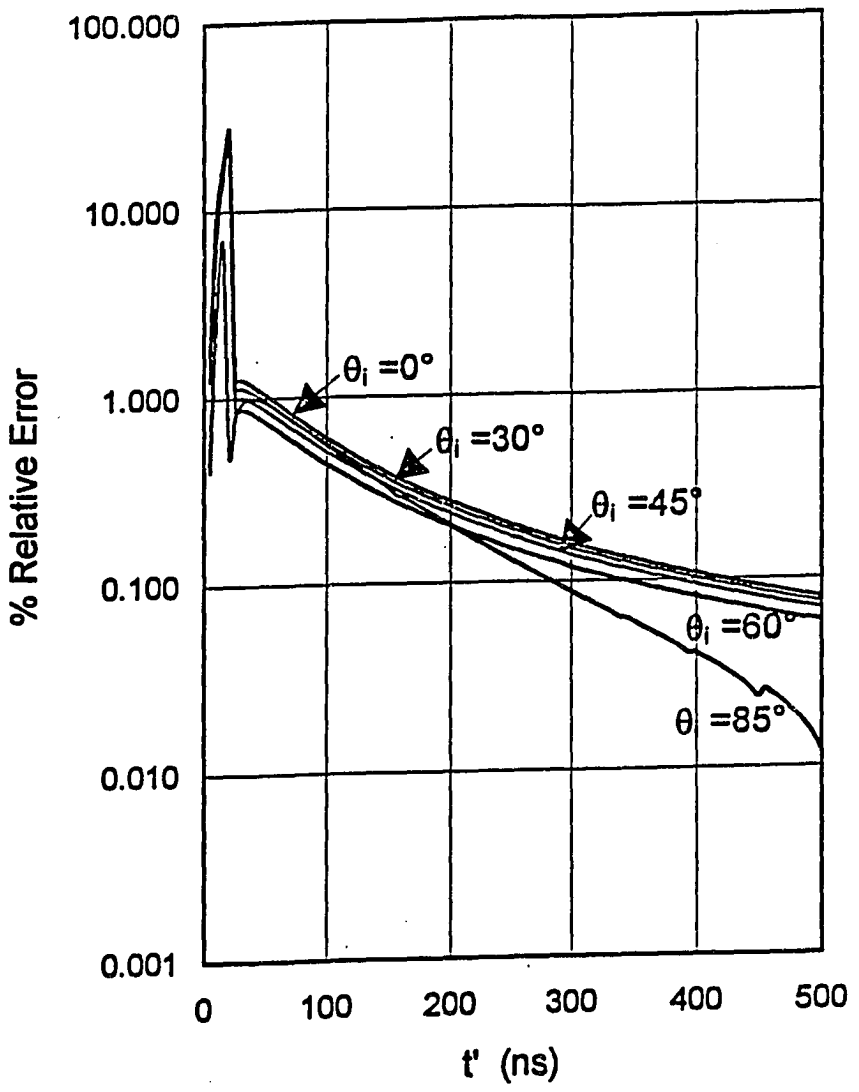


Figure 7.6: The time histories of the percentage relative errors in $H_y^{(t)}$ for different incidence angles, $\theta_i$ (TM case). The parameters are defined as $z = 2m$, $\sigma = 2 \times 10^{-2}\mho/m$, $\epsilon = 10\epsilon_0$, $\mu = \mu_0$, $\theta_i = 45°$.

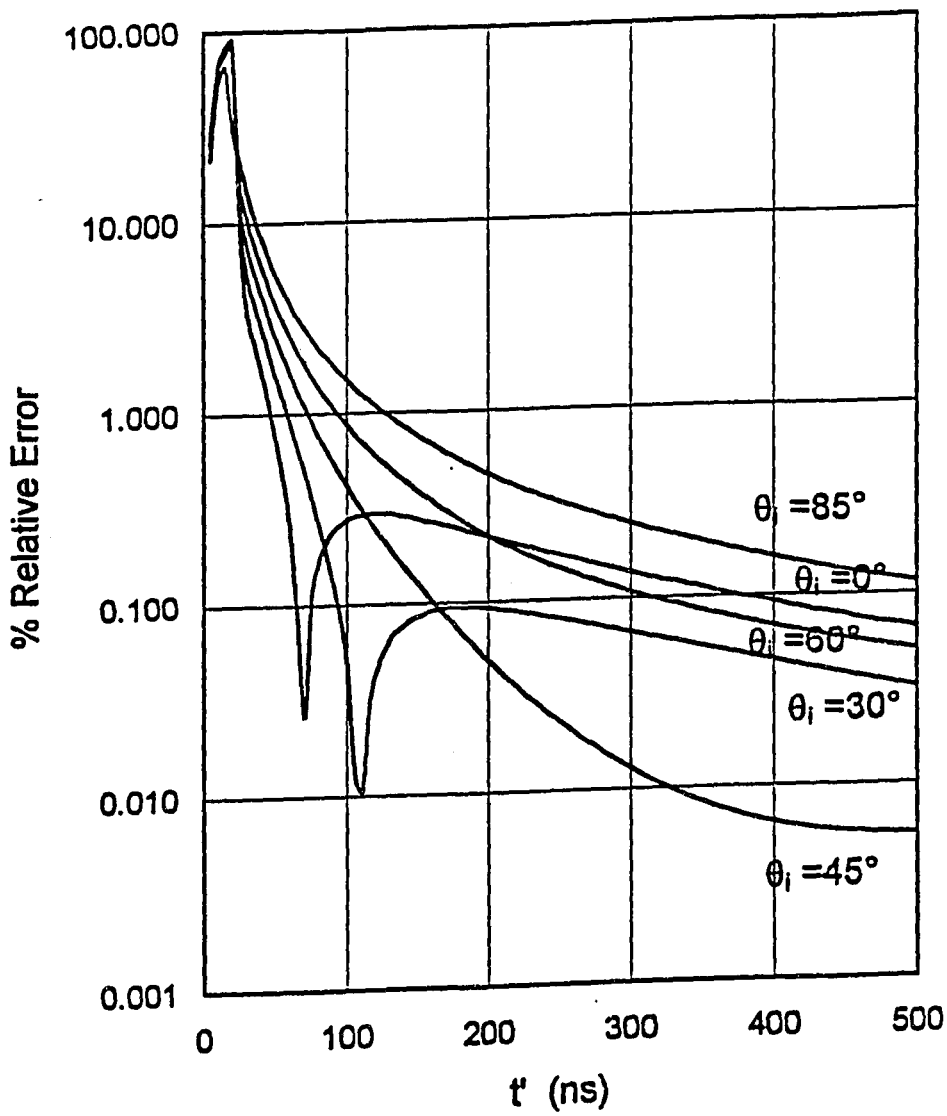


Figure 7.7: The time histories of the percentage relative errors in $E_y^{(t)}$ for different incidence angles, $\theta_i$ (TE case). The parameters are defined as $z = 2m$, $\sigma = 2 \times 10^{-2}\mho/m$, $\epsilon = 10\epsilon_0$, $\mu = \mu_0$.

Figs. 7.8 and 7.9 show the time histories of the percentage relative errors for different permittivities, $\epsilon$. Fig. 7.10 provides a more detailed description of the dependence on changes in $\epsilon$. Since $t \gg \max\left(\frac{z}{\hat{v}}\cos\hat{\theta}_t, \epsilon/\sigma\right)$, larger errors are encountered for larger value of $\epsilon$ (also see (7.25) and (7.27)).

In conclusion, we obtained the diffusion approximations by neglecting the displacement current in the conductive medium. A comparison with the exact transient field representations shows that the diffusion approximation violates causality. However, as has been known for many years [14, 48], the diffusion approximation accurately models the late-time transient behavior, i.e., $t \gg \max\left(\frac{z}{\hat{v}}\cos\hat{\theta}_t, \epsilon/\sigma\right)$.

In the past, the diffusion approximation was used to obtain approximate closed-form expressions for the transient fields. However, as we have demonstrated in this dissertation, exact, closed-form expressions are now available for these fields. Therefore, with some added complexity, the exact, closed-form transient field expressions can be used in place of the diffusion field approximations.

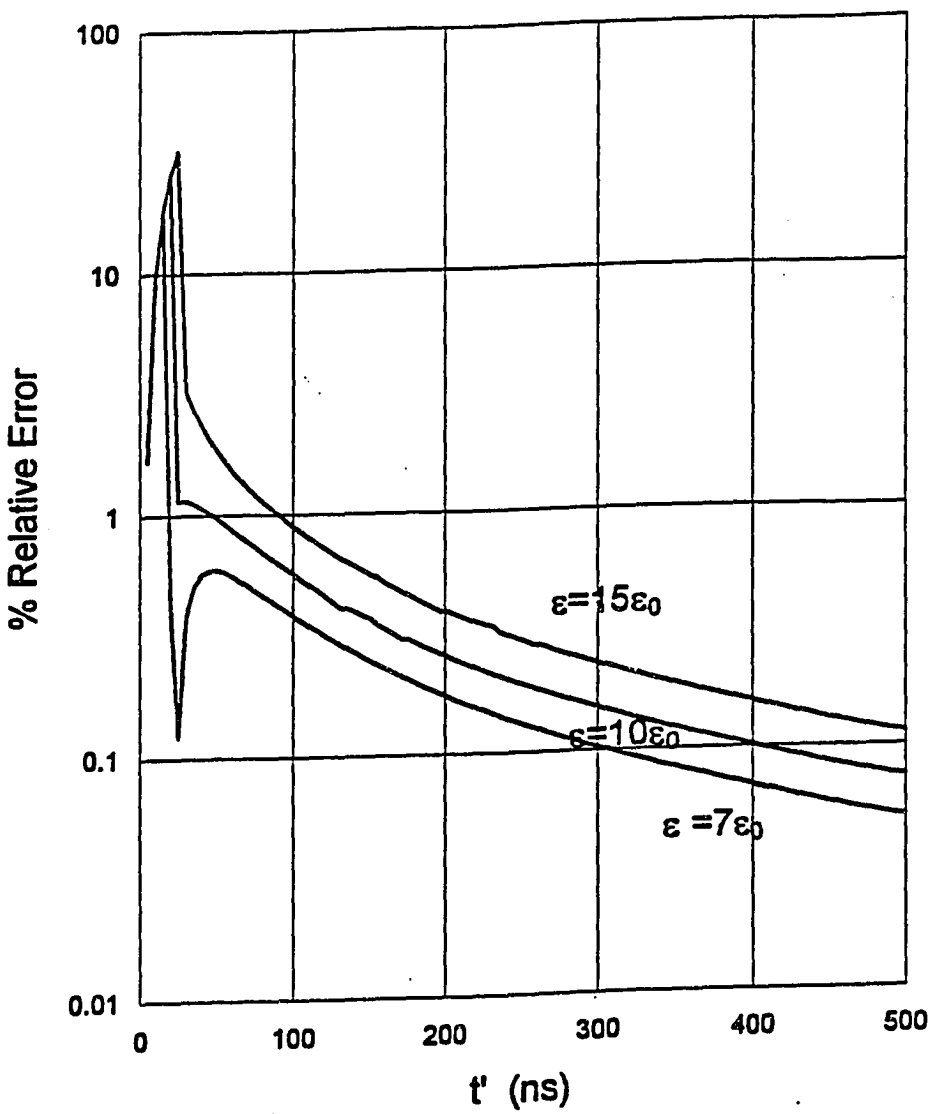


Figure 7.8: The time histories of the percentage relative errors in $H_y^{(t)}$ for different permittivities, $\epsilon$ (TM case). The parameters are defined as $z = 2m$, $\sigma = 2\times10^{-2}\mho/m$, $\theta_i = 30°$.

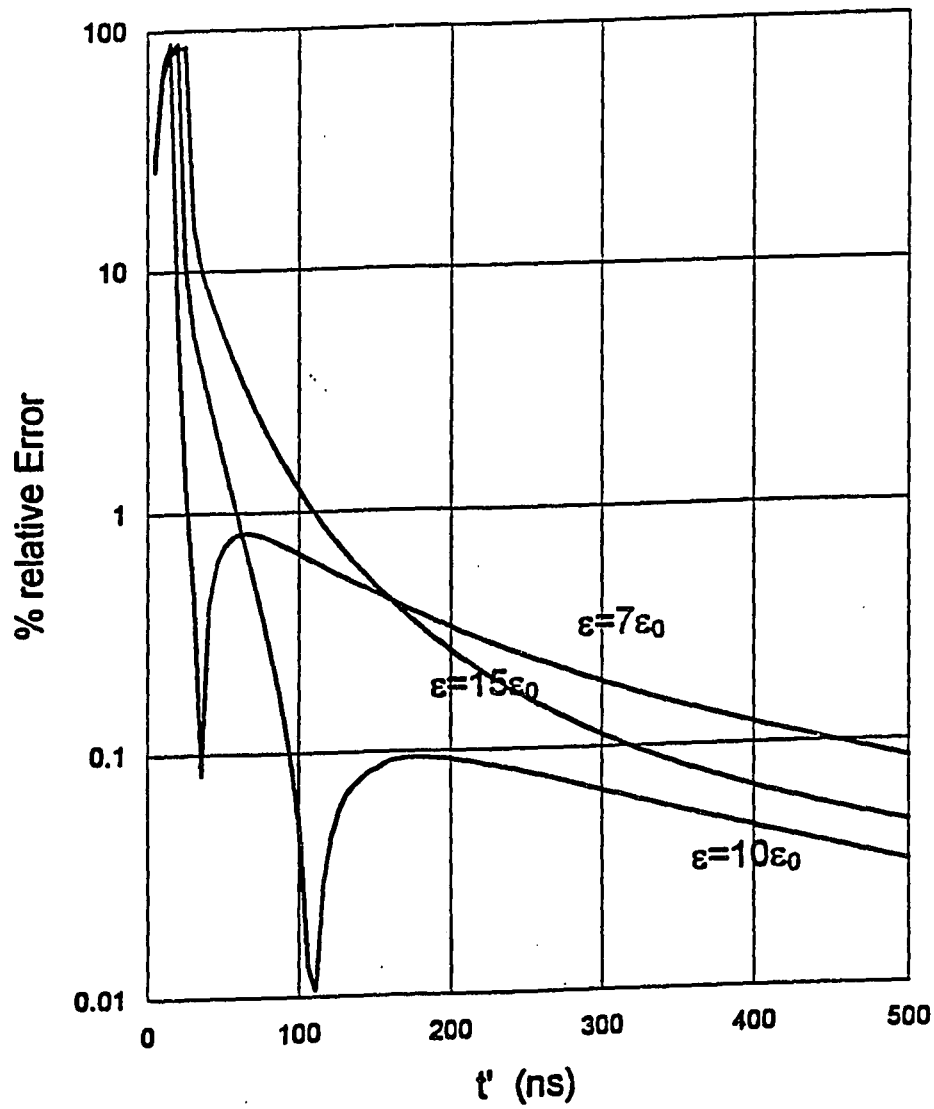


Figure 7.9: The time histories of the percentage relative errors in $E_y^{(t)}$ for different permittivities, $\epsilon$ (TE case). The parameters are defined as $z = 2m$, $\sigma = 2 \times 10^{-2} \mho/m$, $\theta_i = 30°$.

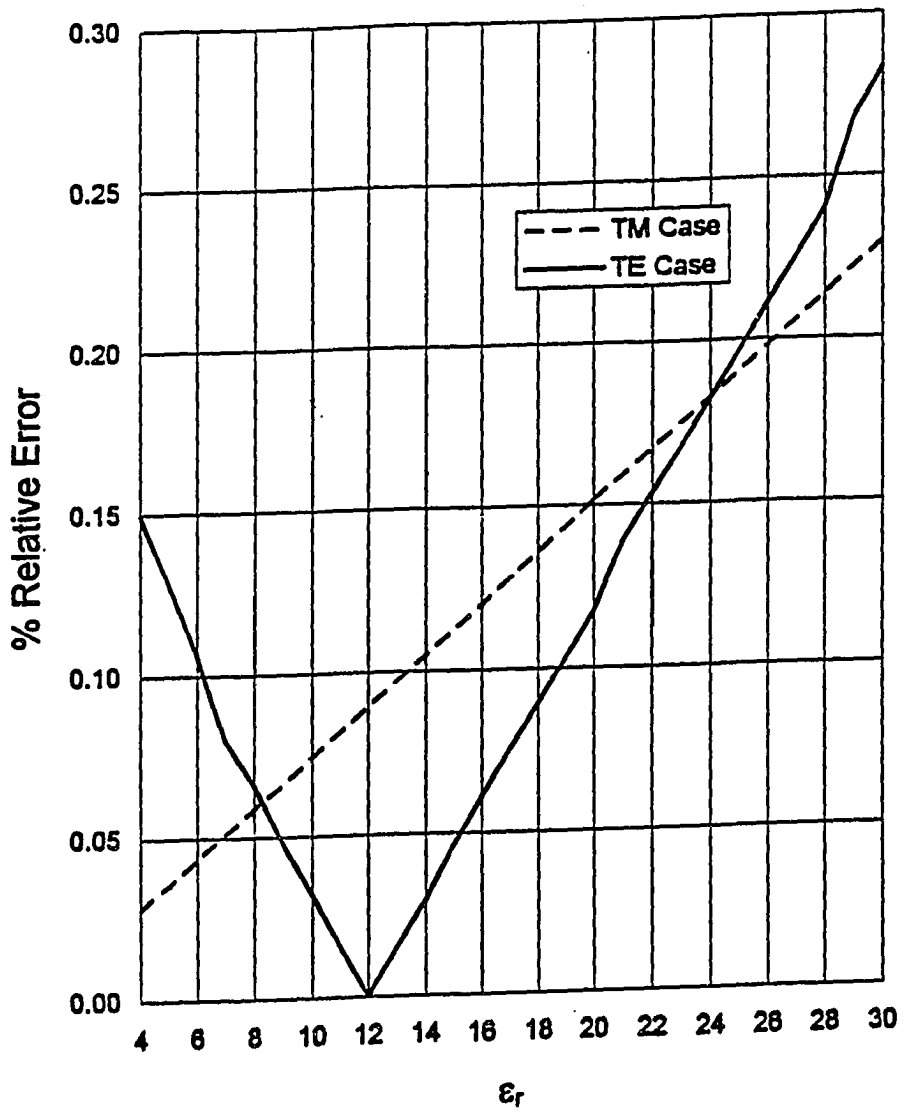


Figure 7.10: The percentage relative errors in $H_y^{(t)}$ and $E_y^{(t)}$ as a function of the relative permittivity, $\epsilon_r$. The parameters are defined as $\sigma = 2 \times 10^{-2} \mho/m$, $\epsilon = 10\epsilon_0$, $\mu = \mu_0$, $\theta_i = 45°$, $t' = 500ns$.

# CHAPTER 8

## Conclusions and Further Work

In this treatise, we have derived exact, closed-form analytical solutions for the interaction between a transient plane wave and a conductive half-space. This is the first time that a closed-form solution has been obtained for this important canonical problem. We began by obtaining expressions for the electromagnetic wave in the Laplace domain. We assumed that the electrical properties of the media are frequency independent. In general, any obliquely incident electromagnetic plane wave is derivable as a linear combination of the two basic polarizations: transverse electric (TE) and transverse magnetic (TM) [15]. By using Maxwell's equations in the Laplace domain and the boundary conditions at the plane interface, we obtained expressions for the electromagnetic fields in all regions.

To return to the time-domain, we multiplied the expressions for the electromagnetic fields in the Laplace domain by the input pulse spectra and then applied an inverse Laplace transform. The inverse Laplace transform integral representations for the fields were shown to possess canonical forms, thereby we were able to express them in terms of two canonical integrals, $f(\beta)$ and $e(\beta)$. These canonical integrals have closed-form analytical expressions involving ILHIs, which are readily computable special functions. In our modeling results, we obtained excellent agreement between

the exact, closed-form solutions and previously published results as well as numerical integration results. We also demonstrated that the closed-form solutions are superior to using an FFT algorithm. The results computed using numerical integration or the FFT required more CPU time than when the closed-form expressions were employed.

The asymptotic expression for the ILHIs was used to formulate relatively simple late-time expressions for the canonical integrals $f(\beta)$ and $e(\beta)$. These late-time expressions proved to be very useful for computing the late-time fields.

The closed-form transient field expressions were used to study the effects of neglecting the displacement currents in the earth. We first derived a relatively simple diffusion approximation for the TE and TM polarization by neglecting the displacement current in the conductive medium. A comparison with the exact transient field representations showed that the diffusion approximation violates causality. However, as has been known for many years [14, 48] the diffusion approximation accurately models the late-time transient behavior, i.e., $t \gg \max\left(\frac{z}{\hat{v}}\cos\hat{\theta}_t, \epsilon/\sigma\right)$.

## 8.1 Future Work

An application that we would like to recommend for further work involves using the results we developed to extract the electrical properties for a conductive half-space. The coordinate system is illustrated in Fig. 8.1. A transient electromagnetic plane wave is assumed normally incident on a conductive half-space such as the earth. A

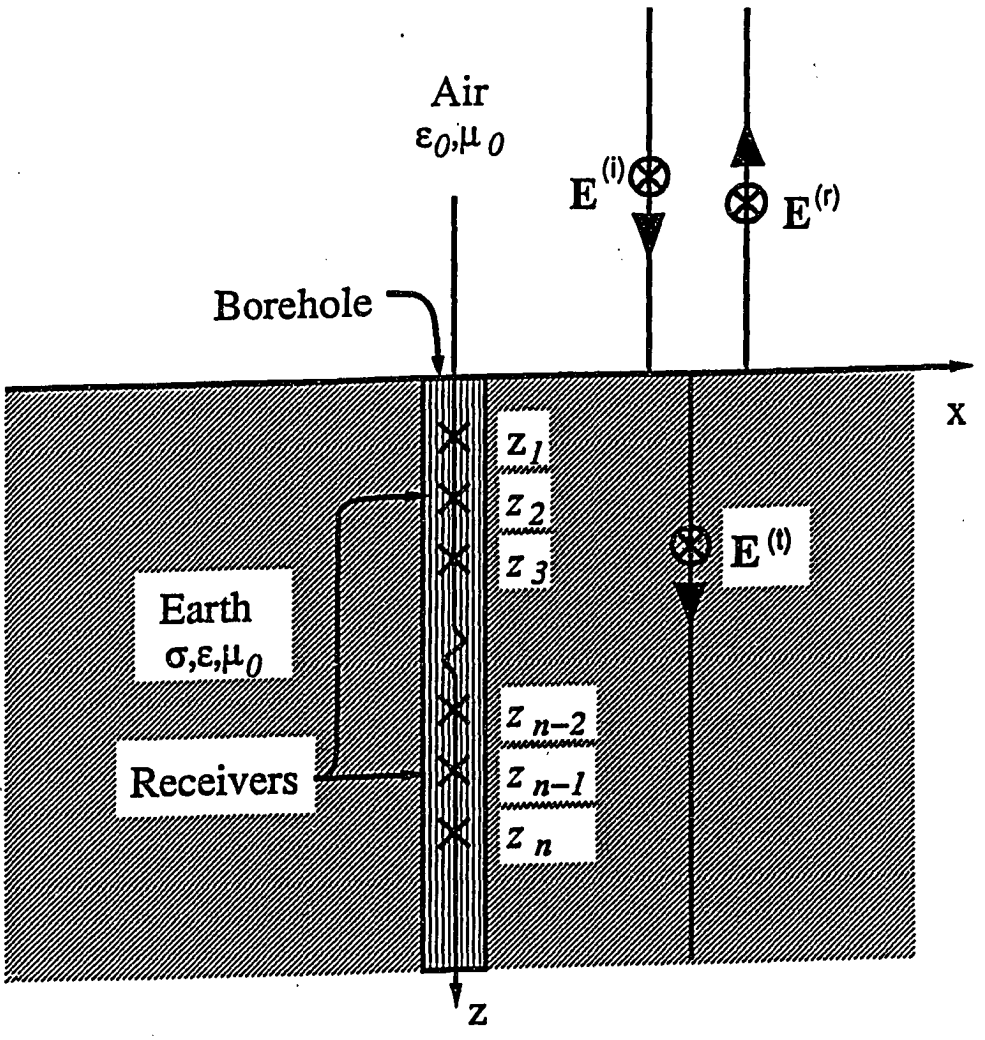


Figure 8.1: System coordinate a plane wave normally incident on a conductive half-space and the borehole where the receivers located.

borehole is drilled perpendicular to the interface. The receivers are located at various depths in the borehole. The source we considered is a unit-step function.

By the standard Laplace transform pair [1]

$$e^{\alpha t} \longleftrightarrow \frac{1}{s-\alpha}, \tag{8.1}$$

the exponential in the time domain corresponds to a pole at $s = \alpha$ in the Laplace domain. For the TE case, if we let the receiver remain stationary, then the transmitted electrical field is proportional to

$$E_y^{(t)} \sim \frac{1}{\sqrt{2\pi a t}}. \tag{8.2}$$

It is clear that this function does not have a pole in the Laplace domain. However, the transmitted electrical field will have a pole if we simulate a moving receiver, i.e.,

$$E_y^{(t)} \sim \frac{e^{-a\chi(\cosh\psi - 1)}}{\sqrt{2\pi a\chi}}, \tag{8.3}$$

where

$$\chi = \sqrt{t^2 - \left(\frac{z}{\hat{v}}\right)^2}, \tag{8.4}$$

and

$$\psi = \tanh^{-1}\frac{z}{\hat{v}t}. \tag{8.5}$$

Thus, the electric field sampled by a moving receiver at a sampling velocity $v_s = \frac{z}{t}$ has a pole at

$$a(\cosh\psi - 1) = \frac{\sigma}{2\epsilon}(\cosh\psi - 1), \tag{8.6}$$

thereby, we obtain

$$a = \frac{\sigma}{2\epsilon}, \tag{8.7}$$

in the Laplace transform domain. Thus, this pole can be used to extract the electric parameters of the medium.

Note that the variable $\chi$ is related to the generalized time interval which is defined in relativity. Thus, $\chi$ is an invariant quantity. The reason why this transform allows for the extraction of $a$ needs further investigation. We believe that a large amount of interesting physics is embedded in this problem. Using the exact, closed-form analytical results we developed, we plan to further investigate this important physical phenomenon.

# Appendix A

## Numerical Integration

In order to validate the closed-form expressions for the transient fields, we also compute the fields using numerical integration [21]. In this appendix, we derive expressions for the convolution integrals which are then integrated numerically. We employ the convolution integral representation for the fields in order to avoid the singularities and infinite integration range present in the spectral representations (see (4.3) and (4.25)).

From (2.18) and (2.33), the transmitted $E$ field in the Laplace domain is:

Unit-step input

$$\tilde{E}_y^{(t)}(x,z,s) = \frac{2e^{-\frac{x}{v}s\sin\hat{\theta}_t}}{b^2-1}\left[b\left(1+\frac{2a-\alpha_0}{s+\alpha_0}\right)\frac{e^{-\frac{z}{v}\cos\hat{\theta}_t\sqrt{(s+a)^2-a^2}}}{\sqrt{(s+a)^2-a^2}} - \frac{e^{-\frac{z}{v}\cos\hat{\theta}_t\sqrt{(s+a)^2-a^2}}}{s+\alpha_0}\right]. \tag{A.1}$$

Double-exponential excitation

$$\tilde{E}_y^{(t)}(x,z,s) = \frac{2Ae^{-\frac{x}{v}s\sin\hat{\theta}_t}}{b^2-1}\left[b\frac{(2a-\alpha_0)\alpha_0(\alpha_1-\alpha_2)}{(\alpha_0-\alpha_1)(\alpha_0-\alpha_2)}\frac{1}{s+\alpha_0}\frac{e^{-\frac{z}{v}\cos\hat{\theta}_t\sqrt{(s+a)^2-a^2}}}{\sqrt{(s+a)^2-a^2}}\right.$$

$$+\ b\frac{(2a-\alpha_1)\alpha_1}{\alpha_1-\alpha_0}\frac{1}{s+\alpha_1}\frac{e^{-\frac{z}{v}\cos\hat{\theta}_t\sqrt{(s+a)^2-a^2}}}{\sqrt{(s+a)^2-a^2}} - b\frac{(2a-\alpha_2)\alpha_2}{\alpha_2-\alpha_0}\frac{1}{s+\alpha_2}\frac{e^{-\frac{z}{v}\cos\hat{\theta}_t\sqrt{(s+a)^2-a^2}}}{\sqrt{(s+a)^2-a^2}}$$

$$\left.-\ \frac{\alpha_0(\alpha_1-\alpha_2)}{(\alpha_0-\alpha_1)(\alpha_0-\alpha_2)}\frac{1}{s+\alpha_0}e^{-\frac{z}{v}\cos\hat{\theta}_t\sqrt{(s+a)^2-a^2}} - \frac{\alpha_1}{\alpha_1-\alpha_0}\frac{1}{s+\alpha_1}e^{-\frac{z}{v}\cos\hat{\theta}_t\sqrt{(s+a)^2-a^2}}\right.$$

$$+ \quad \frac{\alpha_2}{\alpha_2 - \alpha_0} \frac{1}{s + \alpha_2} e^{-\frac{z}{\hat{v}} \cos\hat{\theta}_t \sqrt{(s+a)^2 - a^2}} \Bigg]. \tag{A.2}$$

We will employ the following Laplace transform pairs [1]:

$$e^{-\frac{x}{\hat{v}} s \sin\hat{\theta}_t} \longleftrightarrow \delta\left(t - \frac{x}{\hat{v}} \sin\hat{\theta}_t\right), \tag{A.3}$$

$$\frac{e^{-\frac{x}{\hat{v}} s \sin\hat{\theta}_t}}{s + s_0} \longleftrightarrow e^{-s_0(t - \frac{x}{\hat{v}} \sin\hat{\theta}_t)} u\left(t - \frac{x}{\hat{v}} \sin\hat{\theta}_t\right), \tag{A.4}$$

$$\frac{e^{-\frac{z}{\hat{v}} \cos\hat{\theta}_t \sqrt{(s+a)^2 - a^2}}}{\sqrt{(s+a)^2 - a^2}} \longleftrightarrow e^{-at} I_0\left(a\sqrt{t^2 - \frac{z^2}{v^2}\cos^2\hat{\theta}_t}\right) u\left(t - \frac{z}{\hat{v}} \cos\hat{\theta}_t\right), \tag{A.5}$$

$$e^{-\frac{z}{\hat{v}} \cos\hat{\theta}_t \sqrt{(s+a)^2 - a^2}} \longleftrightarrow e^{-at}\Bigg[\frac{a\frac{z}{\hat{v}}\cos\hat{\theta}_t}{\sqrt{t^2 - \frac{z^2}{v^2}\cos^2\theta_a}} I_1\left(a\sqrt{t^2 - \frac{z^2}{v^2}\cos^2\hat{\theta}_t}\right)$$

$$\times u\left(t - \frac{z}{\hat{v}} \cos\hat{\theta}_t\right) + \delta\left(t - \frac{z}{\hat{v}} \cos\hat{\theta}_t\right)\Bigg], \tag{A.6}$$

where $I_0(x)$ and $I_1(x)$ are the zeroth and first order modified Bessel functions, respectively.

After substituting (A.3) - (A.6) into (A.1) and (A.2), and employing the convolution property of Laplace transform [32], we find the desired convolution integrals:

Unit-step input:

$$E_y^{(t)}(x, z, t) = \frac{2e^{-a(t - \frac{x}{\hat{v}} \sin\hat{\theta}_t)}}{b^2 - 1} b$$

$$\times I_0\left[a\sqrt{\left(t - \frac{x}{\hat{v}} \sin\hat{\theta}_t\right)^2 - \frac{z^2}{v^2}\cos^2\theta_t}\right] u\left(t - \frac{x}{\hat{v}} \sin\hat{\theta}_t - \frac{z}{\hat{v}} \cos\hat{\theta}_t\right)$$

$$+ \frac{2(2a-\alpha_0)}{b^2-1} b e^{-\alpha_0(t-\frac{x}{\hat{v}}\sin\hat{\theta}_t)} \int_{\frac{z}{\hat{v}}\cos\hat{\theta}_t}^{t-\frac{x}{\hat{v}}\sin\hat{\theta}_t} e^{-(a-\alpha_0)\tau} I_0\left(a\sqrt{\tau^2-\frac{z^2}{v^2}\cos^2\theta_t}\right) d\tau$$

$$- \frac{2e^{-\alpha_0(t-\frac{x}{\hat{v}}\sin\hat{\theta}_t)}}{b^2-1} \int_{\frac{z}{\hat{v}}\cos\hat{\theta}_t}^{t-\frac{x}{\hat{v}}\sin\hat{\theta}_t} \frac{a\frac{z}{\hat{v}}\cos\hat{\theta}_t e^{-(a-\alpha_0)\tau}}{\sqrt{\tau^2-\frac{z^2}{v^2}\cos^2\theta_t}} I_1\left(a\sqrt{\tau^2-\frac{z^2}{v^2}\cos^2\theta_t}\right) d\tau$$

$$- \frac{2e^{-a\frac{z}{\hat{v}}\cos\hat{\theta}_t}}{b^2-1} e^{-\alpha_0(t-\frac{x}{\hat{v}}\sin\hat{\theta}_t-\frac{z}{\hat{v}}\cos\hat{\theta}_t)} u\left(t-\frac{x}{\hat{v}}\sin\hat{\theta}_t-\frac{z}{\hat{v}}\cos\hat{\theta}_t\right). \tag{A.7}$$

Double-exponential excitation:

$$E_y^{(t)}(x,z,t) = \frac{2A}{b^2-1}\left\{\frac{\alpha_0(\alpha_1-\alpha_2)}{(\alpha_0-\alpha_1)(\alpha_0-\alpha_2)} e^{-\alpha_0(t-\frac{x}{\hat{v}}\sin\hat{\theta}_t)}\left[b(2a-\alpha_0)\right.\right.$$

$$\times \int_{\frac{z}{\hat{v}}\cos\hat{\theta}_t}^{t-\frac{x}{\hat{v}}\sin\hat{\theta}_t} e^{-(a-\alpha_0)\tau} I_0\left(a\sqrt{\tau^2-\frac{z^2}{v^2}\cos^2\theta_t}\right) d\tau$$

$$- a\frac{z}{\hat{v}}\cos\hat{\theta}_t \int_{\frac{z}{\hat{v}}\cos\hat{\theta}_t}^{t-\frac{x}{\hat{v}}\sin\hat{\theta}_t} \frac{e^{-(a-\alpha_0)\tau}}{\sqrt{\tau^2-\frac{z^2}{v^2}\cos^2\theta_t}} I_1\left(a\sqrt{\tau^2-\frac{z^2}{v^2}\cos^2\theta_t}\right) d\tau$$

$$\left.- e^{-(a-\alpha_0)\frac{z}{\hat{v}}\cos\hat{\theta}_t} u\left(t-\frac{x}{\hat{v}}\sin\hat{\theta}_t-\frac{z}{\hat{v}}\cos\hat{\theta}_t\right)\right]$$

$$+ \frac{\alpha_1}{\alpha_1-\alpha_0} e^{-\alpha_1(t-\frac{x}{\hat{v}}\sin\hat{\theta}_t)}\left[b(2a-\alpha_1)\int_{\frac{z}{\hat{v}}\cos\hat{\theta}_t}^{t-\frac{x}{\hat{v}}\sin\hat{\theta}_t} e^{-(a-\alpha_1)\tau} I_0\left(a\sqrt{\tau^2-\frac{z^2}{v^2}\cos^2\theta_t}\right) d\tau\right.$$

$$\left.- a\frac{z}{\hat{v}}\cos\hat{\theta}_t \int_{\frac{z}{\hat{v}}\cos\hat{\theta}_t}^{t-\frac{x}{\hat{v}}\sin\hat{\theta}_t} \frac{e^{-(a-\alpha_1)\tau}}{\sqrt{\tau^2-\frac{z^2}{v^2}\cos^2\theta_t}} I_1\left(a\sqrt{\tau^2-\frac{z^2}{v^2}\cos^2\theta_t}\right) d\tau\right.$$

$$- \; e^{-(a-\alpha_1)\frac{z}{\hat{v}}\cos\hat{\theta}_t} u\left(t - \frac{x}{\hat{v}}\sin\hat{\theta}_t - \frac{z}{\hat{v}}\cos\hat{\theta}_t\right)\Bigg]$$

$$- \; \frac{\alpha_2}{\alpha_2 - \alpha_0} e^{-\alpha_2(t-\frac{x}{\hat{v}}\sin\hat{\theta}_t)}\Bigg[b(2a-\alpha_2)\int_{\frac{z}{\hat{v}}\cos\hat{\theta}_t}^{t-\frac{x}{\hat{v}}\sin\hat{\theta}_t} e^{-(a-\alpha_2)\tau} I_0\left(a\sqrt{\tau^2 - \frac{z^2}{v^2}\cos^2\theta_t}\right)\, d\tau$$

$$- \; a\frac{z}{\hat{v}}\cos\hat{\theta}_t \int_{\frac{z}{\hat{v}}\cos\hat{\theta}_t}^{t-\frac{x}{\hat{v}}\sin\hat{\theta}_t} \frac{e^{-(a-\alpha_2)\tau}}{\sqrt{\tau^2 - \frac{z^2}{v^2}\cos^2\theta_t}} I_1\left(a\sqrt{\tau^2 - \frac{z^2}{v^2}\cos^2\theta_t}\right)\, d\tau$$

$$- \; e^{-(a-\alpha_2)\frac{z}{\hat{v}}\cos\hat{\theta}_t} u\left(t - \frac{x}{\hat{v}}\sin\hat{\theta}_t - \frac{z}{\hat{v}}\cos\hat{\theta}_t\right)\Bigg]\Bigg\}. \qquad \text{(A.8)}$$

# REFERENCES

[1] M. Abramowitz and I. E. Stegun, *Handbook of Mathematic Functions with Formulas, Graphs, and Mathematical Tables*, U.S. Government Printing Office, Washington, D. C., 1972.

[2] W. L. Anderson and R. K. Moore, "Frequency Spectra of Transient Electromagnetic Pulses in a Conducting Medium", *IRE Trans. Antennas and Propagat.*, vol. AP-8, pp. 603-607, 1960.

[3] P. R. Barnes and F. M. Tesche, "On the Direct Calculation of a Transient Plane Wave Reflected from a Finitely Conducting Half Space", *IEEE Trans. Electromagnetic Compatibility*, Vol. 33, No. 2, pp. 90-96, 1991.

[4] C. E. Baum, "The Reflection of Pulsed Waves from the Surface of a Conducting Dielectric", Theoretical Note 351, Air Force Weapons Lab., Feb. 18, 1967.

[5] B. K. Bhattacharyya, "Propagation of Transient Electromagnetic Waves in a Medium of Finite Conductivity", *Geophysics*, Vol. 22, pp. 75-88, 1957.

[6] B. K. Bhattacharyya, "Propagation of an Electric Pulse through a Homogeneous and Isotropic Medium", *Geophysics*, Vol. 22, pp. 905-921, 1957.

[7] B. K. Bhattacharyya, "Electromagnetic Fields of a Transient Magnetic Dipole on the Earth Surface", *Geophysics*, Vol. 24, pp. 89-108, 1959.

[8] D. G. Dudley, T. M. Papazoglou, and R. C. White, "On The Interaction of a Transient Electromagnetic Plane Wave and a Lossy Half-Space", *J. Appl. Phys.*, vol. 45, pp. 1171-1175, 1974.

[9] S. L. Dvorak and E. F. Kuester, "Numerical Computation of the Incomplete Lipschitz-Hankel Integral $Je_0(a, z)$", *J. Comput. Phys.*, vol.87, No. 2, pp.301-327, 1990.

[10] S. L. Dvorak, "Exact, Closed-Form Expressions for Transient Fields in Homogeneously Filled Waveguides", *IEEE Trans. Microwave Theory Tech.*, vol. 42, No. 11, pp. 2164-2170, 1994.

[11] S. L. Dvorak, "Applications for Incomplete Lipschitz-Hankel Integrals in Electromagnetics", *IEEE Antennas and Propagation Magazine*, Vol. 36, No. 6, pp. 26-32, 1994.

[12] S. L. Dvorak and D. G. Dudley, "Propagation of Ultra-Wideband Electromagnetic Pulses Through Dispersive Media", *IEEE Trans. Electromagn. Compat.*, vol. 37, pp. 192-200, 1995.

[13] J. A. Fuller and J. R. Wait, "Electromagnetic Pulse Transmission in Homogeneous Dispersive Rock", *IEEE Trans. Antennas and Propagat.*, vol. AP-20, pp. 530-533, 1972.

[14] A. Grumet, "Penetration of Transient Electromagnetic Fields into a Conductor", *J. Appl. Phys.*, Vol. 30, No. 5, pp. 682-686, 1959.

[15] R. F. Harrington, *Time-Harmonic Electromagnetic Fields*, McGraw-Hill Book Company, New York, 1987.

[16] D. A. Hill and J. R. Wait, "Diffusion of Electromagnetic Pulses into the Earth from a Line Source", *IEEE Trans. Antennas and Propagat.*, vol. AP-22, pp. 145-146, 1974.

[17] A. Ishimaru, *Electromagnetic Wave Propagation, Radiation, and Scattering*, Prentice-Hall, Englewood Cliffs, 1991.

[18] J. Keilson and R. V. Row, "Transfer of Transient Electromagnetic Surface Wave into a Lossy Medium", *J. Appl. Phys.*, vol. 30, pp. 1595-1598, 1959.

[19] R. W. King and C. W. Harrison, "The Transmission of Electromagnetic Waves and Pulses into the Earth", *J. Appl. Phys.*, Vol. 39, No. 9, pp. 4444-4452, 1968.

[20] R. W. King, "The Propagation of a Gaussian Pulse in Sea Water and its Application to Remote Sensing", *IEEE Trans. Geoscience and Remote Sensing*, vol. 31, No. 3, pp. 595-605, 1993.

[21] J. J. A. Klaasen, "Time-Domain Analysis of One-Dimensional Electromagnetic Scattering by Lossy Media", Rep. FEL-90-A211, TNO Phys. Electron. Lab., the Hague, Oct. 1990.

[22] E. Kreysig, *Advanced Engineering Mathematics*, Wiley, New York, 1962.

[23] B. R. Levy and J. B. Keller, "Propagation of Electromagnetic Pulses around the Earth", *IRE Trans. Antennas and Propagat.*, vol. AP-6, pp. 56-61, 1958.

[24] P. Lorrain and D. R. Corson, *Electromagnetic Fields And Waves*, W. H. Freeman And Co., San Francisco, 1972.

[25] M. M. Mechaik and S. L. Dvorak, "Series Expansions for the Incomplete Lipschitz-Hankel Integral $Je_0(a,z)$", accepted for publication in *Radio Sci.*.

[26] M. M. Mechaik and S. L. Dvorak, "Series Expansions for the Incomplete Lipschitz-Hankel Integral $Ye_0(a,z)$", accepted for publication in *Radio Sci.*.

[27] P. E. Mijnarends, "Propagation of Electromagnetic Step Function over a Conducting Medium", *J. Appl. Phys.*, vol. 33, pp. 2556-2564, 1962.

[28] R. L. Monroe, "Approximate Step-Function Response of a Vertically Polarized Electromagnetic Plane Wave Reflected at an Imperfectly Conducting Surface", *J. Appl. Phys.*, vol. 40, pp. 3526-3531, 1969.

[29] J. S. Nicolis, "The Distortion of Electromagnetic Pulses Undergoing Total Internal Reflection in a Stratified Troposphere", *IEEE Trans. Antennas and Propagat.*, Vol. AP-15, pp. 706-708, 1967.

[30] J. S. Nicolis, "Comments on Distortion of Electromagnetic Pulses at Totally Reflecting Layers'", *IEEE Trans. Antennas and Propagat.*, Vol. AP-17, p. 388, 1969.

[31] *The NAG Mark 12 Manual*, Numerical Algorithms Group Ltd., Oxford,1987.

[32] A. V. Oppenheim, A. S. Willsky, and I. T. Young, *Signals and Systems*, Prentice-Hall, Englewood Cliffs, 1983.

[33] A. V. Oppenheim, and R. W. Schafer, *Discrete-Time Signal Processing*, Prentice-Hall, Englewood Cliffs, 1989.

[34] T. M. Papazoglou, "Transmission of A Transient Electromagnetic Plane Wave Into A Lossy Half-Space", *J. Appl. Phys.*, vol. 46, pp. 3333-3341, 1975.

[35] W. H. Press, B. P. Flannery, S. A. Teukolsky, and W. T. Vetterling, *Numerical Recipes — The Art of Scientific Computing*, Cambridge University Press, Cambridge University Press, 1986.

[36] P. I. Richards, "Transients in Conducting Media", *IRE Trans. Antennas and Propagat.*, vol. AP-6, pp. 178-182, 1958.

[37] J. A. Stratton, *Electromagnetic Theory*, McGraw-Hill, New York, 1941.

[38] L. M. Vallese, "Diffusion of Pulsed Current in Conductors", *J. Appl. Phys.*, vol. 25, pp. 225-228, 1954.

[39] J. R. Wait, "Transient Electromagnetic Propagation in a Conducting Medium", *Geophysics*, Vol. 16, pp. 213-221, 1951,

[40] J. R. Wait, "The Magnetic Dipole over the Horizontally Stratified Earth", *Canadian Journal of Physics*, Vol. 29, pp. 577-592, 1951,

[41] J. R. Wait, "A Transient Magnetic Dipole Source in a Dissipative Medium", *J. Appl. Phys.*, vol. 24, pp. 341-343, 1953.

[42] J. R. Wait and C. Froese, "Reflection of a Transient Electromagnetic Wave at a Conducting Surface", *Journal of Geophysics Research*, Vol. 60, No. 1 pp. 97-103, 1955.

[43] J. R. Wait, "Transient Fields of a Vertical Dipole over a Homogeneous Curved Ground", *Canadian Journal of Physics*, Vol. 34, pp. 27-35, 1956.

[44] J. R. Wait, "A Note on the Propagation of the Transient Ground Wave", *Canadian Journal of Physics*, Vol. 35, pp. 1146-1151, 1957.

[45] J. R. Wait, "The Transient Behavior of the Electromagnetic Ground Wave on a Spherical Earth", *IRE Trans. Antennas and Propagat.*, vol. AP-5, pp. 198-202, 1957.

[46] J. R. Wait, "Propagation of Electromagnetic Pulses in a Homogeneous Conducting Earth", *IRE Appl. Sci. Res. Section B*, vol. 8, pp. 213-253, 1961.

[47] J. R. Wait, "Distortion of Electromagnetic Pulses at Totally Reflecting Layers", *IEEE Trans. Antennas and Propagat.*, Vol. AP-17, pp. 385-388, 1969.

[48] J. R. Wait, "Electromagnetic Fields of Sources in Lossy Media", in *Antenna Theory*, Ed. by R. E. Collin and F. J. Zucker, Part 2, Chapter 24, McGraw-Hill, New York, pp. 503-505, 1969.

[49] J. R. Wait and K. P. Spies, "Transient Field for an Electric Dipole in a Dissipative Medium", *Canadian Journal of Physics*, Vol. 48, pp. 1858-1862, 1970.

[50] J. R. Wait and K. P. Spies, "Transient Magnetic Field of a Pulsed Electric Dipole in a Dissipative Medium", *IEEE Trans. Antennas and Propagat.*, Vol. AP-18, pp. 714-716, 1970.

[51] J. R. Wait, "Transient Excitation of the Earth by a Line Source of Current", *Proc. IEEE*, Vol. 59, pp. 1287-1288, 1971,

[52] J. R. Wait and D. A. Hill, "Transient Signals from a Buried Magnetic Dipole", *J. Appl. Phys.*, vol. 42, pp. 3866-3869, 1971.

[53] J. R. Wait and R. H. Ott, "On Calculating Transient Electromagnetic Fields of a Small Current-Carrying Loop over a Homogeneous Earth", *PAGEOPH*, Vol. 95, pp.157-162, 1972.

[54] J. R. Wait, "On the Theory of Transient Electromagnetic Sounding over a Stratified Earth", *Canadian Journal of Physics*, Vol. 50, pp. 1055-1061, 1972.

[55] R. Ziemer, W. Tranter and D. Fannin, *Signals and Systems: Continuous and Discrete*, MacMillan Publishing Company, New York, 1993.

[56] S. H. Zisk, "Electromagnetic Transient in Conducting Media", *IRE Trans. Antennas and Propagat.*, vol. AP-8, pp. 229-230, 1960.